

Electronic Thesis and Dissertation Repository

12-15-2011 12:00 AM

Septal Modulation of the Hippocampus

Siew Kian Tai, *The University of Western Ontario*

Supervisor: Dr. Stan Leung, *The University of Western Ontario*

A thesis submitted in partial fulfillment of the requirements for the Doctor of Philosophy degree in Neuroscience

© Siew Kian Tai 2011

Follow this and additional works at: <https://ir.lib.uwo.ca/etd>



Part of the [Systems Neuroscience Commons](#)

Recommended Citation

Tai, Siew Kian, "Septal Modulation of the Hippocampus" (2011). *Electronic Thesis and Dissertation Repository*. 342.

<https://ir.lib.uwo.ca/etd/342>

This Dissertation/Thesis is brought to you for free and open access by Scholarship@Western. It has been accepted for inclusion in Electronic Thesis and Dissertation Repository by an authorized administrator of Scholarship@Western. For more information, please contact wlsadmin@uwo.ca.

SEPTAL MODULATION OF THE HIPPOCAMPUS

(Spine title: Septal Modulation of the Hippocampus)

(Thesis format: Integrated Article)

by

Siew Kian Tai

Graduate Program in Neuroscience

A thesis submitted in partial fulfillment
of the requirements for the degree of
Doctor of Philosophy

The School of Graduate and Postdoctoral Studies
The University of Western Ontario
London, Ontario, Canada

© Siew Kian Tai 2011

THE UNIVERSITY OF WESTERN ONTARIO
School of Graduate and Postdoctoral Studies

CERTIFICATE OF EXAMINATION

Supervisor

Examiners

Dr. L. Stan Leung

Dr. Clayton Dickson

Supervisory Committee

Dr. Steven Laviolette

Dr. Michael Poulter

Dr. Wei-Yang Lu

Dr. Nagalingam Rajakumar

Dr. John Mitchell

Dr. Stephen Lomber

The thesis by

Siew Kian Tai

entitled:

Septal Modulation of the Hippocampus

is accepted in partial fulfillment of the
requirements for the degree of
Doctor of Philosophy

Date

Chair of the Thesis Examination Board

Abstract

The medial septum (MS) is the main source of acetylcholine to the hippocampus, a structure involved in memory and Alzheimer's disease (AD). Learning and memory involve long-term changes in synaptic strengths, and are suggested to be facilitated by a brain wave, theta rhythm in the hippocampus. Since medial septal neurons influence hippocampal neural activity, lesion of two neuronal populations in the MS, cholinergic and GABAergic, was performed by intraseptal infusion of 192 IgG-saporin and orexin-saporin, respectively. I hypothesized that 1) activation of cholinergic cells by vestibular stimulation induces an atropine-sensitive theta rhythm, modulates synaptic transmission and enhances long-term potentiation (LTP), a model of synaptic plasticity, in the hippocampus and 2) GABAergic neurons regulate granule cell activity by inhibiting interneurons in the dentate gyrus (DG).

Vestibular stimulation by passive whole-body rotation induced an atropine-sensitive theta rhythm that was not present in awake immobility. Following systemic cholinergic blockade, septal 192 IgG-saporin or bilateral vestibular lesion, rotation-induced theta and rotation-induced modulation of evoked potential were attenuated. LTP was enhanced when tetanus was delivered during rotation as compared to during immobility. Systemic cholinergic blockade or 192 IgG-saporin lesion abolished LTP enhancement by rotation.

I provided the first report investigating the role of septal GABAergic neurons on dentate neuronal unit activity *in vivo*. In urethane-anesthetized sham-lesion rats, pontis nucleus oralis (PNO) stimulation induced a theta rhythm, increased spontaneous granule

cell activity, facilitated DG population spike and increased paired-pulse depression (PPD) of population spikes. In freely moving rats, PPD was larger during walking as compared to during immobility. Orexin-saporin lesion attenuated theta, and blocked PNO-induced population spike facilitation and PPD in anesthetized rats. Spontaneous granule cell activity decreased while spontaneous interneuronal activity increased in orexin-saporin lesion rats as compared to sham-lesion rats. It is inferred that tonic interneuronal inhibition is increased and granule cells are less likely to be activated in orexin-saporin lesion rats, as compared to sham-lesion rats.

Therefore, vestibular stimulation provides a physiological method to activate septal cholinergic neurons, consistent with improvement of cognition in humans. Vestibular stimulation may ameliorate cholinergic dysfunction deficits and targeting septal GABAergic neurons may improve behavioral functions in AD.

KEYWORDS: medial septum, hippocampus, theta rhythm, population spike, single unit, vestibular system, acetylcholine, GABA, immunotoxin, sensorimotor processing, Alzheimer's disease.

Co-Authorship

This thesis contains materials that were previously published in *Hippocampus* (co-authored by S.K. Tai, J. Ma, K-P. Ossenkopp and L.S. Leung). All experimental work, preparation and writing of the manuscript were performed by S.K. Tai.

Acknowledgments

I will like to express my deepest gratitude to my supervisor Dr. L. Stan Leung for his excellent guidance and support throughout the course of my PhD training. I like to thank my advisory committee members, Drs. Michael Poulter, Nagalingam Rajakumar and Stephen Lomber. Many thanks to Drs. Klaus-Peter Ossenkopp, Jingyi Ma, Jiabi Yang and Min-Ching Kuo for their advice. I thank the previous laboratory members (Tao Luo, Lintao Qu, Bixia Shen, Pascal Peloquin, Thomas Fung, Richard Boyce, Melanie Crutchley, Jennifer Long and Min-Lan Tsai) for technical assistance. Financial support was provided through the generosity of the Canadian Commonwealth Scholarship and School of Graduate and Postdoctoral Studies at the University of Western Ontario. Last but not least, I will like to give special thanks to my family and friends for their continued support and encouragement.

Table of Contents

CERTIFICATE OF EXAMINATION	ii
Abstract.....	iii
Co-Authorship.....	v
Acknowledgments.....	vi
Table of Contents.....	vii
List of Figures.....	xii
Abbreviations.....	xiv
CHAPTER 1: General Introduction and Thesis Overview	1
1.1 Acetylcholine and GABA receptors	2
1.2 Septal region.....	3
1.2.1 Septohippocampal pathway	4
1.2.2 Hippocamposeptal pathway.....	5
1.3 Hippocampal theta rhythm.....	6
1.4 Medial septum as the pacemaker of theta rhythm	10
1.4.1 Septal models of theta generation.....	12
1.4.2 Intrinsic theta oscillators in the hippocampus.....	13
1.5 Functional significance of hippocampal theta rhythm.....	15
1.5.1 Sensorimotor integration.....	16
1.5.2 Synaptic plasticity.....	18
1.5.3 Spatial processing	22
1.6 Physiological characteristics of hippocampal neurons.....	24

1.6.1 Principal cells.....	24
1.6.2 Interneurons	26
1.7 Vestibular system.....	29
1.8 Outline of thesis.....	30
1.9 References.....	32
CHAPTER 2: Activation of Immobility-related Hippocampal Theta by Cholinergic Septohippocampal Neurons during Vestibular Stimulation.....	49
2.1 Introduction.....	49
2.2 Material and methods.....	51
2.2.1 Lesion and control rats.....	51
2.2.2 Electrode implantation and vestibular stimulation	53
2.2.3 Recording and analysis of EEG and evoked potentials	55
2.2.4 Histology.....	56
2.2.5 Statistical analysis.....	58
2.3 Results	58
2.3.1 Labyrinthine integrity	58
2.3.2 Effect of 192-IgG saporin lesion of the medial septum.....	59
2.3.3 Characteristics of theta rhythm during rotation	59
2.3.4 Characteristics of theta rhythm during walking.....	71
2.3.5 Effect of atropine sulfate and 192 IgG-saporin lesion on fEPSP modulation .	73
2.4 Discussion.....	75
2.4.1 Septohippocampal cholinergic neurons generates an atropine-sensitive theta rhythm during rotation	75

2.4.2 Vestibular stimulation of cholinergic activity in the hippocampus	76
2.4.3 Cholinergic septohippocampal and vestibular inputs modulates theta rhythm during walking	78
2.4.4 Vestibular activation modulates hippocampal synaptic transmission	79
2.4.5 Conclusion	80
2.5 References	81
CHAPTER 3: Vestibular Stimulation Enhances Hippocampal Long-term Potentiation via Activation of Cholinergic Septohippocampal Neurons	87
3.1 Introduction	87
3.2 Material and methods	89
3.2.1 Lesion and control rats	89
3.2.2 Electrode implantation	89
3.2.3 Lesion of cholinergic cells in the medial septum	90
3.2.4 Recording and analysis of evoked potentials	91
3.2.5 Experimental design	92
3.2.6 Histology	93
3.2.7 Statistical analysis	95
3.3 Results	95
3.3.1 Induction of basal-dendritic LTP in normal intact rats	98
3.3.2 Effect of muscarinic cholinergic blockade on LTP during rotation	101
3.3.3 Effect of lesion of septohippocampal cholinergic cells on LTP	104
3.4 Discussion	111
3.4.1 Vestibular stimulation enhances LTP	111

3.4.2 Septohippocampal cholinergic modulation of LTP	113
3.4.3 Conclusion	114
3.5 References	116
CHAPTER 4: Activation of Septohippocampal GABAergic Neurons Facilitates Population Spike and Modulates Single Unit Activities in the Dentate Gyrus	123
4.1 Introduction	123
4.2 Material and methods	125
4.2.1 Lesion, sham and control rats	125
4.2.2 Lesion of GABAergic cells in the medial septum	126
4.2.3 Electrophysiological procedure in anesthetized rats	126
4.2.4 Recordings from the 16-channel probe in anesthetized rats	128
4.2.5 Recordings from the tungsten microelectrode in anesthetized rats	129
4.2.6 Electrophysiological procedure and recordings in behaving rats	131
4.2.7 Histology	132
4.2.8 Statistical analysis	133
4.3 Results	134
4.3.1 Effect of orexin-saporin lesion on theta rhythm and population spike in anesthetized rats	134
4.3.2 Effect of orexin-saporin lesion on paired-pulse responses in anesthetized rats	139
4.3.3 Effect of orexin-saporin lesion on single units in anesthetized rats	143
4.3.4 Effect of orexin-saporin lesion in behaving rats	154
4.3.5 Effect of orexin-saporin lesion on cells in the MS	160

4.4 Discussion	160
4.4.1 Orexin-saporin lesion attenuates PNO-induced theta	161
4.4.2 Orexin-saporin lesion blocks PNO-induced population spike facilitation	162
4.4.3 Orexin-saporin lesion blocks changes in paired-pulse population spike response.....	163
4.4.4 Orexin-saporin lesion results in changes in single unit activity	165
4.4.5 Conclusion	166
4.5 References	168
CHAPTER 5: General Discussion	175
5.1 Introduction	175
5.2 Advantages and limitations of immunotoxin lesions	176
5.2.1 192 IgG-saporin lesion of septal cholinergic neurons	177
5.2.2 Orexin-saporin lesion of septal GABAergic neurons	178
5.2.3 Septal glutamatergic neurons.....	178
5.3 Significance of studies	179
5.4 Further studies	181
5.5 References	183
Copyright Transfer Agreement.....	187
Curriculum Vitae	192

List of Figures

Fig. 1.1 A diagrammatic representation of the connections between the MS-DB and hippocampus.....	7
Fig. 1.2 A diagrammatic representation of the sensorimotor integration model.....	19
Fig. 2.1 Photomicrographs of the ampullae of a semicircular canal.....	60
Fig. 2.2 Counts of ChAT-immunopositive cells in the MS and hippocampal sections stained for AChE.....	61
Fig. 2.3 Power spectra of hippocampal EEG during rotation.....	65
Fig. 2.4 Effect of rotational speeds on hippocampal theta rhythm.....	67
Fig. 2.5 Hippocampal theta rhythm is stable during rotation.....	69
Fig. 2.6 Changes in theta peak frequency and power during walking.....	72
Fig. 2.7 Effect of atropine sulfate and septal 192 IgG-saporin lesion on fEPSPs.....	74
Fig. 3.1 Recording of hippocampal basal-dendritic evoked potential and EEG using implanted electrodes in CA1.....	96
Fig. 3.2 Rotation-associated enhancement of basal-dendritic LTP.....	99
Fig. 3.3 Rotation-associated enhancement of LTP was suppressed by atropine sulfate.....	102
Fig. 3.4 Septal cholinergic lesion abolished the difference in LTP induced during immobility and rotation.....	105
Fig. 3.5 Photomicrographs of the MS following immunostaining and the hippocampus stained for AChE.....	107

Fig. 3.6 Counts of ChAT- and Parv-immunopositive cells from MS sections.....	109
Fig. 4.1 Electrode placements and hippocampal theta rhythm following electrical stimulation of PNO.....	135
Fig. 4.2 Averaged evoked potentials and its corresponding current source densities following PNO stimulation.....	137
Fig. 4.3 Paired-pulse responses as a function of interpulse interval.....	141
Fig. 4.4 Identification of interneurons and granule cells.....	144
Fig. 4.5 Probability of unit activation in the 40-ms time window immediately following PNO stimulation and before MPP stimulation.....	146
Fig. 4.6 Normalized peristimulus time histograms of granule cells and interneurons.....	150
Fig. 4.7 Probability of unit activation units by conditioning and test stimulus pulses delivered to the MPP.....	152
Fig. 4.8 Effect of orexin-saporin on theta rhythm and paired-pulse responses in behaving rats.....	155
Fig. 4.9 Counts of ChAT- and Parv-immunopositive cells in MS sections of sham and orexin-lesion rats.....	158

Abbreviations

ACh	acetylcholine
AChE	acetylcholinesterase
AD	Alzheimer's disease
AEP	averaged evoked potential
AHP	afterhyperpolarization
AMPA	2-amino-3-(5-methyl-3-oxo-1,2-oxazol-4-yl) propanoic acid
ANOVA	analysis of variance
CA1	field CA1 of the hippocampus
CA3	field CA3 of the hippocampus
ChAT	choline acetyltransferase
CSD	current source density
DAB	diaminobenzidine tetrahydrochloride
dB	decibel
DB	diagonal band of Broca
DG	dentate gyrus
DHPG	(S)-3,5-dihydroxyphenylglycine
DNQX	6,7-dinitroquinoxaline-2,3-dione
EEG	electroencephalogram
EPSP	excitatory postsynaptic potential
fEPSP	field excitatory postsynaptic potential
FFT	fast Fourier Transform
g	gram

GABA	gamma aminobutyric acid
GAD	glutamic acid decarboxylase
HDB	horizontal limb of Broca
Hz	hertz
i.p.	intraperitoneal
IPI	interpulse interval
IS	interneuron-selective cells
kg	kilogram
LIA	large irregular activity
LS	lateral septum
LSD	least significant difference
LTD	long-term depotentiation
LTP	long-term potentiation
μ A	microampere
μ l	microliter
μ m	micrometer
mA	milliampere
mg	milligram
mGluR	metabotropic glutamate receptors
min	minute
ml	milliliter
mm	millimeter
ms	milisecond

MPO	membrane potential oscillations
MPP	medial perforant path
MS	medial septum
ms	millisecond
mV	millivolt
NGF	nerve growth factor
nm	nanometer
NMDA	N-methyl-D-aspartate
Parv	parvalbumin
PB	phosphate buffer
PCA	principal component analysis
PETH	peristimulus time histogram
PLC β 1	phospholipase C- β 1
PNO	pontis nucleus oralis
PPF	paired pulse facilitation
PPT	pedunclopontine tegmental nucleus
PS	population spike
REM	rapid eye movement
rpm	revolution per minute
s	second
SEM	standard error of the mean
TTX	tetrodotoxin
VDB	vertical limb of Broca

Chapter 1

General Introduction and Thesis Overview

Acetylcholine acts as an excitatory neurotransmitter at the neuromuscular junctions of the peripheral nervous system. In the central nervous system, acetylcholine released from cholinergic neurons in the basal forebrain and brainstem mediates a variety of effects via nicotinic and muscarinic receptors. The cholinergic basal forebrain consists of the nucleus basalis magnocellularis (nucleus basalis of Meynert in humans) and the medial septum. The nucleus basalis projects mainly to the neocortex while the medial septum projects mostly to the hippocampus and entorhinal cortex (Mesulam et al., 1983; McKinney et al., 1983; Saper, 1984). The medial septum in the septal region is the major source of acetylcholine for the hippocampus (Mesulam et al., 1983; Nyakas et al., 1987). Besides cholinergic neurons, GABAergic and glutamatergic neurons in the medial septum also project to the hippocampus (Amaral and Kurz, 1985; Freund and Antal, 1988; Kiss et al., 1990; Sotty et al., 2003; Colom et al., 2005). In a mature mammalian nervous system, GABA and glutamate serve as the main inhibitory and excitatory neurotransmitters, respectively. An important function of the septohippocampal system lies in generating a hippocampal theta rhythm which is of importance in sensorimotor integration, spatial navigation, and learning and memory (O'Keefe and Reece, 1993; Bland and Oddie, 2001; Hasselmo et al., 2002).

Since this thesis focuses on the septohippocampal cholinergic and GABAergic projections, it will begin by describing acetylcholine and GABA receptors in the hippocampus, and the anatomical pathways between the septal region and the hippocampus. Next, I will describe the hippocampal theta rhythm and discuss the pacemaker role of medial septum. I will proceed to discuss the functional significance of theta rhythm and describe the physiological properties of hippocampal principal neurons and interneurons. Lastly, I will conclude with a description of the vestibular system and its role in spatial memory. The term “freely moving animal” and “behaving animal” will be used interchangeably throughout this thesis.

1.1 Acetylcholine and GABA receptors

Acetylcholine receptors are divided into muscarinic and nicotinic receptors. There are five subtypes of muscarinic receptors (M1-M5) coupled to G-proteins, mediating slow synaptic transmission. M1, M3 and M5 receptors are coupled to phospholipase C through G_q , resulting in an increase in intracellular calcium (Ca^{2+}), whereas M2 and M4 receptors are negatively coupled to adenylate cyclase via inhibitory G_i , leading to an reduction in cyclic adenosine monophosphate (cAMP) levels (Lanzafame et al., 2003). In the hippocampus, M1, M3 and M5 receptors are mainly expressed postsynaptically on glutamatergic principal neurons. M2 and M4 receptors are present postsynaptically on principal neurons and GABAergic interneurons, and presynaptically on cholinergic (autoreceptors) and non-cholinergic (heteroreceptors) terminals (Volpicelli and Levey, 2004). Nicotinic receptors are ligand-gated ion channels permeable to sodium (Na^+), Ca^{2+} and potassium (K^+) ions, and are responsible for rapid excitatory action on pre- and

postsynaptic sites. They are made up of a pentameric combination of α ($\alpha 2$ - $\alpha 10$) and β ($\beta 2$ - $\beta 4$) subunits with $\alpha 7$ subtype being the most common in the hippocampus (Fabian-Fine et al., 2001; Nai et al., 2003).

There are three classes of GABA receptors: GABA_A, GABA_B and GABA_C receptors. GABA_A receptors are ligand-gated ion channels permeable to chloride (Cl⁻) and bicarbonate (HCO₃⁻) ions. Like nicotinic receptors, GABA_A receptors are pentamers formed by different combinations of α ($\alpha 1$ - $\alpha 6$), β ($\beta 1$ - $\beta 4$), γ ($\gamma 1$ to $\gamma 3$), δ , ϵ , θ , π and ρ ($\rho 1$ - $\rho 3$) subunits. In adult neurons, GABA_A receptors mediate fast inhibitory postsynaptic potentials (IPSPs) (Benarroch, 2007). In the hippocampus, GABA_A receptors contain two α subunits, two β subunits and either a γ or a δ subunit but not both (Henschel et al., 2008). In contrast, GABA_B receptors are heterodimers made up of GABA_{B1} and GABA_{B2} subunits coupled to G_i protein. They mediate slower and longer-lasting synaptic responses on pre- and postsynaptic membranes, by decreasing adenylyl cyclase activity, activating postsynaptic K⁺ channels and inhibiting presynaptic voltage-gated Ca²⁺ channels (Couve et al., 2000). GABA_C receptors are ionotropic receptors and made up of ρ subunits, however, they are not known to play a major role in the hippocampus.

1.2 Septal region

The septal region is divided into four groups based on their anatomical location: the lateral group, the medial septal group, the posterior group and the ventral group (Risold, 2004). The focus of this thesis is on the medial septal group (MS-DB) which consists of the dorsally-located medial septal nucleus (MS) and the ventrally-situated nucleus of the diagonal band of Broca (DB). The DB is further subdivided into a (dorsal)

vertical limb (VDB) and a (ventral) horizontal limb of Broca (HDB). Throughout this thesis, medial septum and MS-DB will be used interchangeably.

1.2.1 Septohippocampal pathway

The MS-DB, a major subcortical input to the hippocampus, projects via four pathways: the fimbria, dorsal fornix, supracallosal stria and by a ventral route through and around the amygdala (Meibach and Siegel, 1977; Milner and Amaral, 1984; Nyakas et al., 1987; Gaykema et al., 1990; Dutar et al., 1995). Septal fibers terminate in all fields of the hippocampus formation, particularly in the dentate gyrus (DG). In the DG, septal fibers terminate heavily in the hilus (or polymorphic layer) and more lightly in the molecular layer (Gaykema et al., 1990). Although CA1 receives lighter septal innervation than CA3, septal projections terminate more densely in the stratum oriens and to a lesser extent in the stratum radiatum in both fields (Nyakas et al., 1987).

The MS nucleus projections show a clear mediolateral topographic arrangement. Cells located medially in the MS nucleus project preferentially to septal (dorsal) hippocampus and lateral entorhinal cortex whereas cells located laterally in this nucleus innervate the temporal (ventral) hippocampus and medial entorhinal cortex (Gaykema et al., 1990). The DB projects to the hippocampus and entorhinal cortex. The dorsal hippocampus and lateral entorhinal cortex receives afferent input mostly from the caudal VDB and medial HDB. The lateral HDB projects predominately to the olfactory nuclei and the entorhinal cortex. The rostromedial portion of the VDB and from the MS projects throughout the entire hippocampus (Gaykema et al., 1990).

Immunohistochemical studies showed that septal fibers which terminate in the hippocampus are cholinergic, GABAergic or glutamatergic (Lynch et al., 1977; Kohler et al., 1984; Amaral and Kurz, 1985; Freund and Antal, 1988; Kiss et al., 1990; Manns et al., 2003; Sotty et al, 2003; Colom et al., 2005). Cholinergic cells containing choline acetyltransferase (ChAT) are concentrated at the rostral and caudal ends of the MS-DB, whereas middle portion of the MS-DB contains the highest density of GABAergic cells that contain glutamic acid decarboxylase (GAD) and parvalbumin (Parv). On the contrary, glutamatergic cells are equally distributed throughout the rostrocaudal axis (Colom et al., 2005). In addition, cholinergic cells are mostly located lateral to the midline while Parv-containing GABAergic cells are concentrated along the midline (Kiss et al., 1990; Pang et al., 2001). Glutamatergic cells are evenly distributed within the MS-DB (Huh et al., 2010) with more abundance in the VDB and HDB than in the MS (Colom et al., 2005). Axons of cholinergic septal neurons impinge on to both principal cells and GABAergic interneurons of the hippocampus (Leranth and Frotscher, 1987) while GABAergic septal neurons preferentially project to the GABAergic hippocampal interneurons (Freund and Antal, 1988). Glutamatergic septal cells have been shown to project to hippocampal principal cells (Huh et al., 2010; Fig. 1.1).

1.2.2 Hippocamboseptal pathway

The lateral group of the septal region consists of the lateral septal (LS), septofimbrial and septohippocampal nuclei. The hippocampus sends major descending inputs to the LS. These projections are glutamatergic (Joels and Urban, 1984) and are topographically organized such that septo-temporal axis of the hippocampal formation

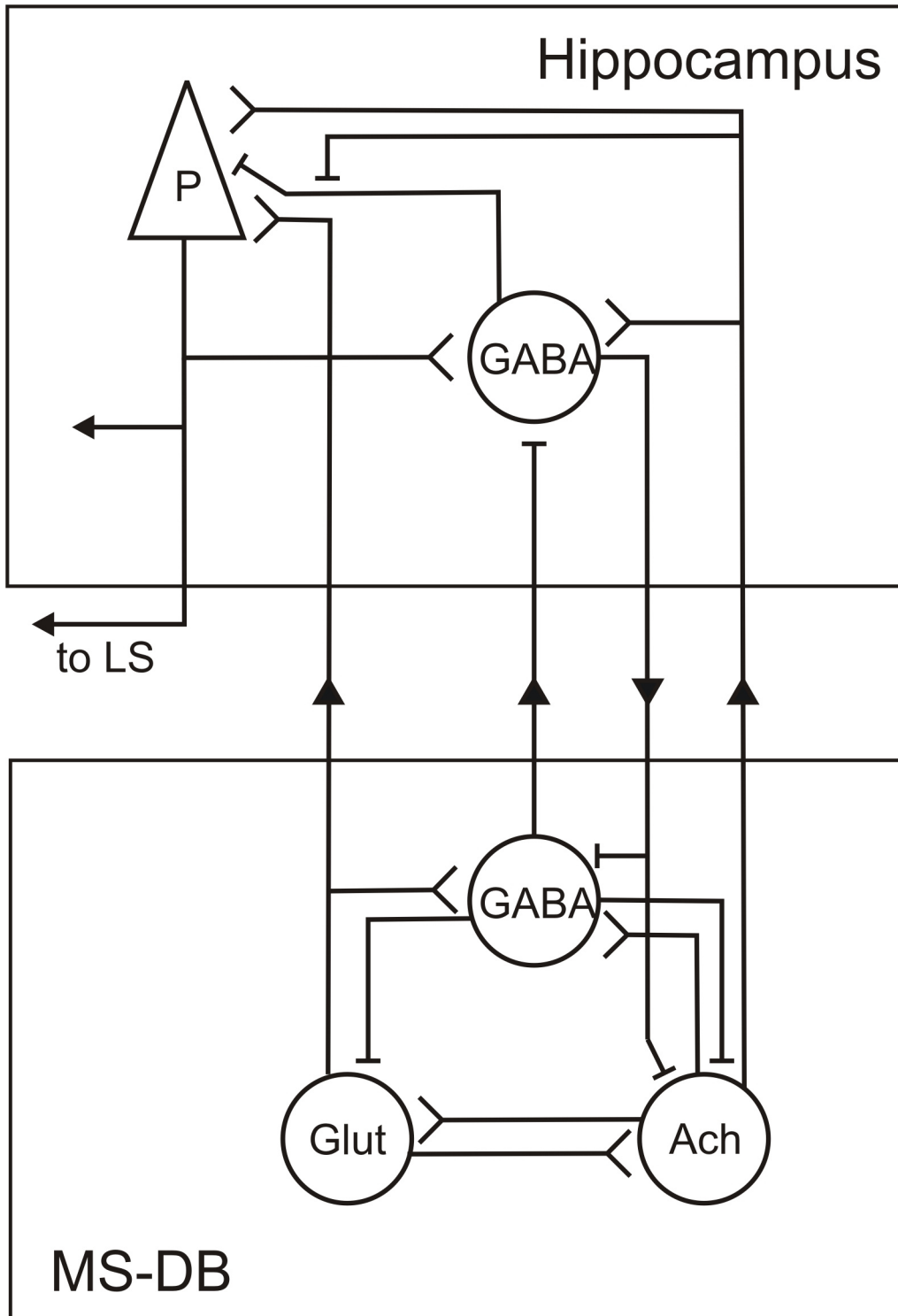
maps onto the dorso-ventral axis of the LS. Specifically, septal portions of the hippocampus project dorsally in the LS and progressively more temporal portions of the hippocampus project more ventrally (Swanson and Cowan, 1977, 1979; Risold and Swanson, 1997).

Apart from hippocampal projections to LS, hippocampal neurons give rise to weaker projections to MS-DB. Hippocampal neurons projecting to the MS-DB are exclusively non-principal cells while those sending axons to the LS appear to be mostly principal neurons (Alonso and Kohler, 1982; Fig. 1.1). Projections from septal and temporal portions of the hippocampus are arranged such that septal axons terminate in dorsal and medial areas of the MS and the anterior and dorsal parts of the VDB. Temporal hippocampal afferents innervate the ventral and lateral parts of the MS and the caudal and ventral parts of the VDB (Gaykema et al., 1991).

1.3 Hippocampal theta rhythm

In the hippocampus of a rat, several types of extracellular field potentials can be detected in electroencephalogram (EEG) which reflects the activity of local neural networks. These field potentials include large irregular activity (LIA), slow oscillation (≤ 1 Hz), theta and gamma rhythms (Buzsaki et al., 1983; Buzsaki, 1986; Lopes da Silva et al., 1990; Wolansky et al., 2006; Colgin and Moser, 2010). Theta and gamma rhythms, LIA and slow oscillation can co-occur whereas theta (and gamma) rhythm and LIA (and slow oscillation) are mutually exclusive. When recorded using depth electrodes, theta rhythm appears as rhythmic (nearly sinusoidal) extracellular oscillations with amplitude

Fig. 1.1 A diagrammatic representation of the connections between the MS-DB and hippocampus. Septal cholinergic neurons (ACh) send projections to the principal neurons (P) and GABAergic interneurons in the hippocampus whereas septal GABAergic neurons innervate hippocampal GABAergic interneurons. Septal glutamatergic neurons (Glut) impinge on to hippocampal principal neurons. The hippocampus sends projections to the lateral septum (LS) and MS-DB. Hippocampal interneurons terminate on septal ACh and GABAergic neurons whereas principal cells project to the LS. (Modified from Huh et al., 2010).



of around 1 mV (Vanderwolf, 1988; Bland, 1986; Buzsaki, 2002). Hippocampal theta frequency ranges from 3-6 Hz in anesthetized rats and 4-10 Hz in behaving animals (Bland, 1986; Buzsaki, 2002). In humans, hippocampal theta frequency ranges from 3-8 Hz (Ekstrom et al., 2005; Watrous et al., 2011; Lega et al., 2011).

Hippocampal gamma rhythm has two distinct frequency bands, a slow (~25-50 Hz) and a fast (~65-150 Hz). The amplitude of a gamma rhythm is largest when they are nested within a theta rhythm (Leung et al., 1982; Buzsaki et al., 1983; Bragin et al., 1995). Within a theta cycle, gamma rhythm bursts at specific times (Soltesz and Deschenes, 1993; Colgin et al., 2009). In CA1, slow gamma oscillations are generated by CA3 and are most apparent during the descending part of a theta cycle whereas fast gamma oscillations, entrained by medial entorhinal cortex, are maximal close to a theta trough (Bragin et al., 1995; Csicsvari et al., 2003; Colgin et al., 2009).

Vanderwolf (1969) was the first to discover the correlation between hippocampal EEG and moment-to-moment behavior in behaving rats. Theta rhythm is observed in conjunction with rapid eye movement (REM) sleep and voluntary movement (e.g. walking and postural shifts) (Vanderwolf, 1969; Whishaw and Vanderwolf, 1973; Kramis et al., 1975; Sainsbury et al., 1987; Vanderwolf, 1988; Oddie and Bland, 1998). In anesthetized rats, theta can occur spontaneously or in response to sensory stimuli (e.g. tail pinch or fur stroking) or during electrical stimulation of the brainstem (Bland, 1986; Herreras et al., 1988a, 1988b; Vertes and Kocsis, 1997; Khanna, 1997; Jiang and Khanna, 2004; Leung and Peloquin, 2010). Slow oscillation is observed during non-REM sleep and anesthesia (Wolansky et al., 2006; Dickson, 2010; Sharma et al., 2010). LIA, but generally not theta rhythm, is observed during non-REM sleep, awake immobility and

automatic movements such as eating, drinking and grooming in the absence of postural shifts (Vanderwolf, 1969; Bland, 1986).

Pharmacological studies indicate that there are two types of theta activity in the hippocampus, namely atropine-sensitive theta and atropine-resistant theta (atropine is a muscarinic cholinergic receptor antagonist) (Kramis et al., 1975; Leung, 1984; Buzsaki et al., 1986; Lawson and Bland, 1993; Leung, 1998; Bland and Oddie, 2001). Atropine-sensitive theta can be induced by an anticholinesterase physostigmine and abolished by anticholinergics (e.g. atropine sulfate and scopolamine). In the behaving rat, theta that remains following administration of atropine is atropine-resistant and appears during voluntary movement (Kramis et al., 1975; Lawson and Bland, 1993). Atropine-sensitive theta can be observed during awake immobility, for example just prior to a jump avoidance response (Vanderwolf, 1969) and during vestibular stimulation (Chapter 2, Tai et al., 2011). In addition, atropine-sensitive theta is generally of a lower frequency (4-7 Hz) as compared to atropine-resistant theta (7-10 Hz) (Vanderwolf, 1975; Bland and Oddie, 2001). Hence, atropine-sensitive theta is also referred to as immobility-related theta and atropine-resistant theta as movement-related theta (Vanderwolf, 1975; Bland, 1986; Bland and Oddie, 2001). In anesthetized rats, atropine eliminated spontaneous theta, but not theta elicited by high intensity electrical stimulation of the brainstem (Kocsis and Li, 2004; Li et al., 2007).

1.4 Medial septum as the pacemaker of theta rhythm

It is well documented that rhythmically bursting cells of the medial septum fire in synchrony with hippocampal theta (Brazhnik and Vinogradova, 1986; Dutar et al., 1986;

Alonso et al., 1987; Stewart and Fox, 1989; Brazhnik and Fox, 1997). When the hippocampus was removed, septal neurons continued firing at a theta frequency (Petsche et al., 1962). Electrolytic lesion of the medial septum permanently abolished theta (Green and Arduini, 1954; Leung, 1987) and septal infusion of a local anesthetic tetracaine temporarily disrupted theta (Mizumori et al., 1989). Therefore, the MS-DB has been regarded as the pacemaker of the hippocampal theta rhythm.

Cholinergic and non-cholinergic (GABAergic and glutamatergic) septal cells were demonstrated to be rhythmically bursting cells projecting to the hippocampus (Stewart and Fox, 1989; Borhegyi et al., 2004; Simon et al., 2006; Huh et al., 2010), and are likely involved in the generation of atropine-sensitive and atropine-resistant theta, respectively. For example, in behaving rabbits, large numbers of septal cells continued to fire rhythmically despite the abolishment of theta with intravenous injections of atropine (Brazhnik and Vinogradova, 1986). In urethane-anesthetized rats, a “residual theta rhythm” of reduced amplitude was observed in both CA1 and DG upon electrical stimulation of septal cells following systemic injections of high doses (100 mg/kg i.p.) of atropine (Stewart and Fox, 1989). In behaving rats, intraseptal injections of 192 IgG-saporin (immunotoxin targeting cholinergic neurons) reduced hippocampal running-induced theta peak power in a dose-dependent manner, but no change in theta peak frequency was observed (Lee et al., 1994). Furthermore, the power of theta, but not its frequency, elicited upon direct activation of the medial septum via intraseptal cholinergic agonist carbachol or by indirect activation upon brainstem stimulation was attenuated in 192 IgG-saporin lesioned rats under urethane (Zheng and Khanna, 2001). In addition, amplitude of walking-induced theta was attenuated in rats infused with kainic acid

(preferentially destroys GABAergic cells) or 192 IgG-saporin in the medial septum. Theta was abolished in rats infused with both kainic acid and 192 IgG-saporin (Yoder and Pang, 2005). In a slice preparation with a half-septum attached to its ipsilateral hippocampus, atropine applied to the hippocampus attenuated the amplitude of theta induced by intraseptal carbachol, but not its frequency (Goutagny et al., 2008). Studies have showed that GABAergic neurons burst at the trough or peak of theta, phasing theta (Borhegyi et al., 2004; Simon et al., 2006). Glutamatergic neurons were recently demonstrated to burst in relation to theta (Huh et al., 2010).

1.4.1 Septal models of theta generation

Prior to the discovery of septohippocampal glutamatergic cells (Manns et al., 2003; Sotty et al, 2003), a model was proposed by Vertes and Kocsis (1997) suggested that the cholinergic and GABAergic septal cells fire in synchrony such that their coordinated burst discharge (burst mode) or pauses (inter-burst mode) drives the negative-going and positive-going phase of extracellular theta, respectively. In addition to the differential projections of the rhythmically bursting cholinergic and GABAergic septal neurons to hippocampal cells, the model was also based on evidence that cholinergic septal cells presynaptically inhibit hippocampal interneurons (Ben-Ari et al., 1981; Krnjevic et al., 1981; Behrends and ten Bruggencate, 1993; Fig. 1.1). During burst mode, cholinergic septal cells excite principal cells directly and inhibit hippocampal interneurons presynaptically while GABAergic septal cells inhibit hippocampal interneurons. Such coordinated action of these septal cells (cholinergic excitation coupled with GABAergic disinhibition) leads to firing of principal cells and drives the positive-

going phase of intracellular theta (negative-going phase of extracellular theta). During inter-burst mode, loss of excitatory input from cholinergic septal cells and inhibitory action on interneurons by GABAergic septal cells leads to inhibition of principal cells by interneurons, giving rise to the negative-going phase of intracellular theta (positive-going phase of extracellular theta).

Although the precise role of septal glutamatergic cells in theta rhythm generation is currently unclear, it has been suggested that these cells work together with septal cholinergic cells to provide a rhythmic excitatory drive to start theta oscillations in the medial septum and subsequently in the hippocampus (Colom, 2006; Huh et al., 2010). According to the model proposed by Colom (2006), activation of the septal cholinergic cells excites septal glutamatergic cells, which in turn recruits more excitatory septal cells, increasing the level of excitation within the medial septum. When this level reaches a threshold, the septo-hippocampal network will begin to oscillate at theta frequencies. Excitatory input from the medial septum depolarizes hippocampal principal cells. This depolarized state is regulated by hippocampal GABAergic interneurons, which maintain a hippocampal theta rhythm.

1.4.2 Intrinsic theta oscillators in the hippocampus

The septal pacemaker hypothesis has been challenged by reports demonstrating that the intrinsic circuitry within the hippocampus is capable of generating a self-sustaining form of theta without the need for afferent inputs. For instance, extracellular recordings of transverse hippocampal slices showed that theta, albeit induced by carbachol, can occur in the absence of inputs from external structures and is atropine-

sensitive (Konopacki et al., 1987). An atropine-resistant theta rhythm of 6-10 Hz in the hippocampal slices was observed following administration of a metabotropic glutamatergic receptor agonist (S)-3,5-dihydroxyphenylglycine (DHPG) (Gillies et al., 2002). Recently, Goutagny and colleagues (2009) provided data showing that the hippocampus can spontaneously generate a theta rhythm in a whole-hippocampus preparation *in vitro*, without application of drugs or stimulation on the medial septum; this *in vitro* rhythm shows properties (e.g. depth profile, atropine-resistance) similar to an *in vivo* preparation. In addition, the fact that when *in vitro* theta was recorded at two locations in CA1 (dorsal and ventral) and local anesthetic procaine applied to the region between, theta at the dorsal site was faster by ~1 Hz than the ventral location, suggested the presence of multiple independent theta oscillators. Judging from the evidence presented, it may seem that the medial septum is not critical for hippocampal theta generation. Nonetheless, the medial septum may synchronize the different hippocampal oscillators along the septotemporal axis (Colgin and Moser, 2009).

Furthermore, hippocampal pyramidal neurons possess intrinsic properties that give rise to theta frequency oscillations and resonance. Early evidence came from intracellular recordings of transverse hippocampal slices which demonstrated the presence of intrinsic theta-frequency membrane potential oscillations (MPOs) following application of carbachol (Bland et al., 1988). Subsequently, a series of intracellular experiments showed that slow voltage-dependent persistent inward Na^+ current I_{NaP} (sensitive to tetrodotoxin TTX and QX-314) and slowly inactivating outward K^+ current I_{m} (sensitive to XE991) are required for MPOs and somatic resonance at theta-frequency (Leung and Yim, 1991; Crill, 1996; Hu et al., 2002, 2007). Blocking I_{NaP} by application

of QX-314 abolished MPOs (Leung and Yim, 1991), and administration of TTX or XE991 suppressed theta-frequency resonance (Hu et al., 2002). Since these currents activate at subthreshold membrane potentials (> -65 mV), only a small depolarization in hippocampal pyramidal cells is sufficient to activate an intrinsic theta-frequency oscillation or resonance (Leung and Yim, 1991; Hu et al., 2002, 2007). However, having the ability to produce MPOs and theta-frequency resonance does not necessarily exclude the purpose of an external oscillator. These small low-threshold currents may act as frequency selectors to promote a theta rhythm at their preferred frequencies when it matches that of an external oscillator (Hutcheon and Yarom, 2000; Hu et al., 2002). Moreover, it was suggested that rhythmic firing of septohippocampal GABAergic neurons may modulate hippocampal theta-frequency resonance via rhythmic disinhibition of pyramidal cells at the soma region where a high density of M-type K^+ channels are concentrated (Hu et al., 2009).

1.5 Functional significance of hippocampal theta rhythm

Electrophysiological recordings indicate that hippocampal theta activity reflects rhythmic oscillations of neurons in information processing. Cell excitation can be observed in correlation with theta and such excitation is theta-rhythmic with peak of cell firing occurring in a temporal relationship to the theta peak (Buzsaki et. al., 1983; Bland, 1986; Buzsaki, 2002; Bland et. al., 2002). In addition, the presence of cellular activity phase-locked to theta in subcortical structures which are involved in hippocampal theta generation (e.g. posterior hypothalamus and brainstem reticular formation) or part of the limbic (e.g. cingulate cortex and amygdala) or sensory system (e.g. superior and inferior

colliculi) (Leung and Borst, 1987; Kirk and McNaughton, 1991; Nunez et al., 1991; Bland et al., 1995; Pedemonte et al., 1996; Kocsis and Vertes, 1997; Natsume et al., 1999; Seidenbecher et al., 2003), represent a widespread function of theta such as the synchronization of neurons across sensory, motor and emotional/motivational centers. Hippocampal theta rhythm has been implicated in sensorimotor integration (Bland and Oddie, 2001), synaptic plasticity (Buzsaki, 2002) and spatial processing (O'Keefe and Reece, 1993).

1.5.1 Sensorimotor integration

Hippocampal theta activation has been linked to sensorimotor integration (Bland, 1986). Bland and Oddie (2001) proposed a sensorimotor integration model of hippocampal function which is based on the assumption that neural circuitry underlying theta is capable of providing voluntary motor systems with continually updated feedback on their performance relative to changing environmental (sensory) conditions. More specifically, there are two separate inputs to the hippocampus, each responsible for generating atropine-sensitive and atropine-resistant theta. Both inputs are active during voluntary movement. In the absence of movement, atropine-sensitive theta occurs alone. The presence of an atropine-sensitive theta indicates that sensory processing is occurring in the hippocampus, whereas atropine-resistant theta serves as the electrical signal of movement-related hippocampal activity (Vanderwolf, 1969).

In this model, ascending brainstem hippocampal synchronizing pathway originates from the pontis nucleus oralis (PNO) and pedunculopontine tegmental nucleus, (PPT) (Vertes et al., 1993, 2004; Takano and Hanada, 2009). Atropine-sensitive

“sensory” input ascend from the PNO and PPT to the midline diencephalic region (posterior hypothalamic and the supramammillary nuclei) then to the medial septum and finally to the hippocampus. If voluntary movement does not occur, only atropine-sensitive input is relayed to motor structures. On the other hand, when voluntary movement is initiated by the motor regions, both atropine-sensitive and atropine-resistant inputs are sent to the midline diencephalic region and loops back to the hippocampus via the medial septum (Fig. 1.2). Thus, activation of the ascending brainstem hippocampal synchronizing pathway provides sensory information required for the initiation of voluntary movement from motor regions which send inputs back, signaling that these movements have been initiated. As movement continues, the combination of atropine-sensitive “sensory” input from the ascending brainstem synchronizing pathways and atropine-resistant “movement-related” input from motor structures are feedback to the hippocampus, allowing the hippocampus to integrate sensory and motor information necessary for the maintenance of voluntary motor behavior. In this context, atropine-sensitive theta may prepare motor systems for movement or signal the intensity of an upcoming movement or arrange a change of an ongoing movement. In contrast, atropine-resistant theta may indicate the level of activation of motor systems engaged in voluntary behaviors (Bland and Oddie, 2001).

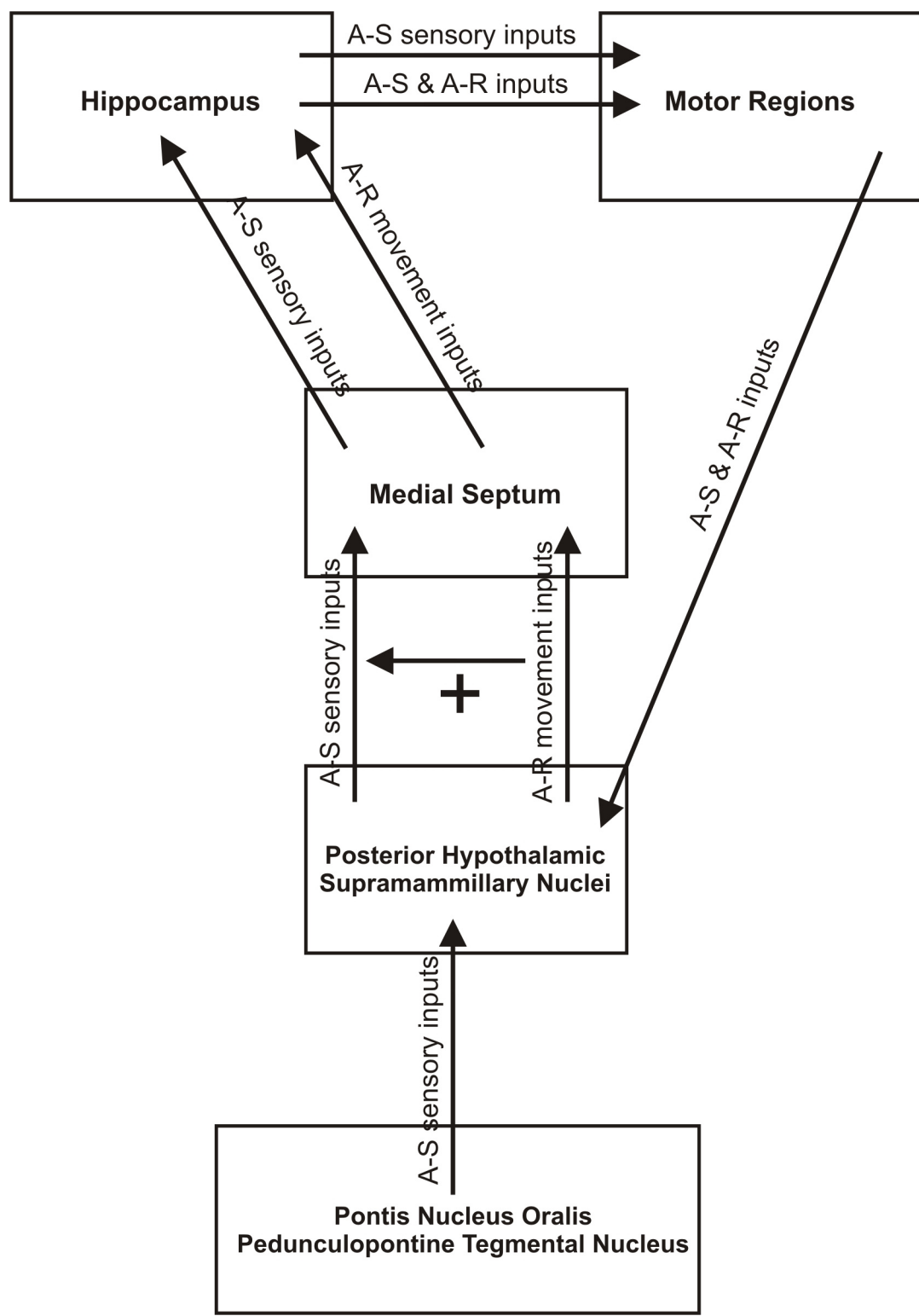
Based on this model, indices of theta (e.g. amplitude, frequency) should increase with speed of movement such that more rapid or intense the movement will require faster sensorimotor transformations. This has been observed in rats (Vanderwolf, 1969; McFarland et al., 1975; Bland et al., 2006), guinea pigs (Rivas et al., 1996), cats (Whishaw and Vanderwolf, 1973), dogs (Arnolds et al., 1979) and humans (Ekstrom et

al., 2005; Watrous et al., 2011; Hinman et al., 2011). Inactivation by a local anesthetic procaine in rats (Hallworth and Bland, 2004) or electrical lesion of the medial septum in rabbits (Green and Arduini, 1954) and cats (Sabatino et al., 1985) abolished theta. Also in agreement with this model, the red nucleus in the brainstem and nuclei in the basal ganglia, which are traditionally associated with motor functions (DeLong, 2000; Kuchler et al., 2002; Muir and Whishaw, 2000), are functionally connected with the neural circuitry involved in the theta generation. For example, in urethane-anesthetized rats, electrical stimulation of the red nucleus led to the transition from LIA to theta in the hippocampus. Moreover, amplitude and frequency of theta was correlated positively with stimulation intensity (Dypvik and Bland, 2004). In addition, electrical stimulation of nuclei in the basal ganglia induced a hippocampal theta rhythm in anesthetized animals (Sabatino et al., 1985, 1986; Hallworth and Bland, 2004). Overall, these findings suggest that these motor-related structures may interact with the hippocampus via the ascending brainstem synchronizing pathways.

1.5.2 Synaptic plasticity

Synaptic plasticity describes the change in strength across the synapse. Long-term potentiation (LTP) and depression (LTD) are two forms of long-lasting synaptic plasticity that can persist for hours. LTP, prolonged enhancement of synaptic transmission arising from temporal coincidence of postsynaptic firing with presynaptic input, is a postulated neural mechanism of learning and memory, especially in the hippocampus (Bliss and Collingridge, 1993). In contrast, LTD is the long-lasting depression of synaptic transmission. Besides the hippocampus, studies have shown that LTP can occur in other

Fig. 1.2 A diagrammatic representation of the sensorimotor integration model which involves two types of inputs to the hippocampus, namely atropine-sensitive (A-S) and atropine-resistant (A-R) inputs. A-S inputs, originating from the pontis nucleus oralis and pedunculopontine tegmental nucleus, carry sensory information for the initiation of voluntary movement to the motor regions. Once voluntary movement is initiated, both A-S sensory and A-R movement inputs are relayed back via the medial septum to hippocampus where sensory and motor information required for the maintenance of voluntary motor behavior are integrated. (Modified from Bland and Oddie, 2001).



structures, such as cerebellum and amygdala (Teyler and Fountain, 1987; Clugnet and LeDoux, 1990).

Theta oscillations modulate hippocampal synaptic plasticity such that the timing of stimulation with respect to the phase of theta determines the direction of synaptic change. For instance, a single pulse (0.1 Hz) or burst (100 Hz) given at the peak of carbachol-induced theta in hippocampal CA1 slices resulted in LTP, but when given at the trough of theta induced LTD (Huerta and Lisman, 1995, 1996). Likewise, in the behaving rat, LTP was recorded in stratum radiatum of CA1, following tetanic burst stimulation delivered on the peak of running-induced theta (Hyman et al., 2003). This is consistent with previous studies in CA1 of anesthetized rats (Holscher et al., 1997), and in DG of anesthetized (Pavrides et al., 1988) and behaving rats (Orr et al., 2001). Meanwhile, stimulation at the trough of theta in behaving rats depotentiates previously potentiated synapses in anesthetized rats (Holscher et al., 1997) and induced LTD in behaving rats (Hyman et al., 2003). Based on these findings, a model was constructed, associating the peak and trough of local theta with memory encoding and retrieval, respectively (Hasselmo et al., 2002). Since tetanic burst stimulation resembles complex spike bursting of hippocampal principal cells, it was suggested that hippocampal synaptic plasticity can be modulated by theta rhythm during behaviors associated with learning and contribute to memory formation. In humans, theta oscillations in the hippocampus were also implicated in memory function (Cornwell et al., 2008; Lega et al., 2011).

The medial septum has been shown to modulate synaptic plasticity in the hippocampus. For example, lesion of the medial septum led to a faster decay of LTP (Rashidy-Pour et al., 1996) and septal stimulation prolonged LTP (Frey et al., 2003). Due

to its implications on Alzheimer's disease in which degeneration of basal forebrain cholinergic neurons is a pathological characteristic (Bartus et al., 1982; Francis et al., 1999; Wu et al., 2005; Wenk, 2006), research has been centered on septohippocampal cholinergic projections. Although acetylcholine can act on a variety of muscarinic and nicotinic cholinergic receptors, attention has been largely focused on muscarinic receptors. Application of carbachol to hippocampal slices facilitated LTP (Blitzer et al., 1990; Auerbach and Segal, 1996; Shimoshige et al., 1997). Hippocampal LTP facilitated by tetanic stimulation of the medial septum was blocked by systemic administration of muscarinic cholinergic antagonists in anesthetized rats (Markevich et al., 1997; Ovsepiyan et al., 2004). In behaving rats, higher level of acetylcholine is released during walking than immobility (Dudar et al., 1979). Hippocampal LTP was facilitated when induced during walking, as opposed to when induced in the absence of theta (i.e. immobility). In addition, systemic scopolamine or 192 IgG-saporin septal lesion or specific M1 receptor antagonist pirenzepine attenuated LTP induced during walking without affecting LTP induced during immobility (Leung et al., 2003; Doralp and Leung, 2008). There is some evidence of modulation of synaptic plasticity by nicotinic receptors. In hippocampal slices, nicotine induced LTP in the absence of tetanus (He et al., 2000; Yu et al., 2007) and facilitated LTP following tetanus (Welsby et al., 2006, 2009).

1.5.3 Spatial processing

When running on a treadmill, majority of CA1 pyramidal cells in a behaving rat tends to fire on the positive phase of theta (Fox and Ranck, 1975; Buzsáki et al., 1983). However, in a "natural" environment (e.g. walking on a narrow track), theta phase

relationship of hippocampal pyramidal cells is not constant and can change dynamically as a function of behavior. During walking, pyramidal cells which are preferentially activated with respect to the rat's specific location in the environment are referred to as place cells. Hippocampal place cells were also found in humans (Ekstrom et al., 2003). The region in which a given place cell is maximally activated is called its place field (O'Keefe and Dostrovsky, 1971; O'Keefe, 1976; O'Keefe and Nadel, 1978). As the rat traversed the cell's place field, place cells displayed a systematic phase shift relative to theta. Upon entering a place field, firing consistently began at a particular phase of theta but during traversal of the field, place cells fired at progressively earlier phases of the theta cycle. This phenomenon is termed phase precession (O'Keefe and Recce, 1993; Skaggs et al., 1996).

Maximal firing generally occurred in the middle of the phase shift (O'Keefe and Recce, 1993). However, the phase of spike firing is strongly correlated with the rat's location within the place field and this correlation is higher than the time spent in the field or firing rate demonstrated that this temporal variation in firing transmits information about the rat's spatial location (Huxter et al., 2003). In addition, when theta phase relationship was considered together with firing rates, localization of the rat's position improved significantly (Jensen and Lisman, 2000). Lastly, it is interesting to note that the signal strength of place cells is greater during theta than during LIA (Muller, 1996).

1.6 Physiological characteristics of hippocampal neurons

Although EEG and field potential allow us to examine synchronous activity of a large number of neurons in a given brain region, neighboring neurons may not always respond in the same manner. In order to attain a more complete picture, recording of individual neuronal responses (single unit) is required. The electrophysiological characteristics of hippocampal principal neurons, including those in DG, have been documented in a number of studies (e.g. Kandel and Spencer, 1961; Fox and Ranck, 1975, 1981). Based on their anatomical and physiological properties such as firing rates, waveform and relative position in the hippocampus, two classes of cells were identified in the rat hippocampus; complex spike cells and theta cells. Complex spike cells were located in the stratum pyramidale and stratum granulosum whereas theta cells were found in all layers of the hippocampus (Fox and Ranck, 1975). Since most principal cells innervate adjacent interneurons via axon collaterals, an increased probability of firing in theta cells follow shortly after action potentials in the principal cells (Csicsvari et al., 1998). Complex spike and theta cells are generally recognized as principal cells and interneurons, respectively.

1.6.1 Principal cells

Hippocampal principal cells have relatively low firing frequency (≤ 2 Hz) and long duration action potentials (0.4-1 ms). These cells can be antidromically activated by electrical stimulation of the hippocampal efferent pathways (Fox and Ranck, 1975; Fox and Ranck, 1981; Vertes and Kocsis, 1997). Moreover, principal cells possess a

distinctive firing pattern known as burst firing which can be recorded extracellularly in the form of 'complex spike'. A complex spike comprises of a series of 2 to 10 action potentials (spikes) with short interspike intervals (3-10 ms), in which the amplitude of individual spike decreases during the series (Kandel and Spencer, 1961; Ranck, 1973; Fox and Ranck, 1975, 1981). It has been suggested that depolarizing after-potentials such as inward I_{NaP} and R-type Ca^{2+} current are responsible for complex spike bursting (Yue et al., 2005; Metz et al., 2005). Another unique feature is that the frequency of spikes declines during the series and is followed by a slow afterhyperpolarization (AHP) at the end of the series, as a result of gradual activation of K^+ channels (e.g. outward I_m and I_{AHP} , mediated by Ca^{2+} -activated SK channels) (Lancaster and Adams, 1986; Lancaster and Nicoll, 1987). In addition, these cells can fire single isolated spikes and remain silent for long periods of time (Fox and Ranck, 1975, 1981).

Complex spike bursting is implicated in synaptic plasticity and spatial information processing in the hippocampus. In contrast to the former, in hippocampal slice experiments, pairings of synaptic inputs with postsynaptic bursting activity, but not with single postsynaptic action potentials, induced LTP (Thomas et al., 1998; Pike et al., 1999). LTP was not observed following blockade of complex spike bursting by low concentration of TTX without affecting generation of single postsynaptic potential (Thomas et al. 1998). In the latter, place cells are hippocampal principal cells which can fire when animals enter specific spatial locations in the environment. Thus, the hippocampus is likely involved in the construction of a cognitive map of the animal's environment (O'Keefe and Dostrovsky, 1971; O'Keefe, 1976). Mapping of the animal's position, encoded by activation of a place cell, is defined more precisely by burst firing,

rather than by single spikes of the place cell (Otto et al., 1991). Burst firing of place cells is suggested to be “information-rich” and may create a more accurate internal representation of position in the external environment, than single spikes (Lisman, 1997).

1.6.2 Interneurons

Interneurons have relatively high firing frequency (10 Hz to 100 Hz) and short-duration action potentials (< 0.4 ms). These cells generally cannot be antidromically driven from efferent pathways (Vertes and Kocsis, 1997). Distinct from principal cells, interneurons do not fire complex spikes in bursts. Interneurons fire single spikes in bursts, in synchrony with theta rhythm (Fox and Ranck, 1975). In a behaving rat, interneurons can alter their firing rate when the rat is engaged in “theta” activities (e.g. walking), as opposed to when the rat is in “LIA-state” (e.g. immobile), therefore are termed theta cells (Ranck, 1973).

According to a classification system of Colom and Bland (1987), theta cells are divided into theta-ON and theta-OFF cells. Theta-ON cells increase their firing rates during theta activity, whereas theta-OFF cells decrease theirs. In addition, these cells are further categorized into 2 subtypes, phasic and tonic. Phasic cells fire rhythmically with theta and their firing rate is positively (theta-ON) or negatively (theta-OFF) correlated with theta frequency. Tonic cells fire non-rhythmically. On the other hand, neurobiotin-labeled pyramidal cells in CA1 and CA3 were found to behave like phasic and tonic theta-ON cells, suggesting that not all theta cells are interneurons (Bland et al., 2002, 2005).

GABAergic interneurons are involved in network forms of inhibition (e.g. feedback and feedforward inhibition) which spatially limit the flow of excitation to pyramidal cells to provide stability to the principal cell population. In feedback inhibition, an excitatory input arrives directly to a principal cell, whose excitatory input is fed-back to an interneuron through recurrent axon collaterals. This interneuron in turn inhibits a number of principal cells including those which initially activated it and also the neighboring principal cells (recurrent and lateral inhibition). In feedforward inhibition, an excitatory input arrives at both a principal cell and an interneuron. This interneuron then suppresses the firing of the principal cell. Feedforward inhibition may participate in “signal-to-noise” information processing in which excitation in a selected population of principal cells occurs against the suppression of background firing of adjacent principal cell populations (Buzsaki, 1984). Moreover, interneuron-selective cells (IS-1, IS-2, and IS-3), which innervate specific subsets of interneurons, may synchronize interneurons that converge onto a particular group of principal cells. They may disinhibit principal cell dendrites targeted by particular excitatory inputs. IS-1 cells can reduce feedback inhibition produced by interneurons (i.e. basket cells) in the principal cell layer. Hence, IS interneurons may play a role in the control of population oscillations and disinhibition in the hippocampal network (Freund and Buzsaki, 1996).

In addition, the network of interneurons serves as a clock, providing a rhythm-based timing signal to the principal cell population. Locally, interneurons can control spike timing via shunting inhibition. Having reversal potential (e.g. -55 mV) for GABAergic events below action potential threshold but above resting membrane potential allows for shunting inhibition in which rapid reversal of the polarity of synaptic

events occurs. Shunting inhibition consists of two temporal events. In the first event, GABA_A-mediated Cl⁻ conductance increases and this reduces membrane resistance and amplitude of excitatory postsynaptic potentials (EPSPs), decreasing the excitability of the postsynaptic cell and prevents it from firing. The membrane is held at subthreshold potential despite concurrent depolarization. In the second event, conductance decays but membrane potential remains depolarized. The postsynaptic cell reaches spike threshold and produces an action potential. In this way, an action potential occurs following a short delay in the presence of a tonic excitatory drive (Stein and Nicoll, 2003; Gullledge and Stuart, 2003). Shunting inhibition is activity-dependent. At high excitation levels, the first inhibitory event dominates, shifting the spike to a later time. However, at low excitation levels, the second excitatory event takes over and shortens the interspike interval (Vida et al., 2006). This allows interneurons to accelerate weakly activated neurons and decelerate strongly activated neurons, increasing the precision of spike time and homogenize firing rates even when the tonic drive to the interneuronal network is heterogeneous (Vida et al., 2006; Mann and Paulsen, 2006, 2007). In addition, synchronization of neuronal populations over longer distances can be achieved through region-spanning axon collaterals of principal cells or by a class of long-range interneurons. These interneurons possess axon trees that span brain regions and hemispheres. They may have a role in the synchronization of spatially distant multiple oscillators and timing of principal cells that are not connected directly with each other (Buzsaki and Chrobak, 1995; Bartos et al., 2007).

1.7 Vestibular system

The vestibular system is traditionally recognized as a system which stabilizes visual images by mechanisms that adjust the eyes (vestibulo-ocular reflex) and the body (vestibulospinal reflex). Damage results in vertigo, imbalance and nausea. The peripheral vestibular apparatus located in the inner ear consists of two otolith organs (utricle and saccule) and three semi-circular canals (anterior, horizontal and posterior canals) which contain receptors are sensitive to linear and angular acceleration of the head. They transmit signals to the vestibular nucleus complex in the brainstem where position, linear and angular velocity are computed (Raphan and Cohen, 2002).

In addition, the vestibular system plays an important role in spatial navigation and memory. Mittelstaedt and Mittelstaedt (1980) showed that mammals can keep track of their relative spatial location by integrating linear and angular motion, even in the absence of vision (path integration). The integration of vestibular signals is suggested to include the hippocampus, which is widely known to be involved in spatial navigation and memory (O'Keefe and Nadel, 1978; McNaughton et al., 1996). To navigate efficiently in an environment, mammals rely on external sensory (e.g. visual landmarks) and self-motion (idiothetic) cues (Etienne, 1992). Connected through several polysynaptic pathways such as the vestibulo-thalamocortical and the hypothalamus-septohippocampal pathway (Smith, 1997; Smith et al., 2005; Hübner et al., 2007) to the hippocampus, the vestibular system may provide self-motion cues to guide navigation, contributing to spatial information processing and the development of spatial memory in the hippocampus (Smith, 1997; Stackman et al., 2002; Russell et al., 2003). Vestibular lesioned rats displayed deficits in hippocampal-dependent spatial learning and memory

tasks such as radial arm maze (Matthews et al., 1989; Ossenkopp and Hargreaves, 1993), Morris water maze (Petrosini, 1984; Stackman and Herbert, 2002), and a food foraging task (Wallace et al., 2002; Zheng et al., 2009). Disruptions in location-specific firing of hippocampal place cells were reported following lesion and temporary inactivation of the vestibular apparatus (Stackman et al., 2002; Russell et al., 2003). Vestibular-damaged humans showed deficits in spatial memory (Hüfner et al., 2007; Guidetti et al., 2008; Hamann et al., 2009) and atrophy in the hippocampus (Brandt et al., 2005). Vestibular stimulation by passive rotation can alter the function of the hippocampus. During passive rotation, place fields of hippocampal neurons were modified in animals (Knierim et al., 1995; Wiener et al., 1995). Humans with unilateral hippocampal lesions showed errors in “vestibular working memory” in which they were unable to orientate themselves back to the initial position before rotation (Wiest et al., 1996).

1.8 Outline of thesis

The medial septum consists of cholinergic, GABAergic and glutamatergic cells that project to the hippocampus. Cholinergic input to the hippocampus, originating mainly from the medial septum (Mesulam et al., 1983; Nyakas et al., 1987), is particularly important for learning and memory (Kesner, 1988; Givens and Olton, 1990). Chapters 2 and 3 will focus on the role of cholinergic septohippocampal cells in hippocampal theta rhythm and synaptic plasticity during vestibular stimulation in freely behaving rats. Although the roles of GABAergic and glutamatergic cells are yet to be clearly defined, their projection patterns to the hippocampus suggest that they exhibit the potential to influence hippocampal activity. In Chapter 4, I will elucidate the contribution

of septal GABAergic cells to hippocampal activity by examining population and unit activity in urethane-anesthetized and behaving rats. These aims were achieved by the use of antibody/ligand conjugated to neurotoxin saporin, 192 IgG-saporin and orexin-saporin, to destroy cholinergic and GABAergic cells respectively.

The following specific hypotheses will be examined in this thesis:

1. It is hypothesized that a cholinergic, atropine-sensitive theta rhythm is generated during vestibular stimulation via passive whole-body rotation in freely behaving rats (Chapter 2).
2. It is hypothesized that septal cholinergic neurons are responsible for a rotation-induced modulation of hippocampal evoked potentials (Chapter 2).
3. It is hypothesized that passive whole-body rotation enhances LTP in CA1 of behaving rats (Chapter 3).
4. It is hypothesized that rotation-induced enhancement of LTP depends on the activation of septal cholinergic neurons (Chapter 3).
5. It is hypothesized that the septal GABAergic neurons are responsible for the facilitation of the dentate population spike following stimulation of PNO (Chapter 4).
6. It is hypothesized that the septal GABAergic cells help maintain granule cell excitability by inhibiting hippocampal interneurons (Chapter 4).

The thesis is concluded in the Chapter 5 with a general discussion of all the results and their implications.

1.9 References

- Alonso A, Gaztelu JM, Buno W Jr, Garcia-Austt E (1987) Cross-correlation analysis of septohippocampal neurons during theta-rhythm. *Brain Res* 413:135-146.
- Alonso A, Kohler C (1982) Evidence for separate projections of hippocampal pyramidal and non-pyramidal neurons to different parts of the septum in the rat brain. *Neurosci Lett* 31:209-214.
- Amaral DG, Kurz J (1985) An analysis of the origins of the cholinergic and noncholinergic septal projections to the hippocampal formation of the rat. *J Comp Neurol* 240:37-59.
- Arnolds DE, Lopes da Silva FH, Aitink JW, Kamp A (1979) Hippocampal EEG and behaviour in dog. I. Hippocampal EEG correlates of gross motor behaviour. *Electroencephalogr Clin Neurophysiol* 46:552-570.
- Auerbach JM, Segal M (1996) Muscarinic receptors mediating depression and long-term potentiation in rat hippocampus. *J Physiol* 492 (Pt 2):479-493.
- Bartos M, Vida I, Jonas P (2007) Synaptic mechanisms of synchronized gamma oscillations in inhibitory interneuron networks. *Nat Rev Neurosci* 8:45-56.
- Bartus RT, Dean RL 3rd, Beer B, Lippa AS (1982) The cholinergic hypothesis of geriatric memory dysfunction. *Science* 217:408-414.
- Behrends JC, ten Bruggencate G (1993) Cholinergic modulation of synaptic inhibition in the guinea pig hippocampus in vitro: excitation of GABAergic interneurons and inhibition of GABA-release. *J Neurophysiol* 69:626-629.
- Ben-Ari Y, Krnjevic K, Reinhardt W, Ropert N (1981) Intracellular observations on the disinhibitory action of acetylcholine in the hippocampus. *Neuroscience* 6:2475-2484.
- Benarroch EE (2007) GABAA receptor heterogeneity, function, and implications for epilepsy. *Neurology* 68:612-614.
- Bland BH (1986) The physiology and pharmacology of hippocampal formation theta rhythms. *Prog Neurobiol* 26:1-54.
- Bland BH, Colom LV, Konopacki J, Roth SH (1988) Intracellular records of carbachol-induced theta rhythm in hippocampal slices. *Brain Res* 447:364-368.

- Bland BH, Jackson J, Derrie-Gillespie D, Azad T, Rickhi A, Abriam J (2006) Amplitude, frequency, and phase analysis of hippocampal theta during sensorimotor processing in a jump avoidance task. *Hippocampus* 16:673-681.
- Bland BH, Konopacki J, Dyck R (2005) Heterogeneity among hippocampal pyramidal neurons revealed by their relation to theta-band oscillation and synchrony. *Exp Neurol* 195:458-474.
- Bland BH, Konopacki J, Dyck RH (2002) Relationship between membrane potential oscillations and rhythmic discharges in identified hippocampal theta-related cells. *J Neurophysiol* 88:3046-3066.
- Bland BH, Konopacki J, Kirk IJ, Oddie SD, Dickson CT (1995) Discharge patterns of hippocampal theta-related cells in the caudal diencephalon of the urethane-anesthetized rat. *J Neurophysiol* 74:322-333.
- Bland BH, Oddie SD (2001) Theta band oscillation and synchrony in the hippocampal formation and associated structures: the case for its role in sensorimotor integration. *Behav Brain Res* 127:119-136.
- Bliss TV, Collingridge GL (1993) A synaptic model of memory: long-term potentiation in the hippocampus. *Nature* 361:31-39.
- Blitzer RD, Gil O, Landau EM (1990) Cholinergic stimulation enhances long-term potentiation in the CA1 region of rat hippocampus. *Neurosci Lett* 119:207-210.
- Borhegyi Z, Varga V, Szilagyi N, Fabo D, Freund TF (2004) Phase segregation of medial septal GABAergic neurons during hippocampal theta activity. *J Neurosci* 24:8470-8479.
- Bragin A, Jando G, Nadasdy Z, Hetke J, Wise K, Buzsaki G (1995) Gamma (40-100 Hz) oscillation in the hippocampus of the behaving rat. *J Neurosci* 15:47-60.
- Brandt T, Schautzer F, Hamilton DA, Bruning R, Markowitsch HJ, Kalla R, Darlington C, Smith P, Strupp M (2005) Vestibular loss causes hippocampal atrophy and impaired spatial memory in humans. *Brain* 128:2732-2741.
- Brazhnik ES, Fox SE (1997) Intracellular recordings from medial septal neurons during hippocampal theta rhythm. *Exp Brain Res* 114:442-453.
- Brazhnik ES, Vinogradova OS (1986) Control of the neuronal rhythmic bursts in the septal pacemaker of theta-rhythm: effects of anaesthetic and anticholinergic drugs. *Brain Res* 380:94-106.
- Buzsaki G (2002) Theta oscillations in the hippocampus. *Neuron* 33:325-340.

- Buzsaki G (1984) Feed-forward inhibition in the hippocampal formation. *Prog Neurobiol* 22:131-153.
- Buzsaki G, Chrobak JJ (1995) Temporal structure in spatially organized neuronal ensembles: a role for interneuronal networks. *Curr Opin Neurobiol* 5:504-510.
- Buzsaki G, Czopf J, Kondakor I, Kellenyi L (1986) Laminar distribution of hippocampal rhythmic slow activity (RSA) in the behaving rat: current-source density analysis, effects of urethane and atropine. *Brain Res* 365:125-137.
- Buzsaki G, Leung LW, Vanderwolf CH (1983) Cellular bases of hippocampal EEG in the behaving rat. *Brain Res* 287:139-171.
- Clugnet MC, LeDoux JE (1990) Synaptic plasticity in fear conditioning circuits: induction of LTP in the lateral nucleus of the amygdala by stimulation of the medial geniculate body. *J Neurosci* 10:2818-2824.
- Colgin LL, Denninger T, Fyhn M, Hafting T, Bonnevie T, Jensen O, Moser MB, Moser EI (2009) Frequency of gamma oscillations routes flow of information in the hippocampus. *Nature* 462:353-357.
- Colgin LL, Moser EI (2010) Gamma oscillations in the hippocampus. *Physiology (Bethesda)* 25:319-329.
- Colgin LL, Moser EI (2009) Hippocampal theta rhythms follow the beat of their own drum. *Nat Neurosci* 12:1483-1484.
- Colom LV (2006) Septal networks: relevance to theta rhythm, epilepsy and Alzheimer's disease. *J Neurochem* 96:609-623.
- Colom LV, Bland BH (1987) State-dependent spike train dynamics of hippocampal formation neurons: evidence for theta-on and theta-off cells. *Brain Res* 422:277-286.
- Colom LV, Castaneda MT, Reyna T, Hernandez S, Garrido-Sanabria E (2005) Characterization of medial septal glutamatergic neurons and their projection to the hippocampus. *Synapse* 58:151-164.
- Cornwell BR, Johnson LL, Holroyd T, Carver FW, Grillon C (2008) Human hippocampal and parahippocampal theta during goal-directed spatial navigation predicts performance on a virtual Morris water maze. *J Neurosci* 28:5983-5990.
- Couve A, Moss SJ, Pangalos MN (2000) GABAB receptors: a new paradigm in G protein signaling. *Mol Cell Neurosci* 16:296-312.
- Crill WE (1996) Persistent sodium current in mammalian central neurons. *Annu Rev Physiol* 58:349-362.

- Csicsvari J, Hirase H, Czurko A, Buzsaki G (1998) Reliability and state dependence of pyramidal cell-interneuron synapses in the hippocampus: an ensemble approach in the behaving rat. *Neuron* 21:179-189.
- Csicsvari J, Jamieson B, Wise KD, Buzsaki G (2003) Mechanisms of gamma oscillations in the hippocampus of the behaving rat. *Neuron* 37:311-322.
- Delong MR (2000) The basal ganglia. In: *Principles of neural science*, 4th edition (Kandel ER, Schwartz JH, Jessell TM eds), pp 853-872. New York: McGraw-Hill, Health Professions Division.
- Dickson CT (2010) Ups and downs in the hippocampus: the influence of oscillatory sleep states on "neuroplasticity" at different time scales. *Behav Brain Res* 214:35-41.
- Doralp S, Leung LS (2008) Cholinergic modulation of hippocampal CA1 basal-dendritic long-term potentiation. *Neurobiol Learn Mem* 90:382-388.
- Dudar JD, Whishaw IQ, Szerb JC (1979) Release of acetylcholine from the hippocampus of freely moving rats during sensory stimulation and running. *Neuropharmacology* 18:673-678.
- Dutar P, Bassant MH, Senut MC, Lamour Y (1995) The septohippocampal pathway: structure and function of a central cholinergic system. *Physiol Rev* 75:393-427.
- Dybvik AT, Bland BH (2004) Functional connectivity between the red nucleus and the hippocampus supports the role of hippocampal formation in sensorimotor integration. *J Neurophysiol* 92:2040-2050.
- Ekstrom AD, Caplan JB, Ho E, Shattuck K, Fried I, Kahana MJ (2005) Human hippocampal theta activity during virtual navigation. *Hippocampus* 15:881-889.
- Ekstrom AD, Kahana MJ, Caplan JB, Fields TA, Isham EA, Newman EL, Fried I (2003) Cellular networks underlying human spatial navigation. *Nature* 425:184-188.
- Etienne AS (1992) Navigation of a small animal by dead reckoning and local cues. *Curr Dir Psych Sci* 1:48-52.
- Fabian-Fine R, Skehel P, Errington ML, Davies HA, Sher E, Stewart MG, Fine A (2001) Ultrastructural distribution of the alpha7 nicotinic acetylcholine receptor subunit in rat hippocampus. *J Neurosci* 21:7993-8003.
- Fox SE, Ranck JB Jr (1981) Electrophysiological characteristics of hippocampal complex-spike cells and theta cells. *Exp Brain Res* 41:399-410.

- Fox SE, Ranck JB, Jr (1975) Localization and anatomical identification of theta and complex spike cells in dorsal hippocampal formation of rats. *Exp Neurol* 49:299-313.
- Francis PT, Palmer AM, Snape M, Wilcock GK (1999) The cholinergic hypothesis of Alzheimer's disease: a review of progress. *J Neurol Neurosurg Psychiatry* 66:137-147.
- Freund TF, Antal M (1988) GABA-containing neurons in the septum control inhibitory interneurons in the hippocampus. *Nature* 336:170-173.
- Freund TF, Buzsaki G (1996) Interneurons of the hippocampus. *Hippocampus* 6:347-470.
- Frey S, Bergado JA, Frey JU (2003) Modulation of late phases of long-term potentiation in rat dentate gyrus by stimulation of the medial septum. *Neuroscience* 118:1055-1062.
- Gaykema RP, Luiten PG, Nyakas C, Traber J (1990) Cortical projection patterns of the medial septum-diagonal band complex. *J Comp Neurol* 293:103-124.
- Gaykema RP, van der Kuil J, Hersh LB, Luiten PG (1991) Patterns of direct projections from the hippocampus to the medial septum-diagonal band complex: anterograde tracing with Phaseolus vulgaris leucoagglutinin combined with immunohistochemistry of choline acetyltransferase. *Neuroscience* 43:349-360.
- Gillies MJ, Traub RD, LeBeau FE, Davies CH, Gloveli T, Buhl EH, Whittington MA (2002) A model of atropine-resistant theta oscillations in rat hippocampal area CA1. *J Physiol* 543:779-793.
- Givens BS, Olton DS (1990) Cholinergic and GABAergic modulation of medial septal area: effect on working memory. *Behav Neurosci* 104:849-855.
- Goutagny R, Jackson J, Williams S (2009) Self-generated theta oscillations in the hippocampus. *Nat Neurosci* 12:1491-1493.
- Goutagny R, Manseau F, Jackson J, Danik M, Williams S (2008) In vitro activation of the medial septum-diagonal band complex generates atropine-sensitive and atropine-resistant hippocampal theta rhythm: an investigation using a complete septohippocampal preparation. *Hippocampus* 18:531-535.
- Green JD, Arduini AA (1954) Hippocampal electrical activity in arousal. *J Neurophysiol* 17:533-557.
- Guidetti G, Monzani D, Trebbi M, Rovatti V (2008) Impaired navigation skills in patients with psychological distress and chronic peripheral vestibular hypofunction without vertigo. *Acta Otorhinolaryngol Ital* 28:21-25.

- Gulledge AT, Stuart GJ (2003) Excitatory actions of GABA in the cortex. *Neuron* 37:299-309.
- Hallworth NE, Bland BH (2004) Basal ganglia--hippocampal interactions support the role of the hippocampal formation in sensorimotor integration. *Exp Neurol* 188:430-443.
- Hamann KF, Weiss U, Ruile A (2009) Effects of acute vestibular lesions on visual orientation and spatial memory, shown for the visual straight ahead. *Ann N Y Acad Sci* 1164:305-308.
- Hasselmo ME, Bodelon C, Wyble BP (2002) A proposed function for hippocampal theta rhythm: separate phases of encoding and retrieval enhance reversal of prior learning. *Neural Comput* 14:793-817.
- He J, Deng CY, Chen RZ, Zhu XN, Yu JP (2000) Long-term potentiation induced by nicotine in CA1 region of hippocampal slice is Ca(2+)-dependent. *Acta Pharmacol Sin* 21:429-432.
- Henschel O, Gipson KE, Bordey A (2008) GABAA receptors, anesthetics and anticonvulsants in brain development. *CNS Neurol Disord Drug Targets* 7:211-224.
- Herreras O, Solis JM, Herranz AS, Martin del Rio R, Lerma J (1988a) Sensory modulation of hippocampal transmission. II. Evidence for a cholinergic locus of inhibition in the Schaffer-CA1 synapse. *Brain Res* 461:303-313.
- Herreras O, Solis JM, Munoz MD, Martin del Rio R, Lerma J (1988b) Sensory modulation of hippocampal transmission. I. Opposite effects on CA1 and dentate gyrus synapses. *Brain Res* 461:290-302.
- Hinman JR, Penley SC, Long LL, Escabi MA, Chrobak JJ (2011) Septotemporal variation in dynamics of theta: speed and habituation. *J Neurophysiol*
- Holscher C, Anwyl R, Rowan MJ (1997) Stimulation on the positive phase of hippocampal theta rhythm induces long-term potentiation that can be depotentiated by stimulation on the negative phase in area CA1 in vivo. *J Neurosci* 17:6470-6477.
- Hu H, Vervaeke K, Graham LJ, Storm JF (2009) Complementary theta resonance filtering by two spatially segregated mechanisms in CA1 hippocampal pyramidal neurons. *J Neurosci* 29:14472-14483.
- Hu H, Vervaeke K, Storm JF (2007) M-channels (Kv7/KCNQ channels) that regulate synaptic integration, excitability, and spike pattern of CA1 pyramidal cells are located in the perisomatic region. *J Neurosci* 27:1853-1867.

- Hu H, Vervaeke K, Storm JF (2002) Two forms of electrical resonance at theta frequencies, generated by M-current, h-current and persistent Na⁺ current in rat hippocampal pyramidal cells. *J Physiol* 545:783-805.
- Huerta PT, Lisman JE (1996) Low-frequency stimulation at the troughs of theta-oscillation induces long-term depression of previously potentiated CA1 synapses. *J Neurophysiol* 75:877-884.
- Huerta PT, Lisman JE (1995) Bidirectional synaptic plasticity induced by a single burst during cholinergic theta oscillation in CA1 in vitro. *Neuron* 15:1053-1063.
- Hufner K, Hamilton DA, Kalla R, Stephan T, Glasauer S, Ma J, Bruning R, Markowitsch HJ, Labudda K, Schichor C, Strupp M, Brandt T (2007) Spatial memory and hippocampal volume in humans with unilateral vestibular deafferentation. *Hippocampus* 17:471-485.
- Huh CY, Goutagny R, Williams S (2010) Glutamatergic neurons of the mouse medial septum and diagonal band of Broca synaptically drive hippocampal pyramidal cells: relevance for hippocampal theta rhythm. *J Neurosci* 30:15951-15961.
- Hutcheon B, Yarom Y (2000) Resonance, oscillation and the intrinsic frequency preferences of neurons. *Trends Neurosci* 23:216-222.
- Huxter J, Burgess N, O'Keefe J (2003) Independent rate and temporal coding in hippocampal pyramidal cells. *Nature* 425:828-832.
- Hyman JM, Wyble BP, Goyal V, Rossi CA, Hasselmo ME (2003) Stimulation in hippocampal region CA1 in behaving rats yields long-term potentiation when delivered to the peak of theta and long-term depression when delivered to the trough. *J Neurosci* 23:11725-11731.
- Jensen O, Lisman JE (2000) Position reconstruction from an ensemble of hippocampal place cells: contribution of theta phase coding. *J Neurophysiol* 83:2602-2609.
- Jiang F, Khanna S (2004) Reticular stimulation evokes suppression of CA1 synaptic responses and generation of theta through separate mechanisms. *Eur J Neurosci* 19:295-308.
- Joels M, Urban IJ (1984) Electrophysiological and pharmacological evidence in favor of amino acid neurotransmission in fimbria-fornix fibers innervating the lateral septal complex of rats. *Exp Brain Res* 54:455-462.
- Kandel ER, Spencer WA (1961) Electrophysiology of hippocampal neurons. II. Afterpotentials and repetitive firing. *J Neurophysiol* 24:243-259.

- Kesner RP (1988) Reevaluation of the contribution of the basal forebrain cholinergic system to memory. *Neurobiol Aging* 9:609-616.
- Khanna S (1997) Dorsal hippocampus field CA1 pyramidal cell responses to a persistent versus an acute nociceptive stimulus and their septal modulation. *Neuroscience* 77:713-721.
- Kirk IJ, McNaughton N (1991) Supramammillary cell firing and hippocampal rhythmical slow activity. *Neuroreport* 2:723-725.
- Kiss J, Patel AJ, Freund TF (1990) Distribution of septohippocampal neurons containing parvalbumin or choline acetyltransferase in the rat brain. *J Comp Neurol* 298:362-372.
- Knierim JJ, Kudrimoti HS, McNaughton BL (1995) Place cells, head direction cells, and the learning of landmark stability. *J Neurosci* 15:1648-1659.
- Kocsis B, Li S (2004) In vivo contribution of h-channels in the septal pacemaker to theta rhythm generation. *Eur J Neurosci* 20:2149-2158.
- Kocsis B, Vertes RP (1997) Phase relations of rhythmic neuronal firing in the supramammillary nucleus and mammillary body to the hippocampal theta activity in urethane anesthetized rats. *Hippocampus* 7:204-214.
- Kohler C, Chan-Palay V, Wu JY (1984) Septal neurons containing glutamic acid decarboxylase immunoreactivity project to the hippocampal region in the rat brain. *Anat Embryol (Berl)* 169:41-44.
- Konopacki J, MacIver MB, Bland BH, Roth SH (1987) Carbachol-induced EEG 'theta' activity in hippocampal brain slices. *Brain Res* 405:196-198.
- Kramis R, Vanderwolf CH, Bland BH (1975) Two types of hippocampal rhythmical slow activity in both the rabbit and the rat: relations to behavior and effects of atropine, diethyl ether, urethane, and pentobarbital. *Exp Neurol* 49:58-85.
- Krnjevic K, Reiffenstein RJ, Ropert N (1981) Disinhibitory action of acetylcholine in the rat's hippocampus: extracellular observations. *Neuroscience* 6:2465-2474.
- Kuchler M, Fouad K, Weinmann O, Schwab ME, Raineteau O (2002) Red nucleus projections to distinct motor neuron pools in the rat spinal cord. *J Comp Neurol* 448:349-359.
- Lancaster B, Adams PR (1986) Calcium-dependent current generating the afterhyperpolarization of hippocampal neurons. *J Neurophysiol* 55:1268-1282.

- Lancaster B, Nicoll RA (1987) Properties of two calcium-activated hyperpolarizations in rat hippocampal neurones. *J Physiol* 389:187-203.
- Lanzafame AA, Christopoulos A, Mitchelson F (2003) Cellular signaling mechanisms for muscarinic acetylcholine receptors. *Receptors Channels* 9:241-260.
- Lawson VH, Bland BH (1993) The role of the septohippocampal pathway in the regulation of hippocampal field activity and behavior: analysis by the intraseptal microinfusion of carbachol, atropine, and procaine. *Exp Neurol* 120:132-144.
- Lee MG, Chrobak JJ, Sik A, Wiley RG, Buzsaki G (1994) Hippocampal theta activity following selective lesion of the septal cholinergic system. *Neuroscience* 62:1033-1047.
- Lega BC, Jacobs J, Kahana M (2011) Human hippocampal theta oscillations and the formation of episodic memories. *Hippocampus*
- Leranth C, Frotscher M (1987) Cholinergic innervation of hippocampal GAD- and somatostatin-immunoreactive commissural neurons. *J Comp Neurol* 261:33-47.
- Leung LS (1998) Generation of theta and gamma rhythms in the hippocampus. *Neurosci Biobehav Rev* 22:275-290.
- Leung LS (1984) Pharmacology of theta phase shift in the hippocampal CA1 region of freely moving rats. *Electroencephalogr Clin Neurophysiol* 58:457-466.
- Leung LS, Peloquin P (2010) Cholinergic modulation differs between basal and apical dendritic excitation of hippocampal CA1 pyramidal cells. *Cereb Cortex* 20:1865-1877.
- Leung LS, Shen B, Rajakumar N, Ma J (2003) Cholinergic activity enhances hippocampal long-term potentiation in CA1 during walking in rats. *J Neurosci* 23:9297-9304.
- Leung LW (1987) Hippocampal electrical activity following local tetanization. I. Afterdischarges. *Brain Res* 419:173-187.
- Leung LW, Borst JG (1987) Electrical activity of the cingulate cortex. I. Generating mechanisms and relations to behavior. *Brain Res* 407:68-80.
- Leung LW, Lopes da Silva FH, Wadman WJ (1982) Spectral characteristics of the hippocampal EEG in the freely moving rat. *Electroencephalogr Clin Neurophysiol* 54:203-219.
- Leung LW, Yim CY (1991) Intrinsic membrane potential oscillations in hippocampal neurons in vitro. *Brain Res* 553:261-274.

- Li S, Topchiy I, Kocsis B (2007) The effect of atropine administered in the medial septum or hippocampus on high- and low-frequency theta rhythms in the hippocampus of urethane anesthetized rats. *Synapse* 61:412-419.
- Lisman JE (1997) Bursts as a unit of neural information: making unreliable synapses reliable. *Trends Neurosci* 20:38-43.
- Lopes da Silva FH, Witter MP, Boeijinga PH, Lohman AH (1990) Anatomic organization and physiology of the limbic cortex. *Physiol Rev* 70:453-511.
- Lynch G, Rose G, Gall C (1977) Anatomical and functional aspects of the septo-hippocampal projections. *Ciba Found Symp* (58):5-24.
- Mann EO, Paulsen O (2007) Role of GABAergic inhibition in hippocampal network oscillations. *Trends Neurosci* 30:343-349.
- Mann EO, Paulsen O (2006) Keeping inhibition timely. *Neuron* 49:8-9.
- Manns ID, Alonso A, Jones BE (2003) Rhythmically discharging basal forebrain units comprise cholinergic, GABAergic, and putative glutamatergic cells. *J Neurophysiol* 89:1057-1066.
- Markevich V, Scorsa AM, Dawe GS, Stephenson JD (1997) Cholinergic facilitation and inhibition of long-term potentiation of CA1 in the urethane-anaesthetized rats. *Brain Res* 754:95-102.
- Matthews BL, Ryu JH, Bockaneck C (1989) Vestibular contribution to spatial orientation. Evidence of vestibular navigation in an animal model. *Acta Otolaryngol Suppl* 468:149-154.
- McFarland WL, Teitelbaum H, Hedges EK (1975) Relationship between hippocampal theta activity and running speed in the rat. *J Comp Physiol Psychol* 88:324-328.
- McKinney M, Coyle JT, Hedreen JC (1983) Topographic analysis of the innervation of the rat neocortex and hippocampus by the basal forebrain cholinergic system. *J Comp Neurol* 217:103-121.
- McNaughton BL, Barnes CA, Gerrard JL, Gothard K, Jung MW, Knierim JJ, Kudrimoti H, Qin Y, Skaggs WE, Suster M, Weaver KL (1996) Deciphering the hippocampal polyglot: the hippocampus as a path integration system. *J Exp Biol* 199:173-185.
- Meibach RC, Siegel A (1977) Efferent connections of the septal area in the rat: an analysis utilizing retrograde and anterograde transport methods. *Brain Res* 119:1-20.

- Mesulam MM, Mufson EJ, Wainer BH, Levey AI (1983) Central cholinergic pathways in the rat: an overview based on an alternative nomenclature (Ch1-Ch6). *Neuroscience* 10:1185-1201.
- Metz AE, Jarsky T, Martina M, Spruston N (2005) R-type calcium channels contribute to afterdepolarization and bursting in hippocampal CA1 pyramidal neurons. *J Neurosci* 25:5763-5773.
- Milner TA, Amaral DG (1984) Evidence for a ventral septal projection to the hippocampal formation of the rat. *Exp Brain Res* 55:579-585.
- Mittelstaedt ML, Mittelstaedt H (1980) Homing by path integration in a mammal. *Naturewissenschaften* 67:556-567.
- Mizumori SJ, McNaughton BL, Barnes CA, Fox KB (1989) Preserved spatial coding in hippocampal CA1 pyramidal cells during reversible suppression of CA3c output: evidence for pattern completion in hippocampus. *J Neurosci* 9:3915-3928.
- Muir GD, Whishaw IQ (2000) Red nucleus lesions impair overground locomotion in rats: a kinetic analysis. *Eur J Neurosci* 12:1113-1122.
- Muller R (1996) A quarter of a century of place cells. *Neuron* 17:813-822.
- Nai Q, McIntosh JM, Margiotta JF (2003) Relating neuronal nicotinic acetylcholine receptor subtypes defined by subunit composition and channel function. *Mol Pharmacol* 63:311-324.
- Natsume K, Hallworth NE, Szgatti TL, Bland BH (1999) Hippocampal theta-related cellular activity in the superior colliculus of the urethane-anesthetized rat. *Hippocampus* 9:500-509.
- Nunez A, de Andres I, Garcia-Austt E (1991) Relationships of nucleus reticularis pontis oralis neuronal discharge with sensory and carbachol evoked hippocampal theta rhythm. *Exp Brain Res* 87:303-308.
- Nyakas C, Luiten PG, Spencer DG, Traber J (1987) Detailed projection patterns of septal and diagonal band efferents to the hippocampus in the rat with emphasis on innervation of CA1 and dentate gyrus. *Brain Res Bull* 18:533-545.
- Oddie SD, Bland BH (1998) Hippocampal formation theta activity and movement selection. *Neurosci Biobehav Rev* 22:221-231.
- O'Keefe J (1976) Place units in the hippocampus of the freely moving rat. *Exp Neurol* 51:78-109.

- O'Keefe J, Dostrovsky J (1971) The hippocampus as a spatial map. Preliminary evidence from unit activity in the freely-moving rat. *Brain Res* 34:171-175.
- O'Keefe J, Recce ML (1993) Phase relationship between hippocampal place units and the EEG theta rhythm. *Hippocampus* 3:317-330.
- O'Keefe J, Nadel L, (1978) *The hippocampus as a cognitive map*. pp 570. Oxford: Clarendon Press ;.
- Orr G, Rao G, Houston FP, McNaughton BL, Barnes CA (2001) Hippocampal synaptic plasticity is modulated by theta rhythm in the fascia dentata of adult and aged freely behaving rats. *Hippocampus* 11:647-654.
- Ossenkopp KP, Hargreaves EL (1993) Spatial learning in an enclosed eight-arm radial maze in rats with sodium arsenite-induced labyrinthectomies. *Behav Neural Biol* 59:253-257.
- Otto T, Eichenbaum H, Wiener SI, Wible CG (1991) Learning-related patterns of CA1 spike trains parallel stimulation parameters optimal for inducing hippocampal long-term potentiation. *Hippocampus* 1:181-192.
- Ovsepian SV, Anwyl R, Rowan MJ (2004) Endogenous acetylcholine lowers the threshold for long-term potentiation induction in the CA1 area through muscarinic receptor activation: in vivo study. *Eur J Neurosci* 20:1267-1275.
- Pang KC, Nocera R, Secor AJ, Yoder RM (2001) GABAergic septohippocampal neurons are not necessary for spatial memory. *Hippocampus* 11:814-827.
- Pavlidis C, Greenstein YJ, Grudman M, Winson J (1988) Long-term potentiation in the dentate gyrus is induced preferentially on the positive phase of theta-rhythm. *Brain Res* 439:383-387.
- Pedemonte M, Pena JL, Velluti RA (1996) Firing of inferior colliculus auditory neurons is phase-locked to the hippocampus theta rhythm during paradoxical sleep and waking. *Exp Brain Res* 112:41-46.
- Petrosini L (1984) Task-dependent rate of recovery from hemilabyrinthectomy: an analysis of swimming and locomotor performances. *Physiol Behav* 33:799-804.
- Petsche H, Stumpf C, Gogolak G (1962) The significance of the rabbit's septum as a relay station between the midbrain and the hippocampus. I. The control of hippocampus arousal activity by the septum cells. *Electroencephalogr Clin Neurophysiol* 14:202-211.

- Pike FG, Meredith RM, Olding AW, Paulsen O (1999) Rapid report: postsynaptic bursting is essential for 'Hebbian' induction of associative long-term potentiation at excitatory synapses in rat hippocampus. *J Physiol* 518 (Pt 2):571-576.
- Ranck JB,Jr (1973) Studies on single neurons in dorsal hippocampal formation and septum in unrestrained rats. I. Behavioral correlates and firing repertoires. *Exp Neurol* 41:461-531.
- Raphan T, Cohen B (2002) The vestibulo-ocular reflex in three dimensions. *Exp Brain Res* 145:1-27.
- Rashidy-Pour A, Motamedi F, Semnanian S, Zarrindast MR, Fatollahi Y, Behzadi G (1996) Effects of reversible inactivation of the medial septal area on long-term potentiation and recurrent inhibition of hippocampal population spikes in rats. *Brain Res* 734:43-48.
- Risold PY, (2004) The septal region. In: *The rat nervous system*, 3rd edition (Paxinos G ed),Amsterdam, Boston: Elsevier Academic Press.
- Risold PY, Swanson LW (1997) Connections of the rat lateral septal complex. *Brain Res Brain Res Rev* 24:115-195.
- Rivas J, Gaztelu JM, Garcia-Austt E (1996) Changes in hippocampal cell discharge patterns and theta rhythm spectral properties as a function of walking velocity in the guinea pig. *Exp Brain Res* 108:113-118.
- Russell NA, Horii A, Smith PF, Darlington CL, Bilkey DK (2003) Long-term effects of permanent vestibular lesions on hippocampal spatial firing. *J Neurosci* 23:6490-6498.
- Sabatino M, Ferraro G, Liberti G, Vella N, La Grutta V (1985) Striatal and septal influence on hippocampal theta and spikes in the cat. *Neurosci Lett* 61:55-59.
- Sabatino M, La Grutta V, Ferraro G, La Grutta G (1986) Relations between basal ganglia and hippocampus: action of substantia nigra and pallidum. *Rev Electroencephalogr Neurophysiol Clin* 16:179-190.
- Sainsbury RS, Heynen A, Montoya CP (1987) Behavioral correlates of hippocampal type 2 theta in the rat. *Physiol Behav* 39:513-519.
- Saper CB (1984) Organization of cerebral cortical afferent systems in the rat. II. Magnocellular basal nucleus. *J Comp Neurol* 222:313-342.
- Seidenbecher T, Laxmi TR, Stork O, Pape HC (2003) Amygdalar and hippocampal theta rhythm synchronization during fear memory retrieval. *Science* 301:846-850.

- Sharma AV, Wolansky T, Dickson CT (2010) A comparison of sleeplike slow oscillations in the hippocampus under ketamine and urethane anesthesia. *J Neurophysiol* 104:932-939.
- Shimoshige Y, Maeda T, Kaneko S, Akaike A, Satoh M (1997) Involvement of M2 receptor in an enhancement of long-term potentiation by carbachol in Schaffer collateral-CA1 synapses of hippocampal slices. *Neurosci Res* 27:175-180.
- Simon AP, Poindessous-Jazat F, Dutar P, Epelbaum J, Bassant MH (2006) Firing properties of anatomically identified neurons in the medial septum of anesthetized and unanesthetized restrained rats. *J Neurosci* 26:9038-9046.
- Skaggs WE, McNaughton BL, Wilson MA, Barnes CA (1996) Theta phase precession in hippocampal neuronal populations and the compression of temporal sequences. *Hippocampus* 6:149-172.
- Smith PF (1997) Vestibular-hippocampal interactions. *Hippocampus* 7:465-471.
- Smith PF, Horii A, Russell N, Bilkey DK, Zheng Y, Liu P, Kerr DS, Darlington CL (2005) The effects of vestibular lesions on hippocampal function in rats. *Prog Neurobiol* 75:391-405.
- Soltesz I, Deschenes M (1993) Low- and high-frequency membrane potential oscillations during theta activity in CA1 and CA3 pyramidal neurons of the rat hippocampus under ketamine-xylazine anesthesia. *J Neurophysiol* 70:97-116.
- Sotty F, Danik M, Manseau F, Laplante F, Quirion R, Williams S (2003) Distinct electrophysiological properties of glutamatergic, cholinergic and GABAergic rat septohippocampal neurons: novel implications for hippocampal rhythmicity. *J Physiol* 551:927-943.
- Stackman RW, Clark AS, Taube JS (2002) Hippocampal spatial representations require vestibular input. *Hippocampus* 12:291-303.
- Stackman RW, Herbert AM (2002) Rats with lesions of the vestibular system require a visual landmark for spatial navigation. *Behav Brain Res* 128:27-40.
- Stein V, Nicoll RA (2003) GABA generates excitement. *Neuron* 37:375-378.
- Stewart M, Fox SE (1989) Detection of an atropine-resistant component of the hippocampal theta rhythm in urethane-anesthetized rats. *Brain Res* 500:55-60.
- Swanson LW, Cowan WM (1977) An autoradiographic study of the organization of the efferent connections of the hippocampal formation in the rat. *J Comp Neurol* 172:49-84.

- Tai SK, Ma J, Ossenkopp KP, Leung LS (2011) Activation of immobility-related hippocampal theta by cholinergic septohippocampal neurons during vestibular stimulation. *Hippocampus* doi: 10.1002/hipo.20955.
- Takano Y, Hanada Y (2009) The driving system for hippocampal theta in the brainstem: an examination by single neuron recording in urethane-anesthetized rats. *Neurosci Lett* 455:65-69.
- Teyler TJ, Fountain SB (1987) Neuronal plasticity in the mammalian brain: relevance to behavioral learning and memory. *Child Dev* 58:698-712.
- Thomas MJ, Watabe AM, Moody TD, Makhinson M, O'Dell TJ (1998) Postsynaptic complex spike bursting enables the induction of LTP by theta frequency synaptic stimulation. *J Neurosci* 18:7118-7126.
- Vanderwolf CH (1988) Cerebral activity and behavior: control by central cholinergic and serotonergic systems. *Int Rev Neurobiol* 30:225-340.
- Vanderwolf CH (1975) Neocortical and hippocampal activation relation to behavior: effects of atropine, eserine, phenothiazines, and amphetamine. *J Comp Physiol Psychol* 88:300-323.
- Vanderwolf CH (1969) Hippocampal electrical activity and voluntary movement in the rat. *Electroencephalogr Clin Neurophysiol* 26:407-418.
- Vertes RP, Colom LV, Fortin WJ, Bland BH (1993) Brainstem sites for the carbachol elicitation of the hippocampal theta rhythm in the rat. *Exp Brain Res* 96:419-429.
- Vertes RP, Hoover WB, Viana Di Prisco G (2004) Theta rhythm of the hippocampus: subcortical control and functional significance. *Behav Cogn Neurosci Rev* 3:173-200.
- Vertes RP, Kocsis B (1997) Brainstem-diencephalo-septohippocampal systems controlling the theta rhythm of the hippocampus. *Neuroscience* 81:893-926.
- Vida I, Bartos M, Jonas P (2006) Shunting inhibition improves robustness of gamma oscillations in hippocampal interneuron networks by homogenizing firing rates. *Neuron* 49:107-117.
- Volpicelli LA, Levey AI (2004) Muscarinic acetylcholine receptor subtypes in cerebral cortex and hippocampus. *Prog Brain Res* 145:59-66.
- Wallace DG, Hines DJ, Pellis SM, Whishaw IQ (2002) Vestibular information is required for dead reckoning in the rat. *J Neurosci* 22:10009-10017.

- Watrous AJ, Fried I, Ekstrom AD (2011) Behavioral correlates of human hippocampal delta and theta oscillations during navigation. *J Neurophysiol* 105:1747-1755.
- Welsby P, Rowan M, Anwyl R (2006) Nicotinic receptor-mediated enhancement of long-term potentiation involves activation of metabotropic glutamate receptors and ryanodine-sensitive calcium stores in the dentate gyrus. *Eur J Neurosci* 24:3109-3118.
- Welsby PJ, Rowan MJ, Anwyl R (2009) Intracellular mechanisms underlying the nicotinic enhancement of LTP in the rat dentate gyrus. *Eur J Neurosci* 29:65-75.
- Wenk GL (2006) Neuropathologic changes in Alzheimer's disease: potential targets for treatment. *J Clin Psychiatry* 67 Suppl 3:3-7; quiz 23.
- Whishaw IQ (1976) Neuromuscular blockade: the effects on two hippocampal RSA (theta) systems and neocortical desynchronization. *Brain Res Bull* 1:573-581.
- Whishaw IQ, Vanderwolf CH (1973) Hippocampal EEG and behavior: changes in amplitude and frequency of RSA (theta rhythm) associated with spontaneous and learned movement patterns in rats and cats. *Behav Biol* 8:461-484.
- Wiener SI, Korshunov VA, Garcia R, Berthoz A (1995) Inertial, substratal and landmark cue control of hippocampal CA1 place cell activity. *Eur J Neurosci* 7:2206-2219.
- Wiest G, Baumgartner C, Deecke L, Olbrich A, Steinhoff N, Müller C (1996) Effects of hippocampal lesions on vestibular memory in whole-body rotation. *Journal of Vestibular Research* 6:S17-S17.
- Wolansky T, Clement EA, Peters SR, Palczak MA, Dickson CT (2006) Hippocampal slow oscillation: a novel EEG state and its coordination with ongoing neocortical activity. *J Neurosci* 26:6213-6229.
- Wong RK, Prince DA (1978) Participation of calcium spikes during intrinsic burst firing in hippocampal neurons. *Brain Res* 159:385-390.
- Wu CK, Thal L, Pizzo D, Hansen L, Masliah E, Geula C (2005) Apoptotic signals within the basal forebrain cholinergic neurons in Alzheimer's disease. *Exp Neurol* 195:484-496.
- Yoder RM, Pang KC (2005) Involvement of GABAergic and cholinergic medial septal neurons in hippocampal theta rhythm. *Hippocampus* 15:381-392.
- Yu JP, He J, Liu D, Deng CY, Zhu XN, Wang XL, Wang Y, Chen RZ (2007) Noradrenaline release by activation of kappa-bungarotoxin-sensitive nicotinic acetylcholine receptors participates in long-term potentiation-like response induced by nicotine. *Sheng Li Xue Bao* 59:814-820.

- Yue C, Remy S, Su H, Beck H, Yaari Y (2005) Proximal persistent Na⁺ channels drive spike afterdepolarizations and associated bursting in adult CA1 pyramidal cells. *J Neurosci* 25:9704-9720.
- Zheng F, Khanna S (2001) Selective destruction of medial septal cholinergic neurons attenuates pyramidal cell suppression, but not excitation in dorsal hippocampus field CA1 induced by subcutaneous injection of formalin. *Neuroscience* 103:985-998.
- Zheng Y, Goddard M, Darlington CL, Smith PF (2009) Long-term deficits on a foraging task after bilateral vestibular deafferentation in rats. *Hippocampus* 19:480-486.

Chapter 2

Activation of Immobility-related Hippocampal Theta by Cholinergic Septohippocampal Neurons during Vestibular Stimulation[♦]

2.1 Introduction

The vestibular apparatus is traditionally recognized as a system which stabilizes visual images by mechanisms that adjust the eyes (vestibulo-ocular reflex) and the body (vestibulospinal reflex). Damage results in vertigo, imbalance and nausea. Receptors in the semi-circular canals and otolith organs are sensitive to angular and linear acceleration of the head respectively, providing signals to the vestibular nucleus complex in the brainstem where the position, linear and angular velocity are computed (Raphan and Cohen, 2002).¹

In addition, the vestibular system plays an essential role in spatial navigation and memory. A seminal paper by Mittelstaedt and Mittelstaedt (1980) showed that mammals can keep track of relative spatial location by integrating linear and angular motion (path integration). The integration of vestibular signals is suggested to include the hippocampus, which is widely known to be involved in spatial navigation and memory (O'Keefe and Nadel, 1978; McNaughton et al., 1996; Stackman et al., 2002). Animal

[♦] Data presented in this chapter has been published as: Tai S.K., Ma J., Ossenkopp K-P. and Leung L.S. (2011) Activation of immobility-related hippocampal theta by cholinergic septohippocampal neurons during vestibular stimulation. *Hippocampus* doi: 10.1002/hipo.20955.

studies have showed that damage to the vestibular system produces deficits in hippocampal-dependent spatial learning and memory tasks such as radial arm maze (Matthews et al., 1989; Ossenkopp and Hargreaves, 1993), Morris water maze (Petrosini, 1984; Stackman and Herbert, 2002), and a food foraging task (Wallace et al., 2002; Zheng et al., 2009). Moreover, vestibular-damaged humans displayed spatial memory deficits (Hüfner et al., 2007; Guidetti et al., 2008; Hamann et al., 2009) and a substantial (16.9%) decrease in hippocampal volume relative to healthy subjects (Brandt et al., 2005). Stimulation of the vestibular system by passive rotation can alter the function of the hippocampus. During passive rotation, place fields of hippocampal neurons were modified in animals (Knierim et al., 1995; Wiener et al., 1995), and errors in “vestibular working memory” developed in humans with unilateral hippocampal lesions in which they were unable to orientate themselves back to the initial position before rotation (Wiest et al., 1996).

Vestibular modulation of hippocampal function may be mediated by a hippocampal theta rhythm. The hippocampal theta rhythm, a 4-10 Hz oscillatory electrical activity, is most prominent during voluntary movement and rapid-eye movement sleep (Vanderwolf, 1969, 1988), and is disrupted by vestibular lesion (Russell et al., 2006). On the other hand, passive body rotation also induced a hippocampal theta rhythm in curarized (Winson, 1976) and undrugged rats (Gavrilov et al., 1995, 1996), and in freely behaving mice (Shin et al., 2005; Shin, 2010). There is evidence that suggests the theta rhythm during passive rotation is atropine-sensitive. In phospholipase C- β 1 (PLC β 1) knockout mice, cholinergic muscarinic receptor (M1, M3 and M5) signaling was blocked and the theta rhythm during passive rotation was abolished (Shin et al.,

2005). In wild-type mice, theta during passive rotation was abolished by systemic atropine sulfate injection (Shin, 2010). However, muscarinic signaling and systemic receptor blockade may occur outside of the septohippocampal system. In this study, I hypothesize that the cholinergic septohippocampal neurons are involved in the generation of the hippocampal theta rhythm during passive rotations. In addition, I tested whether cholinergic afferents are responsible for a rotation-induced modulation of Schaffer-collateral/commissural hippocampal evoked potentials. Preliminary results of this report were presented in an abstract (Tai et al., 2007).

2.2 Material and methods

2.2.1 Lesion and control rats

The experiments were performed on 31 adult male Long Evans hooded rats, weighing 250-380 g (Charles River Canada, St. Constance, Quebec, Canada). They were housed in pairs in Plexiglas cages and kept on a 12/12 h light/dark cycle, at a temperature of 22 ± 1 °C. Rats were given food and water ad libitum. Five groups of rats were used: (i) intact rats with no lesions, (ii) rats with peripheral vestibular receptors lesioned by ototoxin, sodium arsenite (Na^+ arsenite), (iii) sham-lesion rats with saline injected intratympanically, (iv) rats with cholinergic neurons in the medial septum (MS) lesioned by 192 IgG-saporin, and (v) sham-lesion rats with saline infused in the MS. All experimental procedures were approved by the local Animal Use Committee and conducted according to the guidelines of Canadian Council for Animal Care. All efforts were taken to minimize the pain and suffering of animals.

Lesion of cholinergic neurons in the MS was carried out using 192 IgG-saporin (Advanced Targeting Systems, San Diego, CA) under sodium pentobarbital (60 mg/kg i.p.) anesthesia. It consists of the monoclonal p75 receptor antibody 192 IgG which is disulfide-linked to saporin, a ribosome-inactivating toxin. Since cholinergic neurons are the only cells in the MS region that express p75 receptor, 192 IgG-saporin destroys cholinergic neurons without affecting non-cholinergic cells (Wiley et al., 1991; Wrenn and Wiley, 1998; Ma et al., 2004). 192 IgG-saporin was diluted to 0.35 $\mu\text{g}/\mu\text{l}$ with sterile saline, and 0.4 μl was infused bilaterally (A +0.5, L \pm 0.5) into each ventral site (V 5.7 and 7.8; atlas of Paxinos and Watson (1997) of the MS at a constant rate of 0.5 μl in 10 minutes by an infusion pump (Harvard Apparatus, South Natick, MA), via 30-gauge Hamilton syringe (Ma et al., 2004). To allow for diffusion, the infusion needle remained in place for 10 minutes before retraction. Sham lesion rats were infused with equal volumes of saline. 192 IgG-saporin and saline-infused rats were implanted with depth electrodes immediately or 1-2 days after MS infusion. Hippocampal EEGs and evoked potentials were recorded 2-4 weeks following lesion.

To lesion the vestibular cells, sodium arsenite, an ototoxic compound, was injected intratympanically following the procedure of Horn et al. (1981). Sodium arsenite was reported to damage the secretory cells of the cristae, which in turn disrupts the osmolarity and eventually kills the hair cells (Anniko and Wersall, 1977), resulting in equilibrium problems similar to labyrinthectomy (Hunt et al., 1987). Rats were anesthetized with ketamine-xylazine anesthesia, and in each ear, an injection needle was inserted through the tympanic membrane until resistance by the auditory ossicles was encountered. Then, intratympanic injection of 0.1 ml of 300 mg/ml sodium arsenite

solution (in sterile saline), or 0.1 ml of sterile saline, was made within 2 s. Following each injection, the ear canal was tightly packed with Surgifoam (Ferrosan). The arsanilate dose used in this study was shown to impair spatial learning and memory (Ossenkopp and Hargreaves, 1993; Stackman and Herbert, 2002). Implantation of depth electrodes was done three days after vestibular lesion.

To test for the integrity of vestibular function, a contact-righting test was performed. Rats were placed in a supine position on a horizontal surface (table) and another horizontal surface (a sheet of Plexiglas) was placed lightly in contact with the soles of the animal's feet. Normal rats will right themselves immediately. In contrast, rats with vestibular dysfunction will remain supine, with their backs in contact with the table and their feet in contact with the Plexiglas sheet, and will not right themselves. Lesion rats will continue walking with respect to the ventral surface (Plexiglas sheet), as long as their hind feet are in contact with it (Shoham et al., 1989; Ossenkopp and Hargreaves, 1993). Once the Plexiglas sheet was no longer in contact with all four feet, lesion rats will display a righting response.

2.2.2 Electrode implantation and vestibular stimulation

Under sodium pentobarbital (60 mg/kg i.p.) anesthesia, the rat's head was fixed on to a stereotaxic frame using blunt ear bars to avoid damage to the tympanic membrane and the skull adjusted to fit the bregma and lambda in the same horizontal plane. Bipolar electrode pairs were placed bilaterally in the hippocampus, with the deep electrode targeting the stratum radiatum or the stratum lacunosum-moleculare and the shallow electrode targeting the alveus or stratum oriens of the dorsal CA1 region (P +3.8 mm, L

± 2.5 mm; insert in Fig. 2.3A). The dorsal-ventral depth was determined by monitoring field potentials while stimulating the contralateral CA1. Each electrode comprised of a 125- μ m stainless steel wire insulated with Teflon, except at the cut end. A jeweler's screw, placed over the occipital bone plate, served as recording reference. All electrodes and the screw were fixed on the skull with dental cement.

After allowing at least 7 days to recover from the last surgery, hippocampal EEG was recorded during awake immobility, walking and passive rotation. During awake immobility, the motionless rat was in an alert state with eyes opened and head held above the ground. Walking behavior consisted of horizontal walking and rearing. For rotation, the rat was placed in a small container (26 x 23 x 21 cm) and electrodes connected through a slide-wire commutator. A steel rod connected to the base of the container was inserted into the shaft of a vertical drill that was adjusted to rotate at various speeds in a vertical axis – low (20-35 rpm), medium (36-49 rpm) and high (50-70 rpm), in the light and dark conditions. Behavior of the rat was visually monitored during rotation in a brightly lit room, whereas only a red light was used for experiment in the dark. The light intensity emitted between 300-600 nm by the red light was less than 1% of the total light intensity measured by a spectrophotometer (S2000, Ocean Optics). There is little or no emission below 600 nm which is the limit of cone detection in rats (Neitz and Jacobs, 1986; Jacobs et al., 2001). Illumination at 300-600 nm during the dark condition, measured inside the rat's cage during rotation, was estimated to be < 0.1 lux. In some experiments, rats were injected with 50 mg/kg atropine sulfate i.p. or 50 mg/kg atropine methyl nitrate i.p. (peripheral blockade of muscarinic cholinergic receptors) 15 min prior to rotation.

2.2.3 Recording and analysis of EEG and evoked potentials

EEG was sampled at 200 Hz after averaging 5 consecutive samples digitized at 1 KHz, which contributed 3 dB and 10 dB attenuation points at 84 Hz and 180 Hz, respectively. Artifact-free segments of the EEG were manually selected, with each segment consisting of 1024 points or 5.12 s duration. A power spectrum was constructed from at least 6 segments, and after smoothing and averaging, spectral estimates had 0.195 Hz resolution, 2.15 Hz bandwidth (interval of smoothing) and >60 degrees of freedom (Leung, 1985). Power spectra were plotted in arbitrary logarithmic units, with the calibration of 5.8 log units = 1 mV peak-to-peak amplitude of a sine wave. An increase of 1 logarithmic power unit signified a 10-fold increase in the squared amplitude of the EEG at a specific frequency. The “rise” of a theta peak was measured as the difference in logarithmic power between a minimum at 3-6 Hz to a maximum at 6-10 Hz. The rise of the theta peak gives a good estimate of the strength of the rhythmic theta signal (Leung and Shen, 2007). Time-frequency spectral analysis during rotation (up to 1 min) was computed using the “spectrogram” function in MATLAB (Natick, MA), with segment length of 256 points (1.28 s) and 200 overlapping points. The spectrogram shows how the EEG power at different frequency changes with time. The coherence spectrum is a measure of the correlation between two EEG signals as a function of frequency and is calculated as the z -transform coherence value which is $0.5 \ln(1 + c)/\ln(1 - c)$, where c is the linear coherence, and \ln is the natural logarithm (Leung et al., 1982).

Field excitatory postsynaptic potentials (fEPSPs) were recorded at CA1 electrodes, following stimulation of the contralateral CA1 (repeated at 0.1 Hz). The

contralateral CA1 stimulus activated CA3 commissural fibers that evoked a population apical dendritic excitatory postsynaptic potential, recorded as a negative peak at the apical dendrites of CA1 or stratum radiatum, and a positive peak at CA1 stratum oriens. In each rat, an average fEPSP (average of 8 sweeps) was recorded at the apical dendrites following stimulation at two times the stimulus threshold (15-50 μ A, 0.2 ms pulse duration). The maximal slope of the average fEPSP during the falling phase (over 2 ms interval) was measured and expressed as a ratio of that evoked during awake immobility.

2.2.4 Histology

At the end of experiments, rats were deeply anesthetized with 30% urethane and perfused through the heart with 400 ml of cold saline followed by 500 ml of cold 4% paraformaldehyde solution in 0.1 M phosphate buffer (PB; pH 7.4). The brain was removed and post-fixed in the latter solution at 4°C. Acetylcholinesterase (AChE) staining and choline acetyltransferase (ChAT) immunohistochemistry were performed on hippocampal and MS sections respectively. Using a freezing microtome, the hippocampus was sectioned at 40 μ m within 12 hrs of fixing while the rest of the brain was kept in 18% sucrose in phosphate-buffered saline for at least 72 hrs at 4°C. For the AChE staining, hippocampal sections were mounted on chrome-alum gelatin coated slides. AChE staining protocol was modified from the Koelle copper thiocholine method (Koelle and Friedenwald, 1949), using acetylthiocholine iodide as a false substrate to tag the AChE enzyme and ethopropazine as an inhibitor of non-specific cholinesterases.

For the ChAT staining, the MS was sectioned at 40 μ m and they were first incubated in 1% sodium borohydride in 0.1 M PB for 15 minutes and subsequently rinsed

in PB. To block non-specific labeling, they were incubated in 10% normal goat serum (Sigma) in 0.1 M PB containing 0.1% Triton X-100 (Sigma) for 1 hr at room temperature. The sections were rinsed briefly in PB and incubated at 4°C for 48 hrs in primary antibody solution containing mouse monoclonal ChAT (1:200; Cedarlane) in 1% normal goat serum. Sections were washed in three changes of PB and followed by incubation in biotin-conjugated goat anti-mouse secondary antiserum (1:200; Jackson ImmunoResearch) for 1 hr in room temperature. The sections were then washed several times in PB. ABC complex solution (Vector Laboratories) was prepared 20 minutes before use by adding equal volumes of solutions A and B in PB (1:1:100). The sections were incubated in the ABC complex solution for 1 hr at room temperature. Following three washes in PB, the sections were incubated in a solution containing 0.05% diaminobenzidine tetrahydrochloride (DAB, Sigma) and 0.03% hydrogen peroxide in PB at room temperature in a fume hood until they reached the desired color intensity (1-3 min). The sections were then washed several times in PB, mounted on glass slides. Finally, they were dehydrated in a series of 70%, 95% and 100% ethyl alcohol, cleared in xylene (5 minutes x 2) and cover-slipped with DePex (BDH) mounting medium.

The number of ChAT-positive cells was quantified in three representative coronal sections (40 μm) at anterior (~A 0.7), middle (~A 0.4) and posterior (~A 0.2) levels of the medial septum-diagonal band of Broca region. Images of selected sections were captured with a digital camera using x100 magnification in a microscope, and cells were counted from the digital images by another person who was unaware of the treatment history. Electrode placements were histologically verified in 40 μm thionin-stained brain sections.

Histology of the vestibular apparatus was carried out on sham lesion and sodium arsenite lesioned rats. Following perfusion, the temporal bones were removed and placed in a decalcification solution (Decalcifier I, Surgipath Medical Ind. Inc.) for a week. The tissue was then rinsed through a graded alcohol series and xylene, and embedded in paraffin for sectioning. Sections of 7 μm thickness were mounted on slides, heated briefly, dried overnight and finally stained with hematoxylin and eosin (H & E).

2.2.5 Statistical analysis

Data was analyzed using one-way or two-way analysis of variance (ANOVA) and Student's t-tests where appropriate (GraphPad Prism 4.0). Significance was set at $P < 0.05$.

2.3 Results

2.3.1 Labyrinthine integrity

Within 24 h after administration of sodium arsenite, rats displayed vestibular system dysfunction such as exaggerated head dorsiflexion, severe ataxia, increased circling behavior and a wide-based stance. When given the contact-righting test, all arsenite lesion rats treated the Plexiglas sheet placed on their feet as the “real” ground – they walked upside down with their backs on the table, and were unable to right themselves. In contrast, sham lesion rats displayed no behavioral abnormalities and righted themselves quickly in the contact-righting test.

Inner ear histology revealed the degeneration of the crista ampullaris of a semicircular canal in an arsenite-lesioned rat (Fig. 2.1C, D). Neuroepithelial cell

pathology was characterized by the collapse of the epithelial layer, the erosion of the supporting stroma and complete loss of sensory hairs. No obvious structural damage was observed in sham lesion rats (Fig. 2.1A, B).

2.3.2 Effect of 192-IgG saporin lesion of the medial septum

A decrease in the number of ChAT-immunopositive cells in the MS was found in 192 IgG-saporin lesion rats ($n = 8$) as compared to control sham-lesion rats ($n = 5$; Fig. 2.2A, B). There was a significant reduction in the number of ChAT-immunoreactive neurons in 192 IgG-saporin lesion rats when compared to sham-lesion rats (Fig. 2.2B), as confirmed by a significant group effect in 2-way (group x section location) ANOVA ($F_{(1, 33)} = 422, P < 0.0001$; Fig. 2.2A). Bonferroni post-hoc test showed that a significant decrease in the number of ChAT-immunoreactive cells in lesion as compared to sham-lesion rats in all three frontal levels (anterior: 24 ± 8 vs 214 ± 12 ; middle: 49 ± 7 vs 207 ± 9 ; posterior: 35 ± 9 vs 240 ± 26 ; $P < 0.001$, respectively). 192 IgG-saporin lesion rats also showed a paler AChE staining in the hippocampus as compared to sham control rats (Fig. 2.2C).

2.3.3 Characteristics of theta rhythm during rotation

At the start of a medium- or high-speed rotation, a rat typically “braced” itself by extending its forelimbs, flexing its hind limbs and tilting its head, and then remained in the same posture, without head and limb movements, until the rotation was stopped. This “bracing” behavior was observed in all rats, including vestibular and 192 IgG-saporin

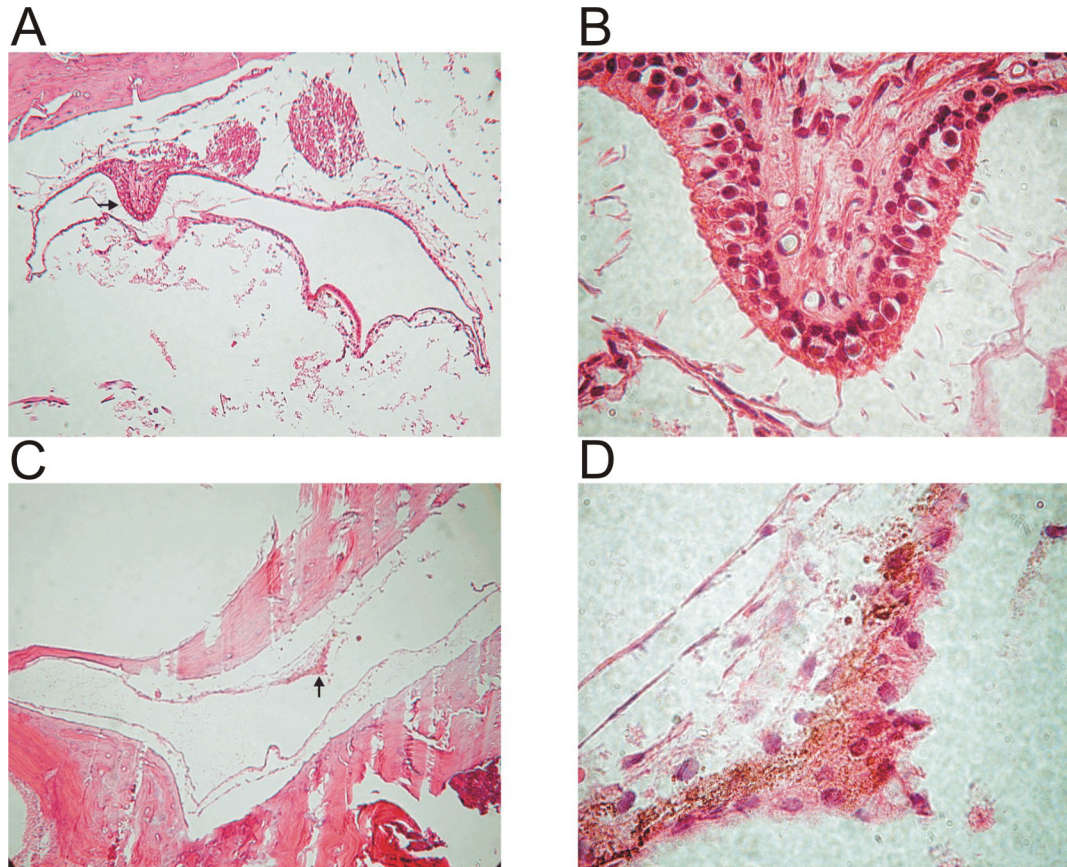
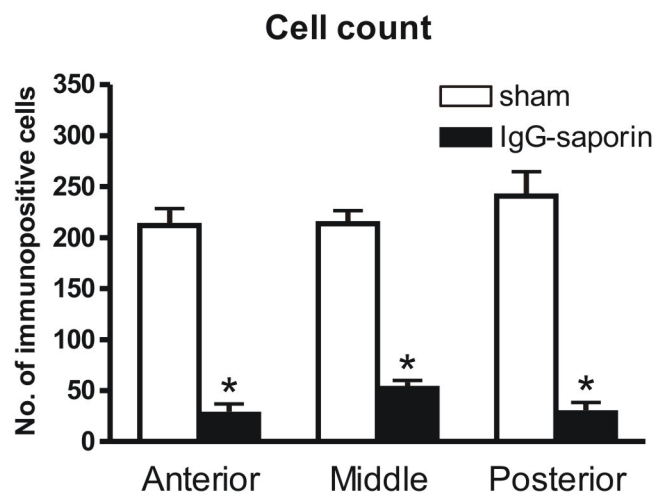


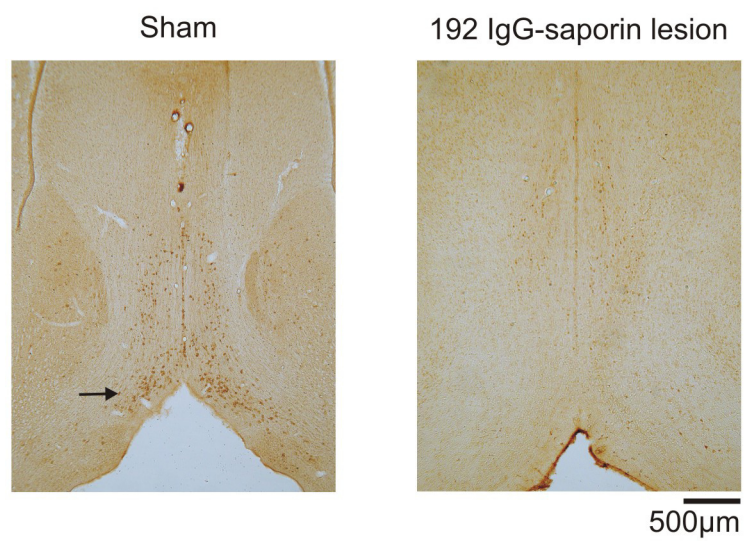
Fig. 2.1. Photomicrographs of the ampullae of a semicircular canal containing the cristae (arrow) of an intact (A, B) and a sodium arsenite lesion rat (C, D). Note that the integrity of the hair cells was lost in the lesioned rat. Left, x 100 magnification; right, x 1000 magnification. Hematoxylin and eosin stain.

Fig. 2.2 Counts of choline acetyltransferase (ChAT)-immunopositive cells and coronal sections of the medial septum (MS), and coronal sections of the hippocampus stained for acetylcholinesterase (AChE) of 192 IgG-saporin lesion rats and sham lesion rats. A significant decrease in the number of ChAT-immunopositive cholinergic neurons was observed in all three different coronal MS sections (A) following bilateral injections of 192 IgG-saporin in the MS (n = 8) as compared to sham (n = 5). Arrow points to a ChAT-immunopositive cell (B). Depletion of AChE in dorsal CA1 was also observed. Note the lighter stain of the hippocampus in the lesion rat (C). Values are expressed as mean \pm SEM. * $P < 0.001$: difference between lesion and sham rats at a particular level, using Bonferroni test after a significant two-way ANOVA.

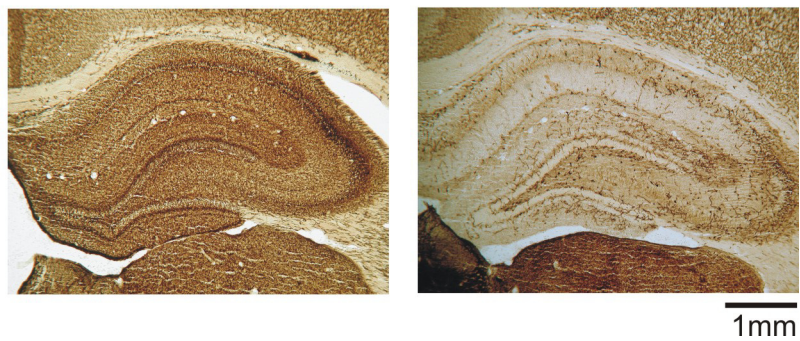
A



B



C



lesion rats. The period of immobility during rotation was invariably accompanied by a steady and stable theta rhythm (Fig. 2.3A, 2.4A and 2.5). More spontaneous movements usually accompanied a low-speed rotation, but theta rhythm was also found during periods of immobility. In intact rats, theta peak frequency changed significantly with rotation speed (Fig. 2.4A; repeated measures one-way ANOVA $F_{(2, 14)} = 5.04$, $P < 0.05$). Newman-Keuls post-hoc test showed a significant difference between high and medium, and between high and low speeds ($P < 0.05$, respectively). However, repeated measures two-way ANOVA revealed no significant difference between the light and the dark condition, when either theta peak frequency ($F_{(1, 14)} = 0.054$, $P = 0.82$) or theta power ($F_{(1, 14)} = 2.02$, $P = 0.18$) during rotation was evaluated.

The stability of the theta rhythm during rotation was confirmed by a time-frequency spectral analysis. The time-frequency spectrogram showed that a minute-long medium-speed rotation was accompanied by a stable theta power and peak frequency (5.5-6.7 Hz) that did not change substantially with time (arrow; Fig 2.5A). The power spectra obtained from 2 s segments showed that peak theta frequency and theta power fluctuated around a mean frequency (6.15 ± 0.07 Hz) and power (0.95 ± 0.02 log units) during the 1-min rotation (Fig. 2.5B). Similarly stable theta frequency and power were found during a 5-min rotation (data not shown).

Atropine sulfate (50 mg/kg i.p.) strongly attenuated rotation-induced hippocampal theta rhythm and theta power compared to that during the drug-free condition (Fig. 2.3A, 2.4A). After atropine sulfate, the rise of the theta peak was not detected in 5 of 8 intact rats, and as a group, theta peak rise averaged 0.06 log units ($n = 8$), which was 9 times smaller than the no-drug baseline (0.55 log units). For experiments in the dark, repeated

measures two-way ANOVA showed a significant reduction in theta power during rotation following injection of atropine sulfate ($F_{(1, 14)} = 47.8$, $P < 0.0001$; Fig. 2.4A). Bonferroni post-hoc test revealed that a difference in theta power between drug-free and atropine-sulfate groups was observed in any one of the three rotation speeds ($P < 0.01$, respectively). Rotation in the light condition yielded similarly significant difference in theta power between drug-free and atropine-sulfate groups (main effect $F_{(1, 14)} = 92.30$, $P < 0.0001$; $P < 0.001$ at any speed, Bonferroni post-hoc test). Following injection of atropine methyl nitrate (Fig. 2.3B), both theta power ($F_{(1, 4)} = 0.022$, $P = 0.89$) and theta peak frequency ($F_{(1, 4)} = 0.906$, $P = 0.40$) were not affected.

When compared to control sham-lesion rats, rotation-induced theta power was attenuated in both 192 IgG-saporin lesion rats (Fig. 2.3C) and vestibular lesion rats (Fig. 2.3D). Two-way ANOVA showed a significant decrease in theta power in 192 IgG-saporin lesion rats ($F_{(1, 21)} = 97.2$, $P < 0.0001$; Fig. 2.4B), and in vestibular lesion rats ($F_{(1, 24)} = 76.8$, $P < 0.0001$; Fig. 2.4C), as compared to the respective control sham-lesion rats. A comparison between lesion and sham rats showed a decrease in theta power across all rotational speeds (at least $P < 0.05$; Bonferroni post-hoc tests; Fig. 2.4B, 2.4C). For example, during medium speed rotation, 192 IgG-saporin lesion rats only showed a small theta peak rise (0.12 ± 0.03 log units), whereas the large peak rise was observed in MS sham-lesion rats (0.64 ± 0.07 log units; Fig. 2.3C, 2.4B). Similarly, vestibular lesion rats displayed a smaller theta peak rise (0.30 ± 0.04 log units, Fig. 2.3D, 2.4C) than vestibular sham-lesion rats (0.80 ± 0.13 log units).

The rotation-induced theta peak frequency in all animals tested ranged from 3.88 Hz to 6.59 Hz. No significant difference in theta peak frequency was found between

Fig. 2.3 Power spectra of hippocampal EEG during rotation. Power spectra were obtained from artifact-free EEG segments during rotation using fast Fourier Transform (FFT) and plotted in arbitrary logarithmic units. The strength of the rhythmic theta signal was determined by the rise of a theta peak, which is the difference in logarithmic power between a minimum at 3-6 Hz to a peak at 6-10 Hz (indicated by the open arrow). Corresponding EEG traces are showed on the right. Frequencies are displayed next to the theta peaks (θ). Speed of rotation ranged from 60 to 68 revolutions per minute (rpm). A representative coronal section of the dorsal hippocampus, stained with thionin, showing the location of the recording electrode (R1) in the stratum lacunosum-moleculare of CA1 (insert, A). Rotation-induced theta rhythm recorded at stratum radiatum/fissure and theta peak power observed during the drug-free condition (dotted red line) were abolished following injection of atropine sulfate (50 mg/kg i.p., solid black line, A). In contrast, the same dose of atropine methyl nitrate did not elicit any appreciable changes (solid black line, B). When compared to sham rats (dotted red line), theta peak power during rotation was attenuated in MS cholinergic (IgG-saporin) lesion (solid black line, C) and vestibular (Na arsenite) lesion rats (solid black line, D).

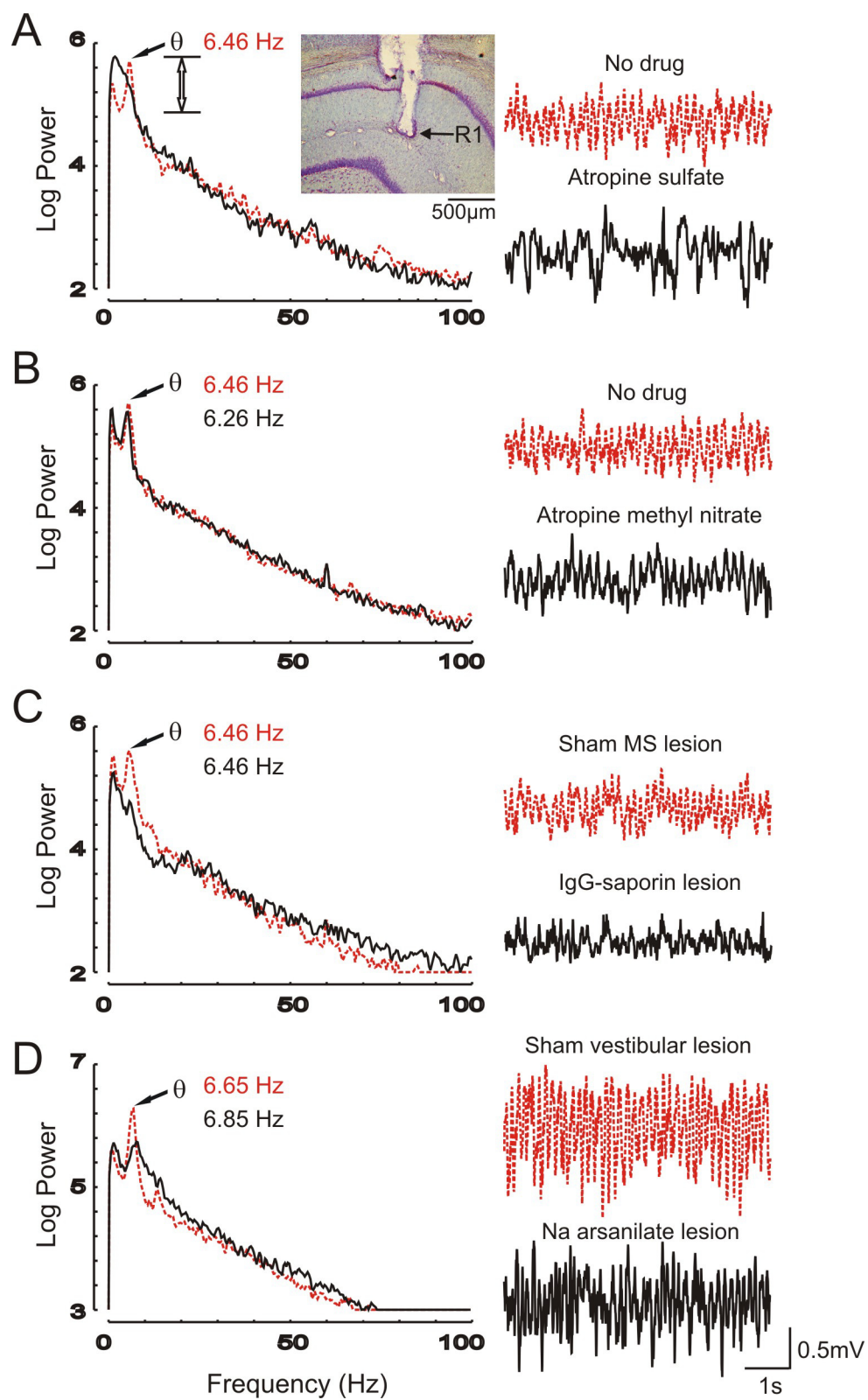


Fig. 2.4 Effect of rotational speeds on hippocampal theta rhythm. The rise of the theta peak in logarithmic power (right) and theta peak frequency (left) were plotted against various rotation speeds: low (20-35 rpm), medium (36-49 rpm) and high (50-70 rpm). Data was derived from experiments performed in the dark. In intact rats, atropine sulfate reduced theta power significantly at all speeds (A). Lesion of MS cholinergic neurons by 192 IgG-saporin (B) and lesion of vestibular receptors by Na arsenilate (C) significantly attenuated theta power at all speeds, when compared to sham lesion animals. Values are expressed as mean \pm SEM. * $P < 0.05$, ** $P < 0.01$, *** $P < 0.001$: difference between no drug and atropine sulfate, and between sham and lesion rats using Bonferroni test after a significant repeated measures two-way ANOVA respectively. # $P < 0.05$: difference across rotational speeds in intact drug-free rats using Newman-Keuls test following a significant repeated measures one-way ANOVA (A).

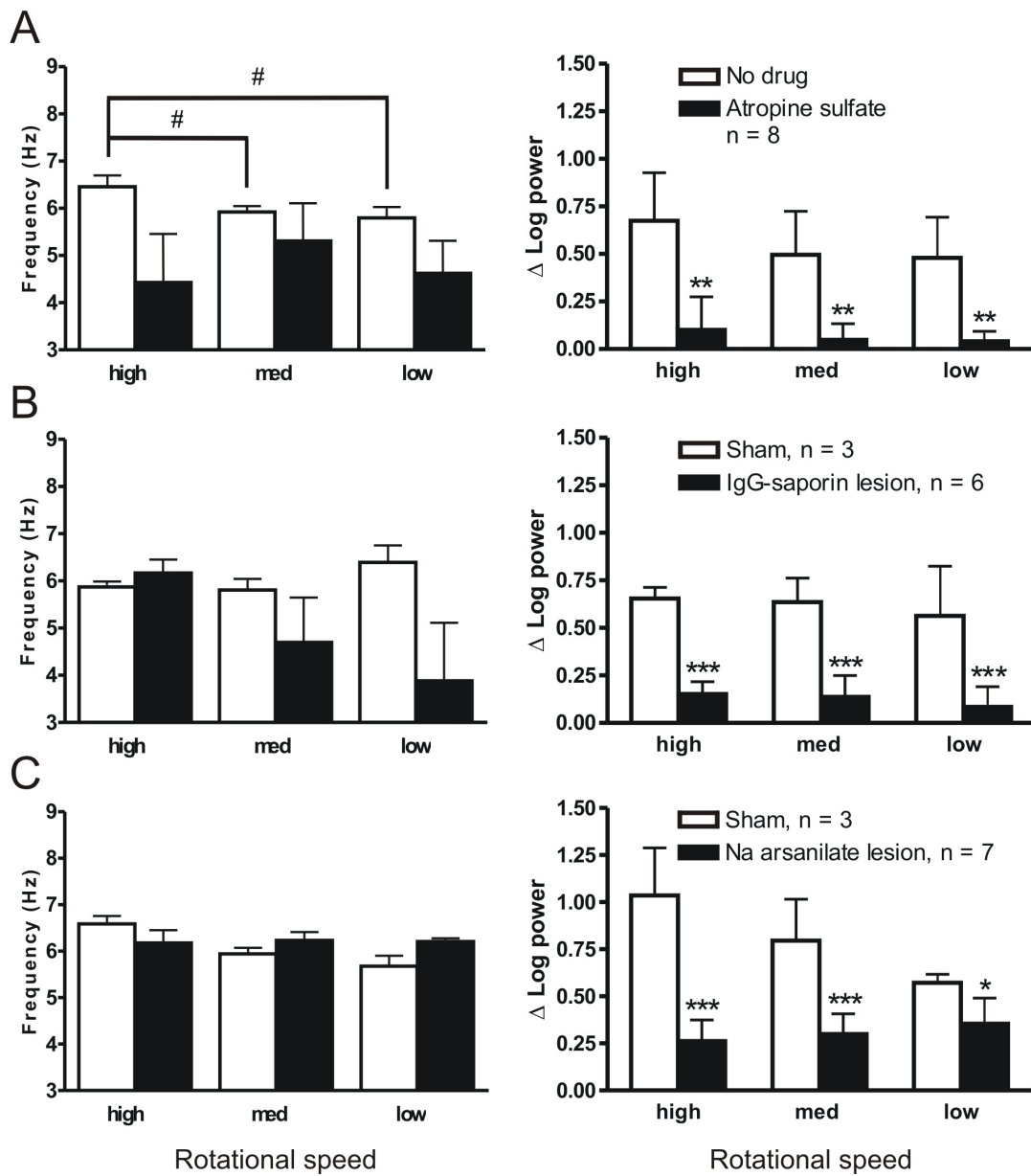
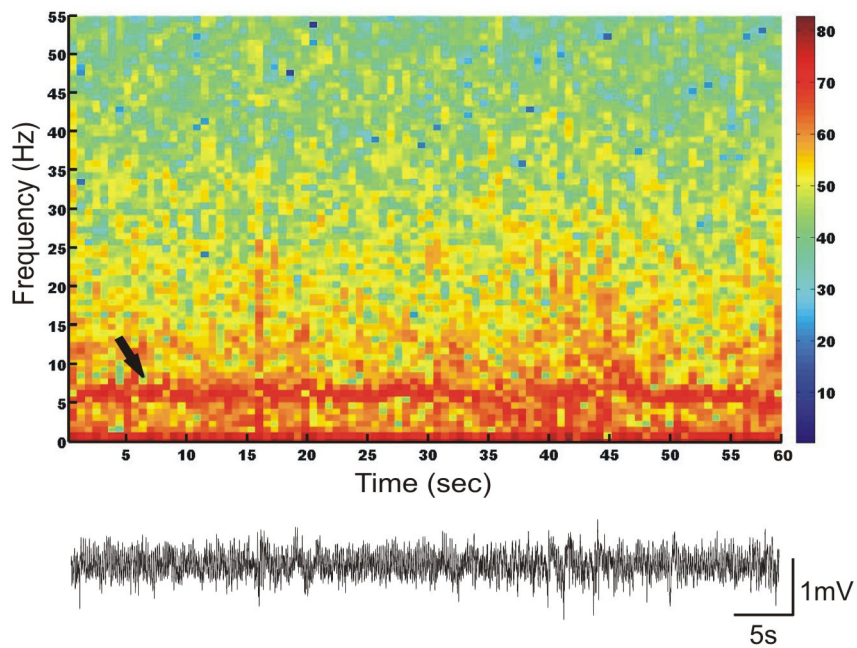
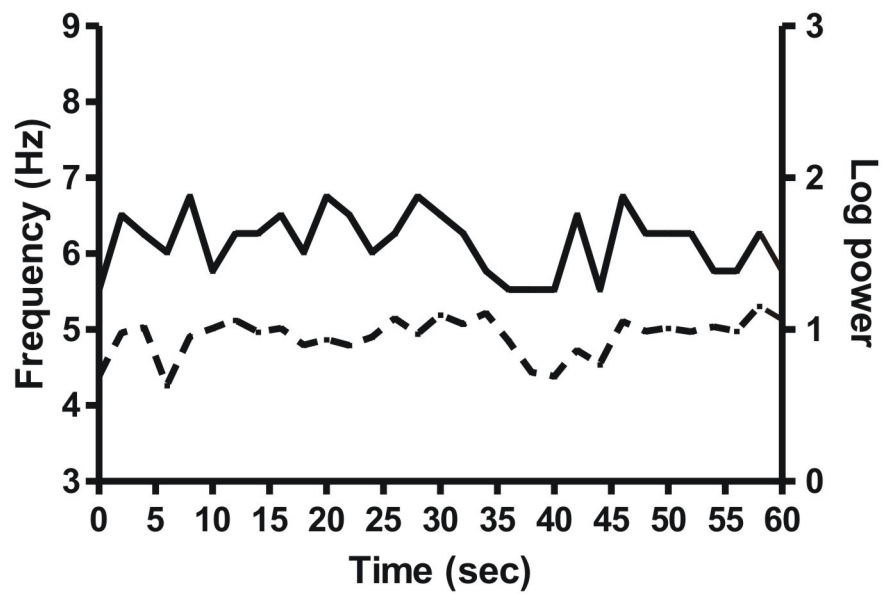


Fig. 2.5 Hippocampal theta rhythm is stable during rotation. A) Time-frequency spectrogram (top panel) calculated using short-time Fourier transform was obtained from artifact-free EEG (bottom panel) during 1 min of medium-speed rotation of an intact rat. The horizontal axis represents time (s) and the left vertical axis represents frequency (Hz), and the color intensity of each pixel in the image (calibration panel on right) indicates the amplitude (dB) at a particular frequency and time. 1 mV peak-to-peak sine wave gives a 75.7 dB power peak in the spectrogram. B) Theta peak frequency (solid line), and rise of theta peak (dotted line; 20 dB = 1 log unit) are plotted for same data. Note that the theta peak frequency (arrow in A) and rise of theta peak did not vary greatly with time (B), i.e., continuous rotation did not result in habituation of the theta rhythm.

A



B



drug-free and atropine-sulfate conditions ($F_{(1, 14)} = 2.77$, $P = 0.12$; Fig. 2.4A), between 192 IgG-saporin ($F_{(1, 21)} = 2.03$, $P = 0.17$; Fig. 2.4B) and sham control groups, or between vestibular lesion ($F_{(1, 24)} = 0.55$, $P = 0.46$; Fig. 2.4C) and sham lesion rats.

Gamma rhythm (30-100 Hz band) in lesion and control rats was not significantly altered by rotation, before or after treatment with atropine sulfate (Fig. 2.3A) or atropine methyl nitrate (Fig. 2.3B).

2.3.4 Characteristics of theta rhythm during walking

Theta power and frequency were evaluated during walking in different groups of rats. In intact rats, atropine sulfate reduced the rise of the theta peak during walking (0.48 ± 0.05 log units, $n = 8$), compared to the drug-free condition (1.05 ± 0.09 log units; $P < 0.001$, paired-t test; Fig. 2.6A). The walking theta peak rise was not significantly different in 192 IgG-saporin lesion (0.87 ± 0.10 log units, $n = 6$) and vestibular lesion rats (0.91 ± 0.09 log units, $n = 7$), as compared to their respective control sham-lesion rats (MS sham: 1.04 ± 0.25 log units, $n = 3$; vestibular sham: 1.15 ± 0.04 units, $n = 3$).

No significant difference in theta peak frequency was observed between drug-free (7.71 ± 0.13 Hz) and atropine sulfate conditions (7.30 ± 0.12 Hz) ($P = 0.0936$; paired t-test; Fig. 2.6B), or between 192 IgG-saporin lesion rats (7.66 ± 0.19 Hz) and sham-MS lesion rats (7.31 ± 0.07 Hz; $P = 0.24$; unpaired t-test; Fig. 2.6B). However, vestibular lesion rats (7.12 ± 0.14 Hz) showed a significantly lower theta peak frequency compared to the respective sham lesion rats (7.70 ± 0.07 ; $P < 0.05$; unpaired t-test).

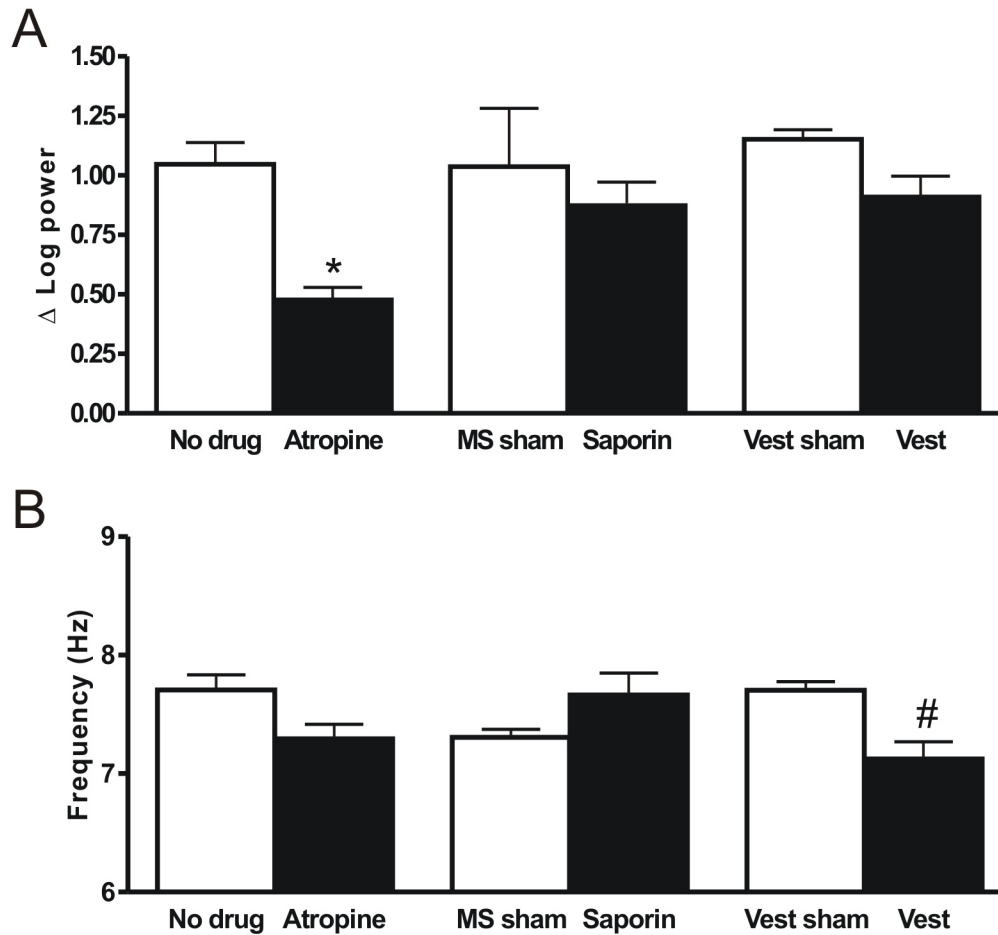


Fig. 2.6 Changes in theta peak frequency and power during walking. A) A reduction in the rise of the theta peak (log power) was observed following atropine sulfate (Atropine) when compared to the drug-free condition (No drug, $n = 8$), but no change in 192 IgG-saporin (Saporin, $n = 6$) and vestibular lesion (Vest, $n = 7$) animals, compared to their respective sham controls ($n = 3$, respectively). B) There was no significant difference in theta peak frequency between drug-free condition and atropine sulfate, and between MS sham and 192 IgG-saporin lesion rats. Vestibular lesion rats display a lower theta peak frequency compared to vestibular sham rats. Values are expressed as mean \pm SEM. * $P < 0.001$: difference between drug-free condition and atropine sulfate (paired t-test). # $P < 0.05$: difference between vestibular lesion and sham lesion rats (unpaired t-test).

2.3.5 Effect of atropine sulfate and 192 IgG-saporin lesion on fEPSP modulation

The commissurally evoked apical dendritic fEPSP in CA1 was used to assess cholinergic function during different behaviors (Leung, 1980, 1998). In drug-free intact rats, the slope of the commissural fEPSP (average of eight sweeps) was smaller during walking than awake-immobility ($P < 0.05$; paired t-test, $n = 5$). Similarly, the slope of the commissural fEPSP was smaller during medium speed rotation than that during awake-immobility ($P < 0.05$; paired t-test, $n = 5$, Fig. 2.7). Consistent with an inference of increased cholinergic inputs during rotation, atropine sulfate significantly increased the rotation-to-immobility fEPSP slope ratio from a pre-drug baseline of 0.83 ± 0.10 to 0.99 ± 0.05 ($P < 0.05$; paired t-test; Fig. 2.7). The walking-to-immobility fEPSP slope ratio also increased after atropine sulfate, from 0.78 ± 0.11 to 0.91 ± 0.13 , but this increase was not statistically significant ($P = 0.088$; paired t-test, $n = 5$).

The rotation-to-immobility fEPSP slope ratio was higher in 192 IgG-saporin lesion rats (1.00 ± 0.02 , $n = 8$) than sham-lesion rats (0.83 ± 0.03 , $n = 5$; $P < 0.01$; unpaired t-test). The walking-to-immobility fEPSP slope ratio was not significantly different between saporin- and sham-lesion rats (0.92 ± 0.04 vs 0.78 ± 0.05 ; $P = 0.051$; unpaired t-test).

When individual fEPSP sweeps were analyzed, fEPSP slope during rotation was significantly smaller than that during immobility in all drug-free intact rats ($n = 5$). However, in vestibular lesion rats ($n = 2$), no difference in the slope of fEPSP was observed between immobility and rotation. The intact ($n = 5$) and lesion groups ($n = 2$)

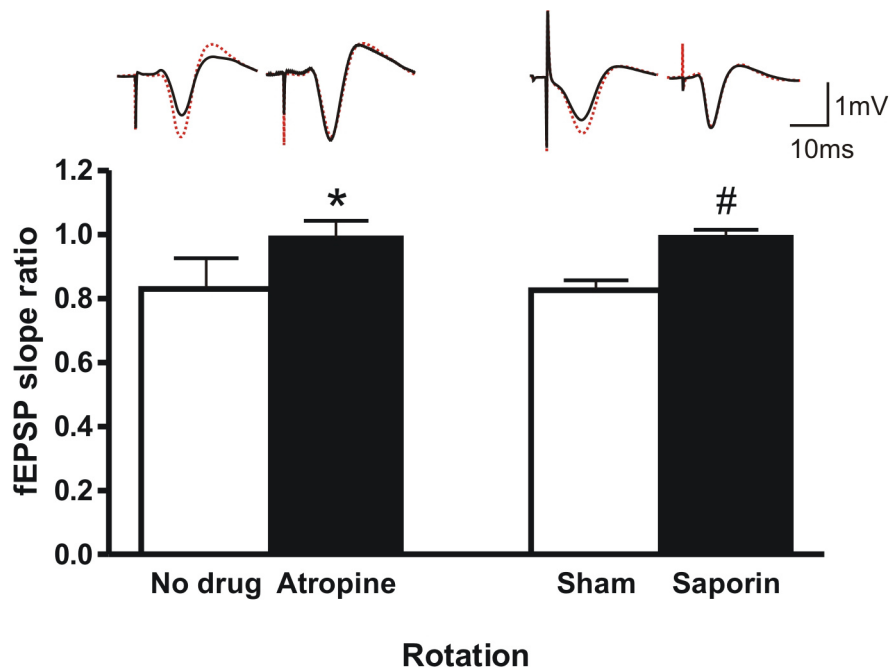


Fig. 2.7 Effect of atropine sulfate and medial septal 192 IgG-saporin lesion on hippocampal field excitatory postsynaptic potentials (fEPSPs). Top traces: average commissural evoked potentials (average of eight sweeps) recorded in CA1 of a representative rat, during immobility (dotted red traces) and medium-speed rotation (solid black traces). The ratio of the rising slope of the fEPSP during rotation to that during awake-immobility (mean \pm SEM) was approximately 0.8 without drug, and it increased significantly after atropine sulfate (left panel), and was higher in rats with septal cholinergic lesion (Saporin) as compared to sham lesion rats. * $P < 0.05$: difference between drug-free condition and atropine sulfate in intact rats ($n = 5$; paired t-test). # $P < 0.01$: difference between sham rats ($n = 5$) and saporin lesion rats ($n = 8$; unpaired t-test).

are different in the frequency occurrence of rotation-modulated fEPSPs ($P < 0.05$; Fisher's exact test).

2.4 Discussion

This study demonstrated that whole body rotation elicits an atropine-sensitive theta rhythm in the hippocampus of freely behaving undrugged rats. Continuous (1 min or longer) rotation activated a stable and continuous hippocampal theta, extending previous studies that stimulated the vestibular system for several seconds (Gavrilov et al., 1995, 1996; Shin et al., 2005; Shin, 2010). The rotation-induced theta was strongly attenuated by central muscarinic, but not peripheral, cholinergic blockade. Rotation-induced theta was also attenuated after lesion of the septal cholinergic neurons or bilateral vestibular lesion. The activation of cholinergic inputs to the hippocampus was confirmed by a modulation of hippocampal fEPSP during rotation as compared to during immobility. The cholinergic modulation of fEPSPs was sensitive to muscarinic cholinergic blockade, lesion of the septal cholinergic neurons and peripheral vestibular receptors.

2.4.1 Septohippocampal cholinergic neurons generates an atropine-sensitive theta rhythm during rotation

In intact rats, the rotation-induced hippocampal theta rhythm was greatly attenuated following atropine sulfate treatment, although activation of a minor (~10% amplitude) atropine-resistant theta cannot be excluded. Similarly, rotation-induced

hippocampal theta was greatly attenuated in 192-IgG saporin lesion rats as compared to sham lesion rats. Although septal cholinergic efferents project to many areas including entorhinal and cingulate cortices (Woolf, 1991), cholinergic input to the hippocampus originates predominately from the MS (Mesulam et al., 1983). In 192-IgG saporin lesion rats, ChAT-immunopositive neurons decreased by ~83%, and accompanied by a large decrease in AChE-staining in the hippocampus, as compared to sham-lesion rats. The small rotation-induced theta rhythm observed in 192-IgG saporin lesion rats could be caused by residual acetylcholine release in the hippocampus, estimated to remain at 30-40% of control levels (Dornan et al., 1996; McMahan et al., 1997), possibly following compensatory up-regulation of synthesis and storage of acetylcholine (Lapchak et al., 1991; Chang and Gold, 2004).

This study is the first report of a rotation-induced hippocampal theta rhythm in freely behaving rats, although rotation-induced theta rhythm was reported in restrained rats (Gavrilov et al., 1995, 1996), in rats paralyzed with curare (Winson, 1976) or made cataleptic with haloperidol (Shoham et al., 1989). A rotation-induced theta rhythm has been shown in freely behaving mice (Shin et al., 2005; Shin, 2010).

2.4.2 Vestibular stimulation of cholinergic activity in the hippocampus

The attenuation in theta power during rotation in the sodium arsenite-lesioned rats was due to a lack of vestibular stimulation and not a deficit in septohippocampal cholinergic activity. The arsenite-lesioned rats lost righting with contact placing and showed clear damage of the vestibular apparatus, consistent with previous studies (Hunt et al., 1987; Shoham et al., 1989; Ossenkopp et al., 1990). No loss of hippocampal AChE

staining was found in sodium arsenilate-lesioned rats (data not shown). Shoham et al. (1989) showed that rotation on a turntable failed to elicit a theta rhythm in vestibular-intact or -lesioned rats, pretreated with haloperidol and atropine sulfate, and concluded that vestibular signals are not necessary for activation of atropine-resistant theta. I showed that vestibular signals are necessary for the activation of an atropine-sensitive theta. Signals are relayed from the vestibular nucleus complex to the hippocampus through several polysynaptic pathways, among which the hypothalamus-septohippocampal pathway (Smith 1997; Smith et al., 2005; Hüfner et al., 2007) is likely involved in the generation of hippocampal theta activity.

In this study, atropine-sensitive theta induced by rotation was in the low frequency range <7 Hz. Although there are exceptions, atropine-sensitive theta is typically of lower frequency (3-7 Hz) as compared to atropine-resistant theta (7-10 Hz) (Vanderwolf, 1975; Bland and Oddie, 2001). Gavrilov et al. (1995, 1996) speculated that the 7-8.5 Hz (high-frequency) theta recorded during rotation was atropine-resistant, while Shin (2010) showed that rotation induced a 7-10 Hz atropine-sensitive theta in mice. A contributing factor to this discrepancy is likely the phasic nature of vestibular stimulation (over 2.5-4 s) in previous studies as compared to tonic vestibular stimulation (0.5-5 min) in the present study.

I did not find an increase in the power of hippocampal theta activity with higher rotation speed, as reported previously by Gavrilov et al (1996). I did find that the theta peak frequency was positively correlated with the speed of passive rotation in undrugged intact rats. Studies in rats (Vanderwolf, 1969) and dogs (Arnolds et al., 1979) demonstrated that theta peak power and frequency increased with the magnitude of

voluntary movement. Moreover, in a jump avoidance task, theta peak frequency increased with height, prior to and during a jump. Theta peak power decreased with height prior to a jump but did not change with height during a jump (Bland et al., 2006).

2.4.3 Cholinergic septohippocampal and vestibular inputs modulates theta rhythm during walking

Hippocampal theta rhythm was observed during walking, following lesion of septal cholinergic neurons and vestibular cells. My data on theta peak frequency during walking is largely similar to previous studies in which theta peak frequency was unaltered following atropine sulfate (Leung et al., 1982; Shoham et al., 1989) and in 192 IgG-saporin lesion rats (Lee et al., 1994; Yoder and Pang, 2005), but was reduced in vestibular lesion rats (Shoham et al., 1989; Russell et al., 2006). In this study, the rise of the theta peak was significantly lower following atropine sulfate, compared to the drug-free condition, consistent with the proposal that both atropine-resistant and atropine-sensitive components were found in the hippocampal theta rhythm during walking (Vanderwolf, 1988; Leung, 1998; Bland and Oddie, 2001). Hippocampal theta rhythm seen during voluntary movement was abolished by medial septal lesion or inactivation (Green and Arduini, 1954; Leung, 1987; Mizumori et al., 1989). In the absence of septohippocampal cholinergic neurons or muscarinic activation, theta rhythmicity may be maintained by the septohippocampal GABAergic and glutamatergic neurons (Brazhnik and Fox, 1999; Alreja et al., 2000; Yoder and Pang, 2005; Huh et al., 2010).

My study showed a decrease in theta power following atropine sulfate, however, no significant difference was observed in 192 IgG-saporin lesion and vestibular lesion

rats, when compared with their respective sham controls. This contrasted with several previous studies. Shin (2010) showed no change in theta peak power during walking following atropine sulfate in mice, and Russell et al. (2006) reported a reduction in theta peak power after surgical ablation of the vestibular apparatus. Intraseptal injection of 192 IgG-saporin was reported to reduce hippocampal theta peak power (Lee et al., 1994; Yoder and Pang, 2005). These previous studies measured the absolute power at theta peak frequency while my study measured the rise of theta peak, which is a more reliable measure of the magnitude of the theta rhythmic oscillation, since the absolute power at the theta frequency also includes power of the irregular slow activity (Leung et al., 1982).

2.4.4 Vestibular activation modulates hippocampal synaptic transmission

A measure of cholinergic modulation of hippocampal synaptic transmission was shown by the behavioural dependence of the Schaffer-collateral evoked apical-dendritic fEPSPs in CA1 (Leung, 1980; Leung and Vanderwolf, 1980; Leung and Peloquin, 2010). As reported previously in drug-free rats, the slope of fEPSP at the apical dendritic layer of CA1 was smaller during walking than immobility, and this behavioral modulation was abolished by atropine sulfate. The latter behavioural modulation was not found in 192 IgG-saporin and vestibular lesion rats. The present report provides a new result that passive rotation, as compared to awake-immobility, decreased the apical dendritic fEPSPs in CA1, and this decrease was not found in 192 IgG saporin and vestibular lesion rats. The lack of cholinergic modulation during rotation in IgG saporin and vestibular lesion rats is consistent with the concept that vestibular stimulation excites

septohippocampal cholinergic neurons, which releases acetylcholine that modulates hippocampal apical dendritic synaptic transmission (Leung and Peloquin, 2010).

2.4.5 Conclusion

This study highlights the finding that rotation activates a cholinergic input from the medial septum to the hippocampus, mediating synaptic modulation and an atropine-sensitive theta rhythm in the hippocampus of behaving rats. Atropine-sensitive theta induced during vestibular stimulation may participate in sensorimotor processing (Bland and Oddie, 2001), and may represent the cholinergic activation that is necessary for spatial memory function (Givens and Olton, 1995; Hasselmo, 2006; Roland et al., 2008). Studies demonstrating that vestibular stimulation has a positive effect on cognition have been reviewed recently (Smith et al., 2010a, 2010b). In humans, caloric stimulation has been suggested to improve verbal and spatial memory (Bachtold et al., 2001). In addition, galvanic vestibular stimulation relieved symptoms of prosopagnosia (Wilkinson et al., 2005) and spatial neglect (Rorsman et al., 1999). Hippocampal-dependent cognitive abilities are greatly compromised in patients suffering from Alzheimer's disease, with degeneration of cholinergic neurons in the basal forebrain (MS included) as a classic pathology (Wu et al., 2005; Wenk, 2006). Since vestibular stimulation activates a cholinergic septal input to the hippocampus, it may be suggested that vestibular stimulation may remedy some of cognitive deficits of Alzheimer's disease.

2.5 References

- Alreja M, Wu M, Liu W, Atkins JB, Leranath C, Shanabrough M (2000) Muscarinic tone sustains impulse flow in the septohippocampal GABA but not cholinergic pathway: implications for learning and memory. *J Neurosci* 20:8103-8110.
- Anniko M, Wersall J (1977) Experimentally (atoxyl) induced ampullar degeneration and damage to the maculae utriculi. *Acta Otolaryngol* 83:429-440.
- Arnolds DE, Lopes da Silva FH, Aitink JW, Kamp A (1979) Hippocampal EEG and behaviour in dog. I. Hippocampal EEG correlates of gross motor behaviour. *Electroencephalogr Clin Neurophysiol* 46:552-570.
- Bachtold D, Baumann T, Sandor PS, Kritos M, Regard M, Brugger P (2001) Spatial- and verbal-memory improvement by cold-water caloric stimulation in healthy subjects. *Exp Brain Res* 136:128-132.
- Bland BH, Jackson J, Derrie-Gillespie D, Azad T, Rickhi A, Abriam J (2006) Amplitude, frequency, and phase analysis of hippocampal theta during sensorimotor processing in a jump avoidance task. *Hippocampus* 16:673-681.
- Bland BH, Oddie SD (2001) Theta band oscillation and synchrony in the hippocampal formation and associated structures: the case for its role in sensorimotor integration. *Behav Brain Res* 127:119-136.
- Brandt T, Schautzer F, Hamilton DA, Bruning R, Markowitsch HJ, Kalla R, Darlington C, Smith P, Strupp M (2005) Vestibular loss causes hippocampal atrophy and impaired spatial memory in humans. *Brain* 128:2732-2741.
- Brazhnik ES, Fox SE (1999) Action potentials and relations to the theta rhythm of medial septal neurons in vivo. *Exp Brain Res* 127:244-258.
- Chang Q, Gold PE (2004) Impaired and spared cholinergic functions in the hippocampus after lesions of the medial septum/vertical limb of the diagonal band with 192 IgG-saporin. *Hippocampus* 14:170-179.
- Dornan WA, McCampbell AR, Tinkler GP, Hickman LJ, Bannon AW, Decker MW, Gunther KL (1996) Comparison of site-specific injections into the basal forebrain on water maze and radial arm maze performance in the male rat after immunolesioning with 192 IgG saporin. *Behav Brain Res* 82:93-101.
- Gavrilov VV, Wiener SI, Berthoz A (1996) Whole-body rotations enhance hippocampal theta rhythmic slow activity in awake rats passively transported on a mobile robot. *Ann N Y Acad Sci* 781:385-398.

- Gavrilov VV, Wiener SI, Berthoz A (1995) Enhanced hippocampal theta EEG during whole body rotations in awake restrained rats. *Neurosci Lett* 197:239-241.
- Givens B, Olton DS (1995) Bidirectional modulation of scopolamine-induced working memory impairments by muscarinic activation of the medial septal area. *Neurobiol Learn Mem* 63:269-276.
- Green JD, Arduini AA (1954) Hippocampal electrical activity in arousal. *J Neurophysiol* 17:533-557.
- Guidetti G, Monzani D, Trebbi M, Rovatti V (2008) Impaired navigation skills in patients with psychological distress and chronic peripheral vestibular hypofunction without vertigo. *Acta Otorhinolaryngol Ital* 28:21-25.
- Hamann KF, Weiss U, Ruile A (2009) Effects of acute vestibular lesions on visual orientation and spatial memory, shown for the visual straight ahead. *Ann N Y Acad Sci* 1164:305-308.
- Hasselmo ME (2006) The role of acetylcholine in learning and memory. *Curr Opin Neurobiol* 16:710-715.
- Horn KM, DeWitt JR, Nielson HC (1981) Behavioral assessment of sodium arsenite induced vestibular dysfunction in rats. 9:371-378.
- Hufner K, Hamilton DA, Kalla R, Stephan T, Glasauer S, Ma J, Bruning R, Markowitsch HJ, Labudda K, Schichor C, Strupp M, Brandt T (2007) Spatial memory and hippocampal volume in humans with unilateral vestibular deafferentation. *Hippocampus* 17:471-485.
- Huh CY, Goutagny R, Williams S (2010) Glutamatergic neurons of the mouse medial septum and diagonal band of Broca synaptically drive hippocampal pyramidal cells: relevance for hippocampal theta rhythm. *J Neurosci* 30:15951-15961.
- Hunt MA, Miller SW, Nielson HC, Horn KM (1987) Intratympanic injection of sodium arsenite (atoxyl) solution results in postural changes consistent with changes described for labyrinthectomized rats. *Behav Neurosci* 101:427-428.
- Jacobs GH, Fenwick JA, Williams GA (2001) Cone-based vision of rats for ultraviolet and visible lights. *J Exp Biol* 204:2439-2446.
- Kasa P, Rakonczay Z, Gulya K (1997) The cholinergic system in Alzheimer's disease. *Prog Neurobiol* 52:511-535.
- Knierim JJ, Kudrimoti HS, McNaughton BL (1995) Place cells, head direction cells, and the learning of landmark stability. *J Neurosci* 15:1648-1659.

- Koelle GB, Friedenwald JS (1949) A histochemical method for localizing cholinesterase activity. *Proc Soc Exp Biol* 70:617-622.
- Lapchak PA, Jenden DJ, Hefti F (1991) Compensatory elevation of acetylcholine synthesis in vivo by cholinergic neurons surviving partial lesions of the septohippocampal pathway. *J Neurosci* 11:2821-2828.
- Leung LS (1998) Generation of theta and gamma rhythms in the hippocampus. *Neurosci Biobehav Rev* 22:275-290.
- Leung LS (1980) Behavior-dependent evoked potentials in the hippocampal CA1 region of the rat. I. Correlation with behavior and EEG. *Brain Res* 198:95-117.
- Leung LS, Peloquin P (2010) Cholinergic modulation differs between basal and apical dendritic excitation of hippocampal CA1 pyramidal cells. *Cereb Cortex* 20:1865-1877.
- Leung LS, Vanderwolf CH (1980) Behavior-dependent evoked potentials in the hippocampal CA1 region of the rat. II. Effect of eserine, atropine, ether and pentobarbital. *Brain Res* 198:119-133.
- Leung LW (1987) Hippocampal electrical activity following local tetanization. I. Afterdischarges. *Brain Res* 419:173-187.
- Leung LW, Lopes da Silva FH, Wadman WJ (1982) Spectral characteristics of the hippocampal EEG in the freely moving rat. *Electroencephalogr Clin Neurophysiol* 54:203-219.
- Ma J, Shen B, Rajakumar N, Leung LS (2004) The medial septum mediates impairment of prepulse inhibition of acoustic startle induced by a hippocampal seizure or phencyclidine. *Behav Brain Res* 155:153-166.
- Matthews BL, Ryu JH, Bockanek C (1989) Vestibular contribution to spatial orientation. Evidence of vestibular navigation in an animal model. *Acta Otolaryngol Suppl* 468:149-154.
- McMahan RW, Sobel TJ, Baxter MG (1997) Selective immunolesions of hippocampal cholinergic input fail to impair spatial working memory. *Hippocampus* 7:130-136.
- McNaughton BL, Barnes CA, Gerrard JL, Gothard K, Jung MW, Knierim JJ, Kudrimoti H, Qin Y, Skaggs WE, Suster M, Weaver KL (1996) Deciphering the hippocampal polyglot: the hippocampus as a path integration system. *J Exp Biol* 199:173-185.
- Mesulam MM, Mufson EJ, Levey AI, Wainer BH (1983) Cholinergic innervation of cortex by the basal forebrain: cytochemistry and cortical connections of the septal

area, diagonal band nuclei, nucleus basalis (substantia innominata), and hypothalamus in the rhesus monkey *J Comp Neurol* 214:170-197.

Mittelstaedt ML, Mittelstaedt H (1980) Homing by path integration in a mammal. *Naturewissenschaften* 67:556-567.

Mizumori SJ, McNaughton BL, Barnes CA, Fox KB (1989) Preserved spatial coding in hippocampal CA1 pyramidal cells during reversible suppression of CA3c output: evidence for pattern completion in hippocampus. *J Neurosci* 9:3915-3928.

Neitz J, Jacobs GH (1986) Reexamination of spectral mechanisms in the rat (*Rattus norvegicus*). *J Comp Psychol* 100:21-29.

O'Keefe J, Nadel L (1978) The hippocampus as a cognitive map. pp 570. Oxford: Clarendon Press.

Ossenkopp KP, Hargreaves EL (1993) Spatial learning in an enclosed eight-arm radial maze in rats with sodium arsenite-induced labyrinthectomies. *Behav Neural Biol* 59:253-257.

Ossenkopp KP, Prkacin A, Hargreaves EL (1990) Sodium arsenite-induced vestibular dysfunction in rats: effects on open-field behavior and spontaneous activity in the automated digiscan monitoring system. *Pharmacol Biochem Behav* 36:875-881.

Paxinos G, Watson C (1997) The rat brain in stereotaxic coordinates. San Diego: Academic Press.

Petrosini L (1984) Task-dependent rate of recovery from hemilabyrinthectomy: an analysis of swimming and locomotor performances. *Physiol Behav* 33:799-804.

Raphan T, Cohen B (2002) The vestibulo-ocular reflex in three dimensions. *Exp Brain Res* 145:1-27.

Roland JJ, Mark K, Vetreno RP, Savage LM (2008) Increasing hippocampal acetylcholine levels enhance behavioral performance in an animal model of diencephalic amnesia. *Brain Res* 1234:116-127.

Rorsman I, Magnusson M, Johansson BB (1999) Reduction of visuo-spatial neglect with vestibular galvanic stimulation. *Scand J Rehabil Med* 31:117-124.

Russell NA, Horii A, Smith PF, Darlington CL, Bilkey DK (2006) Lesions of the vestibular system disrupt hippocampal theta rhythm in the rat. *J Neurophysiol* 96:4-14.

Schliebs R, Arendt T (2006) The significance of the cholinergic system in the brain during aging and in Alzheimer's disease. *J Neural Transm* 113:1625-1644.

- Shin J (2010) Passive rotation-induced theta rhythm and orientation homeostasis response. *Synapse* 64:409-415.
- Shin J, Kim D, Bianchi R, Wong RK, Shin HS (2005) Genetic dissection of theta rhythm heterogeneity in mice. *Proc Natl Acad Sci U S A* 102:18165-18170.
- Shoham S, Chen YC, DeVietti TL, Teitelbaum P (1989) Deafferentation of the vestibular organ: effects on atropine-resistant EEG in rats. *Psychobiology* 17:307-314.
- Smith PF (1997) Vestibular-hippocampal interactions. *Hippocampus* 7:465-471.
- Smith PF, Darlington CL, Zheng Y (2010a) Move it or lose it--is stimulation of the vestibular system necessary for normal spatial memory? *Hippocampus* 20:36-43.
- Smith PF, Geddes LH, Baek JH, Darlington CL, Zheng Y (2010b) Modulation of memory by vestibular lesions and galvanic vestibular stimulation. *Front Neurol* 1:141.
- Smith PF, Horii A, Russell N, Bilkey DK, Zheng Y, Liu P, Kerr DS, Darlington CL (2005) The effects of vestibular lesions on hippocampal function in rats. *Prog Neurobiol* 75:391-405.
- Stackman RW, Clark AS, Taube JS (2002) Hippocampal spatial representations require vestibular input. *Hippocampus* 12:291-303.
- Stackman RW, Herbert AM (2002) Rats with lesions of the vestibular system require a visual landmark for spatial navigation. *Behav Brain Res* 128:27-40.
- Tai SK, Ma J, Leung LS (2007) Vestibular activation stimulates cholinergic system in the hippocampus. *Soc Neurosci Abstr* 33:11.11/OO13.
- Vanderwolf CH (1988) Cerebral activity and behavior: control by central cholinergic and serotonergic systems. *Int Rev Neurobiol* 30:225-340.
- Wallace DG, Hines DJ, Pellis SM, Whishaw IQ (2002) Vestibular information is required for dead reckoning in the rat. *J Neurosci* 22:10009-10017.
- Wenk GL (2006) Neuropathologic changes in Alzheimer's disease: potential targets for treatment. *J Clin Psychiatry* 67 Suppl 3:3-7; quiz 23.
- Wiener SI, Korshunov VA, Garcia R, Berthoz A (1995) Inertial, substratal and landmark cue control of hippocampal CA1 place cell activity. *Eur J Neurosci* 7:2206-2219.
- Wiest G, Baumgartner C, Deecke L, Olbrich A, Steinhoff N, Müller C (1996) Effects of hippocampal lesions on vestibular memory in whole-body rotation. *Journal of Vestibular Research* 6:S17-S17.

- Wiley RG, Oeltmann TN, Lappi DA (1991) Immunolesioning: selective destruction of neurons using immunotoxin to rat NGF receptor. *Brain Res* 562:149-153.
- Wilkinson D, Ko P, Kilduff P, McGlinchey R, Milberg W (2005) Improvement of a face perception deficit via subsensory galvanic vestibular stimulation. *J Int Neuropsychol Soc* 11:925-929.
- Winson J (1976) Hippocampal theta rhythm. I. Depth profiles in the curarized rat. *Brain Res* 103:57-70.
- Woolf NJ (1991) Cholinergic systems in mammalian brain and spinal cord *Prog Neurobiol* 37:475-524.
- Wrenn CC, Wiley RG (1998) The behavioral functions of the cholinergic basal forebrain: lessons from 192 IgG-saporin. *Int J Dev Neurosci* 16:595-602.
- Wu CK, Thal L, Pizzo D, Hansen L, Masliah E, Geula C (2005) Apoptotic signals within the basal forebrain cholinergic neurons in Alzheimer's disease. *Exp Neurol* 195:484-496.
- Yoder RM, Pang KC (2005) Involvement of GABAergic and cholinergic medial septal neurons in hippocampal theta rhythm. *Hippocampus* 15:381-392.
- Zheng Y, Goddard M, Darlington CL, Smith PF (2009) Long-term deficits on a foraging task after bilateral vestibular deafferentation in rats. *Hippocampus* 19:480-486.

Chapter 3

Vestibular Stimulation Enhances Hippocampal Long-term Potentiation via Activation of Cholinergic Septohippocampal Neurons

3.1 Introduction

Acetylcholine modulates a wide array of cognitive functions, including arousal, attention, learning and memory (Jerusalinsky et al., 1997; Sarter et al., 2005; Hasselmo, 2006). Cholinergic input to the hippocampus originating predominantly from medial septum (MS) is particularly important for learning and memory (Mesulam et al., 1983a; Mesulam et al., 1983b; Kesner, 1988; Givens and Olton, 1990). Selective ablation of septal cholinergic neurons by intraseptal microinjection of the immunotoxin 192 immunoglobulin G-saporin (192 IgG-saporin) caused spatial learning and memory impairments in some (Shen et al., 1996; Walsh et al., 1996; Chang and Gold, 2004) but not all experiments (Berger-Sweeney et al., 1994; Baxter et al., 1995; McMahan et al., 1997). Nonetheless, degeneration of cholinergic neurons in the basal forebrain, including MS, forms the basis of the cholinergic hypothesis of Alzheimer's disease (Bartus et al., 1982; Francis et al., 1999).

Long-term potentiation (LTP), a long-lasting increase in synaptic transmission, was first described in the hippocampus of anesthetized and behaving animals (Bliss and Lomo, 1973; Bliss and Gardner-Medwin, 1973). LTP is widely regarded as a cellular correlate of learning and memory (Martin et al., 2000; Abraham and Williams, 2003; Neves et al., 2008). There is experimental evidence that acetylcholine modulates

hippocampal LTP. Application of cholinergic agonists enhanced hippocampal LTP *in vitro* (Blitzer et al., 1990; Auerbach and Segal, 1996; Shimoshige et al., 1997). In anesthetized rats, hippocampal LTP was facilitated by tetanic stimulation of the MS, and this facilitation was blocked by systemic administration of muscarinic cholinergic antagonists (Ovsepián et al., 2004). However, these studies failed to address the effect of physiologically released acetylcholine on hippocampal LTP in behaving animals.

Our laboratory has reported that basal-dendritic LTP in hippocampal CA1 was enhanced when induced during walking while hippocampal EEG showed a theta rhythm, compared to that induced during immobility when large-amplitude irregular activity was observed. Moreover, the systemic muscarinic cholinergic antagonist scopolamine or lesion of septohippocampal cholinergic neurons by 192 IgG-saporin attenuated LTP induced during walking without affecting LTP induced during immobility (Leung et al., 2003). These results were consistent with previous findings that more acetylcholine was released during walking than immobility (Dudar et al., 1979) and acetylcholine release was highly correlated with the appearance of hippocampal theta rhythm (Zhang et al., 2010) and positively correlated with theta frequency in anesthetized rats (Keita et al., 2000). I have shown recently that vestibular stimulation generated a cholinergic, atropine-sensitive theta rhythm and modulated synaptic transmission in the hippocampus of behaving rats (Chapter 2; Tai et al., 2011). In anesthetized rats, caloric vestibular stimulation resulted in an increase in hippocampal acetylcholine level (Horii et al., 1994; Horii et al., 1995). Therefore, activation of the vestibular system provides a good model to investigate cholinergic modulation of LTP in behaving rats. I hypothesize that (1) basal dendritic LTP in CA1 induced during passive rotation (SPIN) was larger than that

induced during awake-immobility (IMM), and (2) the enhanced LTP induced during SPIN as compared IMM is due to the activity of cholinergic septohippocampal cells.

3.2 Material and methods

3.2.1 Lesion and control rats

Experiments were conducted on 15 adult male Long Evans hooded rats (244-310 g; Charles River Canada, Quebec, Canada). All animals were given food and water ad libitum and housed in pairs in Plexiglas cages under climate-controlled conditions on a 12 h light/dark cycle (lights on at 7:00 A.M.). Three groups of rats were used: (i) intact rats with no lesions, (ii) rats with cholinergic neurons in the MS lesioned by 192 IgG-saporin (192 IgG-SAP), and (iii) sham-lesion rats with saline infused in the MS. All experimental procedures were approved by the local Animal Use Committee and conducted according to the guidelines of Canadian Council for Animal Care. All efforts were taken to minimize the pain and suffering of animals.

3.2.2 Electrode implantation

Under sodium pentobarbital (60 mg/kg i.p.) anesthesia, bipolar electrodes were placed bilaterally in the dorsal hippocampus (P +4.6 mm, L \pm 2.8 mm; P +3.2 mm, L \pm 1.7 mm) as described previously (Leung et al., 2003; Luo and Leung, 2010). Coordinates were adapted from the atlas of Paxinos and Watson (Paxinos and Watson, 1997). Each electrode comprised of a 125 μ m stainless steel wire insulated with Teflon, except at the

cut tip and were used for either recording or stimulating. Recording electrodes were implanted to straddle the cell layer of CA1, with the deep electrode in the stratum radiatum and the surface electrode in the alveus or stratum oriens (referred to as the stratum oriens electrode). Stimulating electrodes were placed in the stratum oriens on the same side anterior to the recording electrodes, or homotopically on the opposite side. Two screws in the skull over the frontal cortex and the cerebellum served as the stimulus anode and the recording ground respectively. The depths of stimulating and recording electrodes were optimized by monitoring evoked potentials during surgery. All electrodes and screws were fixed on the skull with dental cement. Hippocampal EEGs and evoked potentials were recorded at least one week after electrode implantation.

3.2.3 Lesion of cholinergic cells in the medial septum

Cholinergic neurons in the MS were lesioned using 192 IgG-saporin (Advanced Targeting Systems, San Diego, CA) under sodium pentobarbital (60 mg/kg i.p.) anesthesia. It consists of a p75 receptor antibody 192 IgG which is conjugated to saporin, a ribosome-inactivating toxin. Given that cholinergic neurons are the only cells in the MS region that express p75 receptor, 192 IgG-saporin destroys cholinergic neurons without affecting non-cholinergic cells (Wiley et al., 1991; Ma et al., 2004). 192 IgG-saporin was diluted with sterile saline, loaded into a Hamilton syringe, and infused bilaterally into the MS (A +0.5, L \pm 0.5). For each lateral track, the 30-gauge cannula was first lowered to V 5.7, and then to V 7.8. At each of the two depths, 0.4 μ l of 192 IgG-saporin (0.35 μ g/ μ l) was infused at a constant rate of 0.5 μ l/10 minutes by an infusion pump (Harvard Apparatus, South Natick, MA). After each infusion, the needle remained in place for 10

minutes. Sham lesion rats were infused with equal volumes of saline. 192 IgG-saporin and saline-infused rats were implanted with depth electrodes immediately or 1-2 days after MS infusion. Hippocampal EEGs and evoked potentials were recorded 2-4 weeks following lesion.

3.2.4 Recording and analysis of evoked potentials

Animals were habituated to the recording environment for at least 2 days, prior to the start of experiments. Recording was carried out between 10:00 A.M. and 7:00 P.M. Photoisolated current stimulus pulses (0.2 ms) were delivered cathodally to one stimulating electrode, using a screw in the skull as the anode. Monopolar recordings were made with a skull screw serving as both the reference and the ground. A stimulating electrode, ipsi- or contra-lateral to a recording pair of CA1 electrodes, evoked a basal-dendritic field excitatory postsynaptic potential (fEPSP) when a negative field potential was evoked at the surface (stratum oriens) electrode and a positive potential was evoked at the deep (stratum radiatum) electrode. Two channels of evoked responses were filtered at 0.1 Hz to 3 kHz and sampled at 10 kHz, and averaged evoked potentials (AEPs) of eight sweeps were acquired online by a custom microcomputer program.

AEPs were recorded during awake-immobility before and after LTP induction. Baseline AEPs were recorded for 1-2 h. LTP was induced by a high-frequency stimulus train (tetanus) delivered either during awake-immobility or passive rotation described below. The train consisted of 100 pulses at 200 Hz (5 ms interpulse interval) at a stimulus intensity of 1-1.5X the fEPSP threshold (the lowest stimulus intensity at which an evoked response can be visually detected). Generally, tetanus did not evoke an afterdischarge.

However, a few experiments in which a short (<15 s) afterdischarge was evoked were included, since the magnitude of LTP (expressed at a ratio of the baseline) was similar to experiments without afterdischarge (Leung and Shen, 1993). Following tetanus, AEPs were recorded at “fixed” times at 5, 10, 15, 20, 30, 60, 90, 120, 150 and 180 min. Previous data showed that LTP magnitude was not significantly different among test pulses of 1.5-2X threshold intensity (Leung and Shen, 1995); therefore, all AEPs were recorded with test pulse of 1.5X the fEPSP threshold. Input-output curves were obtained from fEPSP responses of five different stimulus intensities (1, 1.2, 1.5, 2 and 4 times the fEPSP threshold) recorded during baseline, at 1 h and 2 h after tetanus. The maximal slope of the fEPSP during the falling or rising phase (within 2 ms interval) was measured from the AEPs. The baseline value was obtained by averaging the last six AEPs (over 30-60 min period) before tetanus. For each experiment, the response after tetanus was normalized by the baseline average.

3.2.5 Experimental design

In the first experiment, intact rats were given tetanus during awake-immobility or rotation. During awake-immobility (IMM), the motionless rat was in an alert state with eyes opened and head held against gravity. For rotation (SPIN), the rat was placed in a small container (26 x 23 x 21 cm) and electrodes connected through a slide-wire commutator. A steel rod connected to the base of the container was inserted into the shaft of a drill that was adjusted to rotate at 36-49 rpm in a vertical axis. In Chapter 2, when the rat was rotated at various speeds - low (20-35 rpm), medium (36-49 rpm) and high (50-70 rpm), a stable hippocampal theta rhythm was observed during periods of

immobility (Tai et al., 2011). In this study, only medium speed (36-49 rpm) was used because it produced more consistent and longer periods of immobility as compared to low speed. LTP was induced during immobility or rotation (during a period of immobility).

In the second experiment, rats were injected with muscarinic cholinergic receptor antagonist atropine sulfate (50 mg/kg, i.p.) or an equal volume of saline 15 min before tetanus during rotation. Experiments were conducted in a random order with at least 5 d between treatments. In the third experiment, instead of injecting atropine sulfate or saline (i.p.), 192 IgG-saporin or sham lesioned rats were used. Tetanus was administered during awake-immobility or rotation.

In all experiments, LTP tests were conducted in a random order using the same tetanic stimulus parameters. Tetanus was given up to 5 times, separated by at least 5 days, in each rat.

3.2.6 Histology

At the end of experiments, rats were deeply anesthetized with 30% urethane and perfused through the heart with 400 ml of cold saline followed by 500 ml of cold 4% paraformaldehyde solution in 0.1 M phosphate buffer (PB; pH 7.4). The brain was removed and post-fixed in the latter solution at 4°C. Acetylcholinesterase (AChE) staining was performed on hippocampal sections. Choline acetyltransferase (ChAT) and parvalbumin (Parv) immunohistochemistry were carried out on MS sections. Using a freezing microtome, the hippocampus was sectioned at 40 µm within 12 hrs of fixing while the rest of the brain was kept in 18% sucrose in phosphate-buffered saline for at

least 72 hrs at 4°C. For the AChE staining, hippocampal sections were mounted on chrome-alum gelatin coated slides. AChE staining protocol was modified from the Koelle copper thiocholine method (Koelle GB and Friedenwald JS, 1949), using acetylthiocholine iodide as a false substrate to tag the AChE enzyme and ethopropazine as an inhibitor of non-specific cholinesterases.

For the ChAT and Parv staining, the MS was sectioned at 40 µm and they were first incubated in 1% sodium borohydride in 0.1 M PB for 15 minutes and subsequently rinsed in PB. To block non-specific labeling, they were incubated in 10% normal goat serum (Sigma-Aldrich, St. Louis, MO) in 0.1 M PB containing 0.1% Triton X-100 (Sigma-Aldrich) for 1 hr at room temperature. The sections were rinsed briefly in PB and incubated at 4°C for 48 hrs in primary antibody solution containing mouse monoclonal ChAT (1:200; Cedarlane, Burlington, Ontario, Canada) or Parv (1:100; Sigma-Aldrich) in 1% normal goat serum. Sections were rinsed in three changes of PB and followed by incubation in biotin-conjugated goat anti-mouse secondary antiserum (1:200; Jackson ImmunoResearch, West Grove, PA) for 1 hr in room temperature. The sections were then rinsed several times in PB. ABC complex solution (Vector Laboratories, Burlington, Ontario, Canada) was prepared 20 minutes before use by adding equal volumes of solutions A and B in PB (1:1:100). The sections were incubated in the ABC complex solution for 1 hr at room temperature. Following three washes in PB, the sections were incubated in a solution containing 0.05% diaminobenzidine tetrahydrochloride (DAB, Sigma-Aldrich) and 0.03% hydrogen peroxide in PB at room temperature in a fume hood until they reached the desired color intensity (1-3 min). The sections were then rinsed several times in PB, mounted on glass slides. Finally, they were dehydrated in a series of

70%, 95% and 100% ethyl alcohol, cleared in xylene (5 minutes x 2) and cover-slipped with DePex (BDH, VWR International Mississauga, Ontario, Canada) mounting medium.

The number of ChAT- and Parv-positive cells was quantified in three representative coronal sections (40 μm) at anterior ($\sim\text{A } 0.7$), middle ($\sim\text{A } 0.4$) and posterior ($\sim\text{A } 0.2$) levels of the medial septum-diagonal band of Broca region. Images of selected sections were captured with a digital camera using x100 magnification in a microscope, and cells were counted from the digital images by another person who was unaware of the treatment history. Electrode placements were histologically verified in 40 μm thionin-stained brain sections.

3.2.7 Statistical analysis

One- or two-way ANOVAs were carried out, followed by Newman-Keuls post-hoc if the main or interaction effect was statistically significant ($P < 0.05$). All statistical analyses were performed using Prism 4.0 (GraphPad Software Inc., La Jolla, CA) and GB Stat (Dynamic Microsystems Inc., Silver Spring, MD).

3.3 Results

Ipsilateral or contralateral stimulation of stratum oriens in CA1 (Fig. 3.1A) evoked a typical basal dendritic fEPSP which was negative at the alveus or stratum oriens electrode and positive at the deep electrode in the stratum radiatum (Fig. 3.1B, C). The hippocampal EEG displayed large-amplitude irregular activity during immobility (IMM;

Fig. 3.1 Recording of hippocampal basal-dendritic evoked potential and EEG using implanted electrodes in CA1. (A, B) Representative coronal sections showing locations of (A) the anterior stratum oriens stimulating electrode L1 at P3.2, L1.7, (B) the posterior surface alvear L4 and deep L3 stratum radiatum recording electrode pair at P4.6, L2.8. (C) Representative basal-dendritic average fEPSP at L3 and L4 following cathodal stimulation of L1; stimulus artifacts are indicated by filled circles. (D, E) EEG from L3 and L4 were recorded around the time of tetanus (Tet; dotted line) during awake-immobility (IMM; D) and rotation (SPIN; E). Note the presence of a theta rhythm during rotation and large-amplitude irregular activity during immobility.

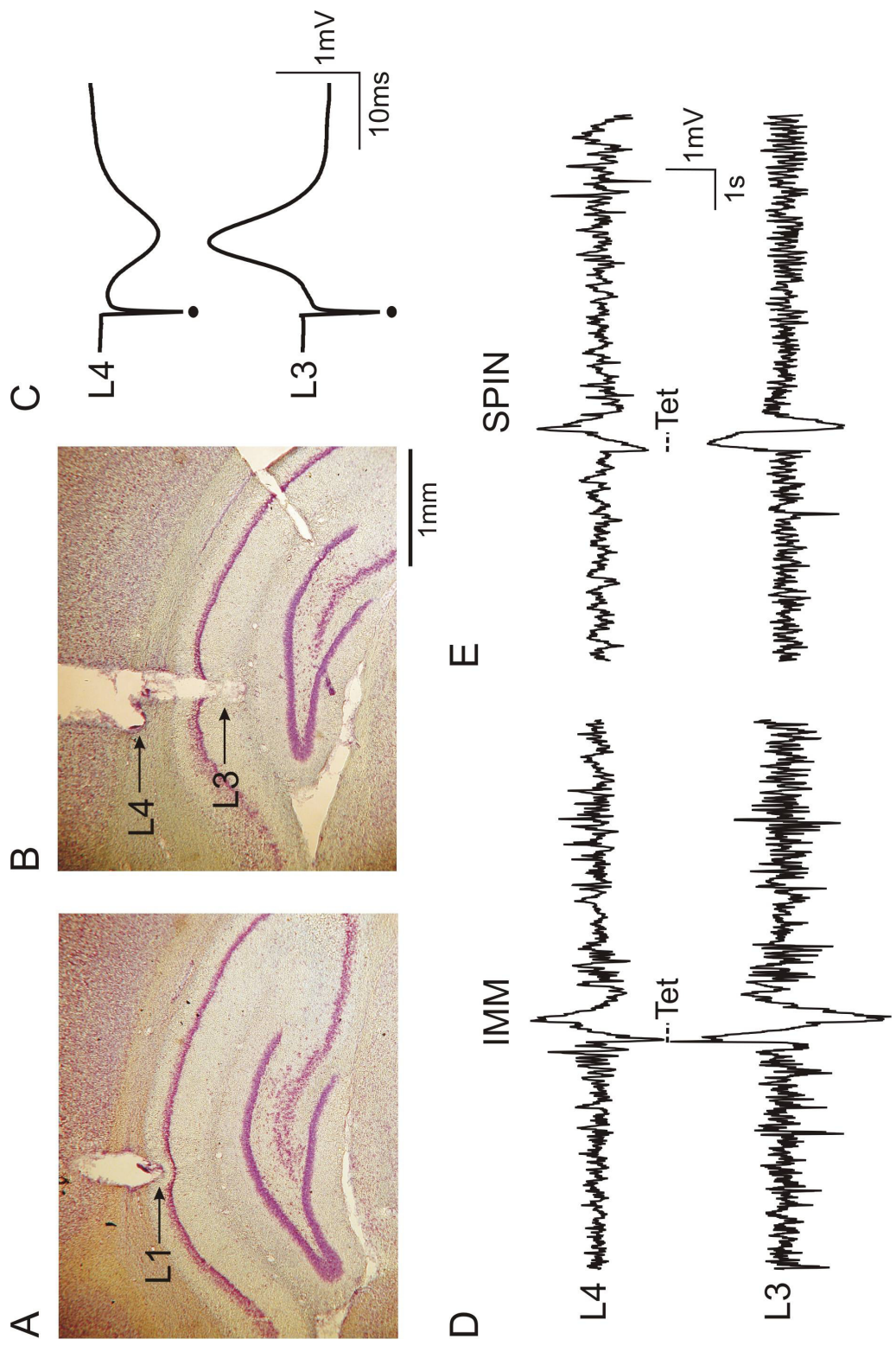


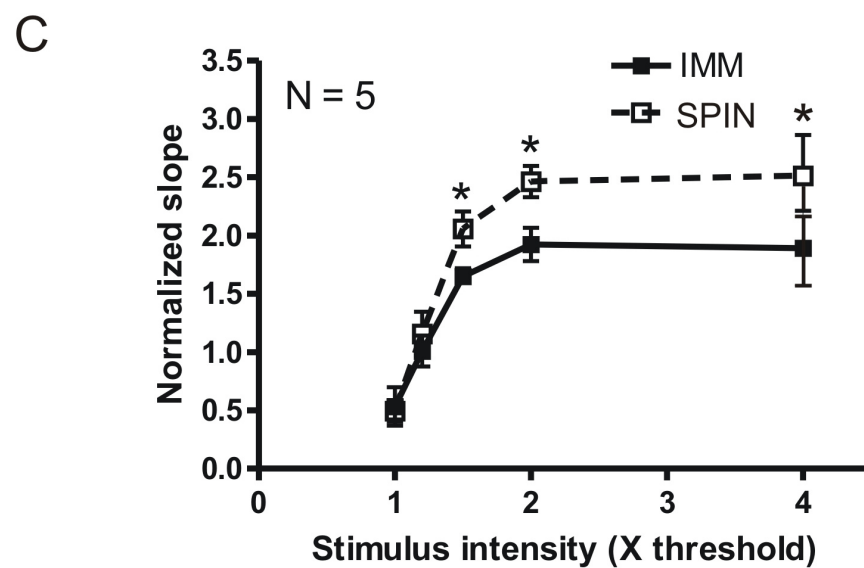
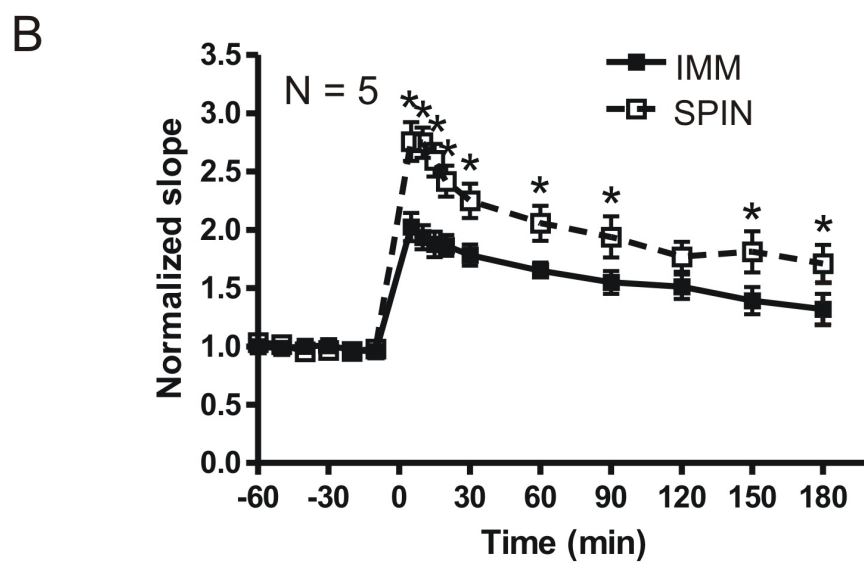
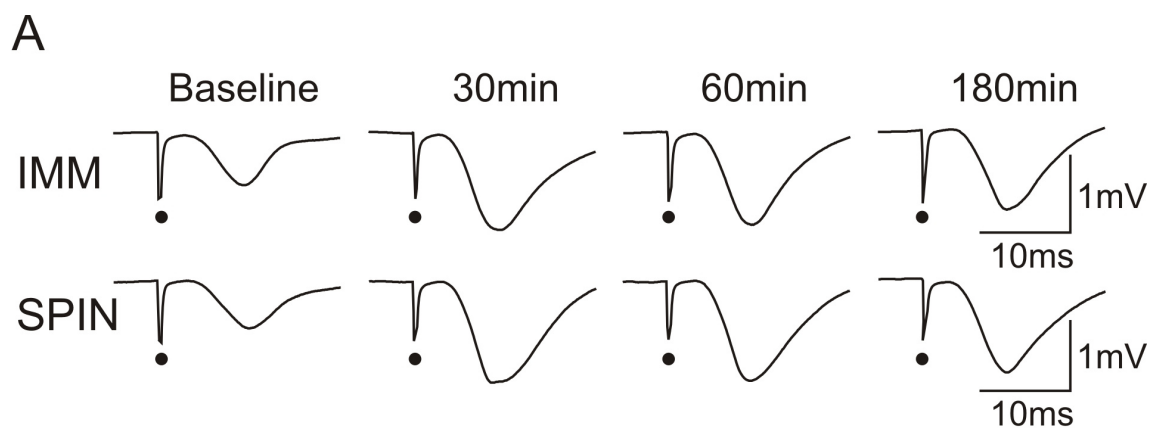
Fig. 3.1D) and a theta rhythm during rotation (SPIN; Fig. 3.1E). The average stimulus intensity for a single-pulse (0.2 ms duration) fEPSP threshold response ($23 \pm 2 \mu\text{A}$, $n = 15$ rats) or for tetanic stimulation ($27 \pm 2 \mu\text{A}$, $n = 30$ sessions), was not significantly different across experimental groups (one-way ANOVA, $P > 0.1$). In each rat, AEPs elicited prior to tetanus by the same stimulus intensity were analyzed. The average slope ($n = 12$ sessions) had decayed to $85.7 \pm 2.9 \%$ at the stratum oriens electrode and $88.3 \pm 3.5 \%$ at the stratum radiatum electrode, compared to the previous session.

After a 0.5-s 200-Hz train stimulation of stratum oriens, enhancement of basal dendritic fEPSPs was found at both stratum oriens and stratum radiatum recording electrodes. The figures will present only the negative fEPSPs recorded at the alveus/stratum oriens electrode, which was directly generated by a basal dendritic excitatory sink in CA1 (Leung and Peloquin, 2010).

3.3.1 Induction of basal-dendritic LTP in normal intact rats

LTP was shown as an increase in the slope and peak of the fEPSPs, above that during baseline. The LTP induced during IMM peaked at about 2 times the average baseline slope immediately after tetanus, and then gradually declined to about 1.5 times baseline slope at 180 min after tetanus (Fig. 3.2A, B). LTP induced during passive rotation (SPIN) showed a magnitude larger than that induced during IMM, but with a similar time course (Fig. 3.2A, B). Repeated measures block two-way ANOVA revealed significant group (SPIN vs IMM) and interaction effects for the potentiation recorded at the stratum oriens electrode (group effect, $F_{(1,4)} = 22.93$, $P < 0.009$; group x time, $F_{(9,36)} = 35.40$, $P < 0.0001$). Newman-Keuls post-hoc tests showed a significant difference

Fig. 3.2 Basal-dendritic LTP was larger when induced during rotation (SPIN) than when induced during immobility (IMM) in intact rats. (A) Traces of fEPSP at the stratum oriens electrode of a representative rat at baseline (before tetanus), 30, 60 and 180 min after tetanus. To facilitate comparison, the fEPSPs were scaled to make the peak amplitudes of the baseline response appear identical. (B) Normalized fEPSP slope (mean \pm SEM) was plotted as a function of time. The maximal falling slope of the fEPSP (within 2 ms interval) after tetanus was normalized by the grand average of the last six average fEPSPs taken prior to tetanus. LTP was larger when tetanus was delivered during SPIN than during IMM, as confirmed by a significant repeated measures block two-way (group x behavior) ANOVA. (C) Normalized fEPSP slope was plotted as a function of stimulus intensity (X threshold) 1h after LTP induction during IMM or SPIN. * $P < 0.01$: difference between IMM and SPIN using Newman-Keuls test following a significant repeated measures block two-way ANOVA.



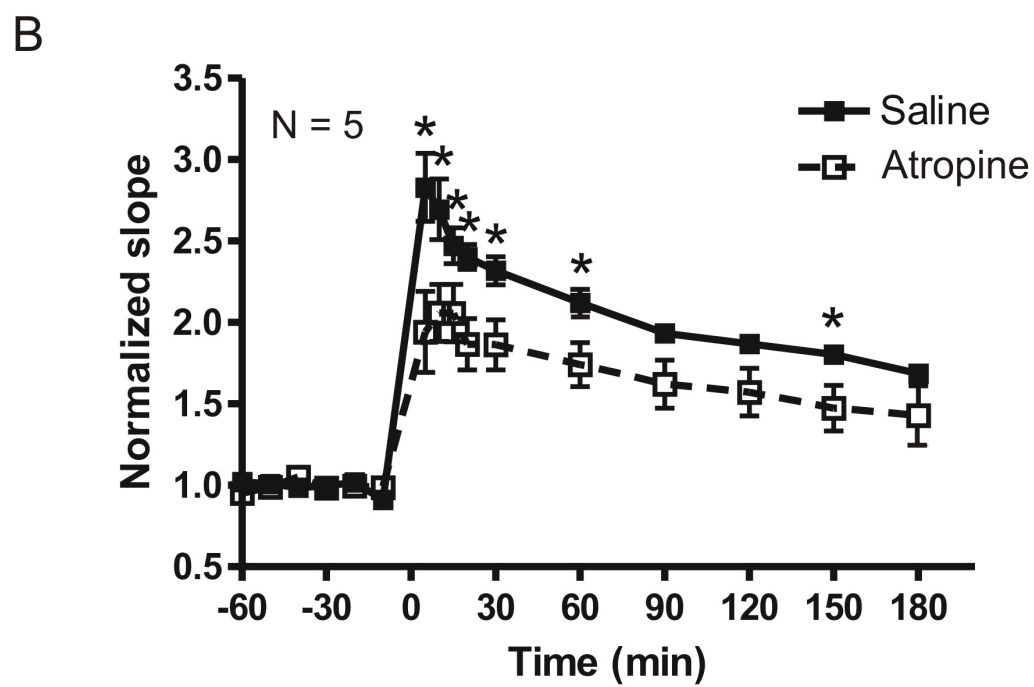
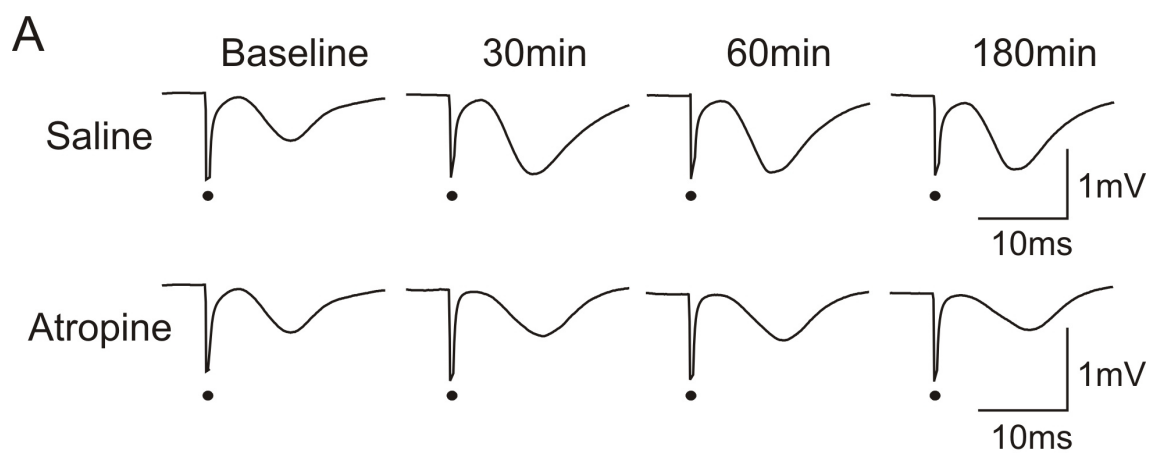
between SPIN and IMM at all time points except 120 min post-tetanus ($P < 0.01$). In addition, there was a significant difference in the LTP at the stratum radiatum electrode (group: $F_{(1,4)} = 17.18$, $P < 0.02$; group x time: $F_{(9,36)} = 9.57$, $P < 0.0001$; repeated measures block two-way ANOVA). For stratum radiatum electrode, Newman-Keuls post-hoc tests revealed significance at 5-15 min post-tetanus ($P < 0.01$).

Input-output curves of the fEPSP slopes at the stratum oriens electrodes, recorded at 1h after tetanus, also confirmed that LTP was larger when induced during SPIN as compared that induced during IMM, at different stimulus intensities (Fig. 3.2C). Repeated measures block two-way ANOVA showed significant group and interaction effects between SPIN and IMM for the potentiation recorded 1h post-tetanus (group: $F_{(1,4)} = 15.51$, $P < 0.02$; group x stimulus intensity: $F_{(4,16)} = 7.11$, $P < 0.002$). Newman-Keuls post-hoc tests revealed that a significant difference between SPIN and IMM at stimulus intensities 1.5-4X fEPSP threshold ($P < 0.01$).

3.3.2 Effect of muscarinic cholinergic blockade on LTP during rotation

Since caloric stimulation of the vestibular receptors increased hippocampal acetylcholine levels (Horii et al., 1994; Horii et al., 1995) and recent evidence suggests that theta rhythm during passive rotation is atropine-sensitive (Tai et al., 2011; Shin et al., 2005; Shin, 2010), the increased cholinergic activity during rotation may be responsible for the facilitation of LTP. Therefore, to elucidate the involvement of cholinergic muscarinic receptors in LTP during rotation, rats were injected with atropine sulfate (50 mg/kg, i.p.) or an equal volume of saline 15 min before tetanus. At the stratum oriens electrode, the average LTP induced during rotation following atropine sulfate injection

Fig. 3.3 Rotation-associated enhancement of LTP was suppressed by muscarinic cholinergic antagonist atropine sulfate (50 mg/kg, i.p.). (A) Traces of fEPSP at the stratum oriens electrode of a representative rat at baseline (before tetanus), 30, 60 and 180 min after tetanus, with tetanus given during rotation at 15min after administration of atropine sulfate or saline. The fEPSPs were scaled to make peak amplitudes of the baseline responses appear identical. (B) Normalized fEPSP slopes (mean \pm SEM) with LTP induced during rotation after injection of either atropine sulfate or saline. A repeated measures block two-way ANOVA revealed a significant treatment effect. * $P < 0.05$: difference between saline and atropine sulfate using Newman-Keuls test following a significant repeated measures block two-way ANOVA.



was smaller than that induced following saline injection (Fig. 3.3). Repeated measures block two-way ANOVA revealed a non-significant main effect ($F_{(1,4)} = 6.68, P = 0.061$), but a significant interaction effect ($F_{(9,36)} = 31.85, P < 0.0001$). Newman-Keuls post-hoc tests showed that LTP, when tetanized during rotation, was significantly smaller after atropine sulfate than after saline at times 5-60 min and 150 min after tetanus ($P < 0.05$). Similarly, when measured at the stratum radiatum electrode, LTP following atropine sulfate was smaller than that following saline as shown by a non-significant main effect ($F_{(1,4)} = 5.53, P = 0.078$) and a significant interaction effect ($F_{(9,36)} = 30.76, P < 0.0001$; repeated measures block two-way ANOVA). Newman-Keuls post-hoc tests revealed significance at 5-15 min post-tetanus (at least $P < 0.05$).

3.3.3 Effect of lesion of septohippocampal cholinergic cells on LTP

To investigate whether cholinergic septohippocampal neurons contribute to hippocampal LTP, cholinergic neurons were lesioned by bilateral infusion of cholinotoxin 192 IgG-SAP into the MS. Both groups of rats, control sham-lesion ($n = 4$) and 192-IgG-SAP lesion ($n = 6$) groups, showed that LTP was induced during either IMM or SPIN, at both stratum oriens and stratum radiatum electrodes. In sham-lesion rats, LTP was larger when the tetanus was delivered during SPIN than during IMM (Fig. 3.4A, C). At the stratum oriens electrode, repeated measures block two-way ANOVA showed significant main ($F_{(1,3)} = 142.45, P < 0.002$) and interaction ($F_{(9,27)} = 2.51, P < 0.04$) effects, with significant differences between SPIN and IMM revealed by Newman-Keuls post-hoc tests at all times except 90 min post-tetanus. At the stratum radiatum electrode, LTP induced during SPIN as compared that induced during IMM was

Fig. 3.4 Cholinergic lesion of the medial septum (MS) abolished the difference in hippocampal basal-dendritic LTP induced during immobility (IMM) and rotation (SPIN). (A, B) Traces of fEPSP at the stratum oriens electrode of representative rats at baseline (before tetanus), 30, 60 and 180 min after tetanus in sham-lesion (A) and 192 IgG-saporin (192 IgG-SAP) lesion rats (B). The fEPSPs were scaled to make peak amplitudes of the baseline responses appear identical in A and B. (C, D) Normalized fEPSPs slopes (mean \pm SEM) were larger when tetanus was induced during SPIN compared to during IMM in sham-lesion rats (C). However, this behavioral modulation of LTP was absent in 192 IgG-SAP lesion rats (D). A repeated measures block two-way ANOVA revealed a significant IMM versus SPIN effect in sham-lesion rats but not in the 192 IgG-SAP lesion rats. * $P < 0.05$: difference between IMM and SPIN using Newman-Keuls test following a significant repeated measures block two-way ANOVA.

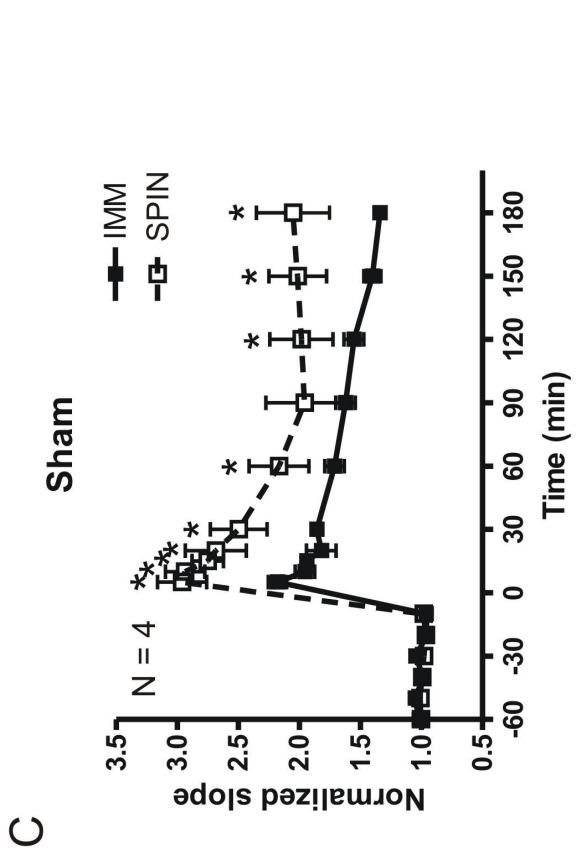
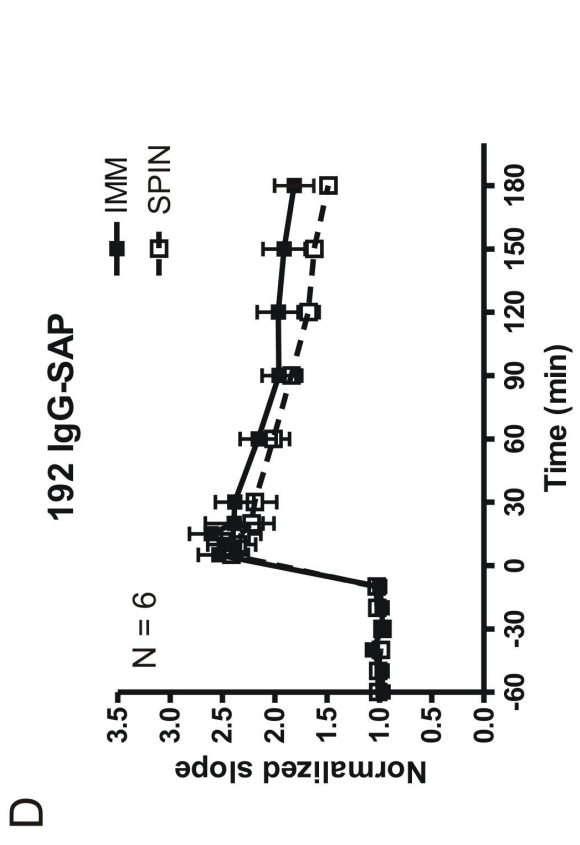
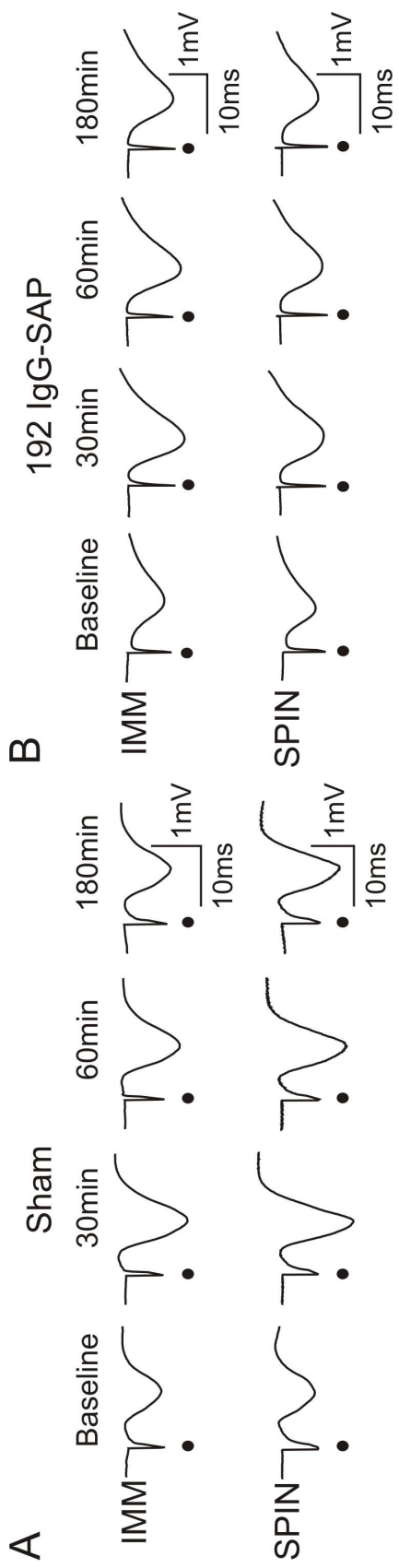
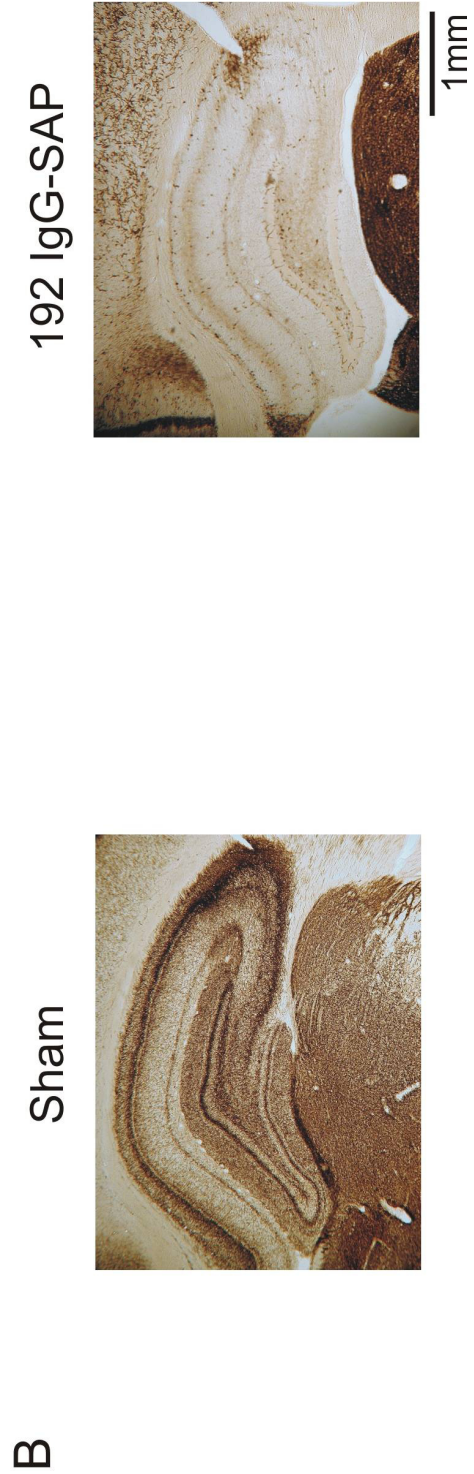
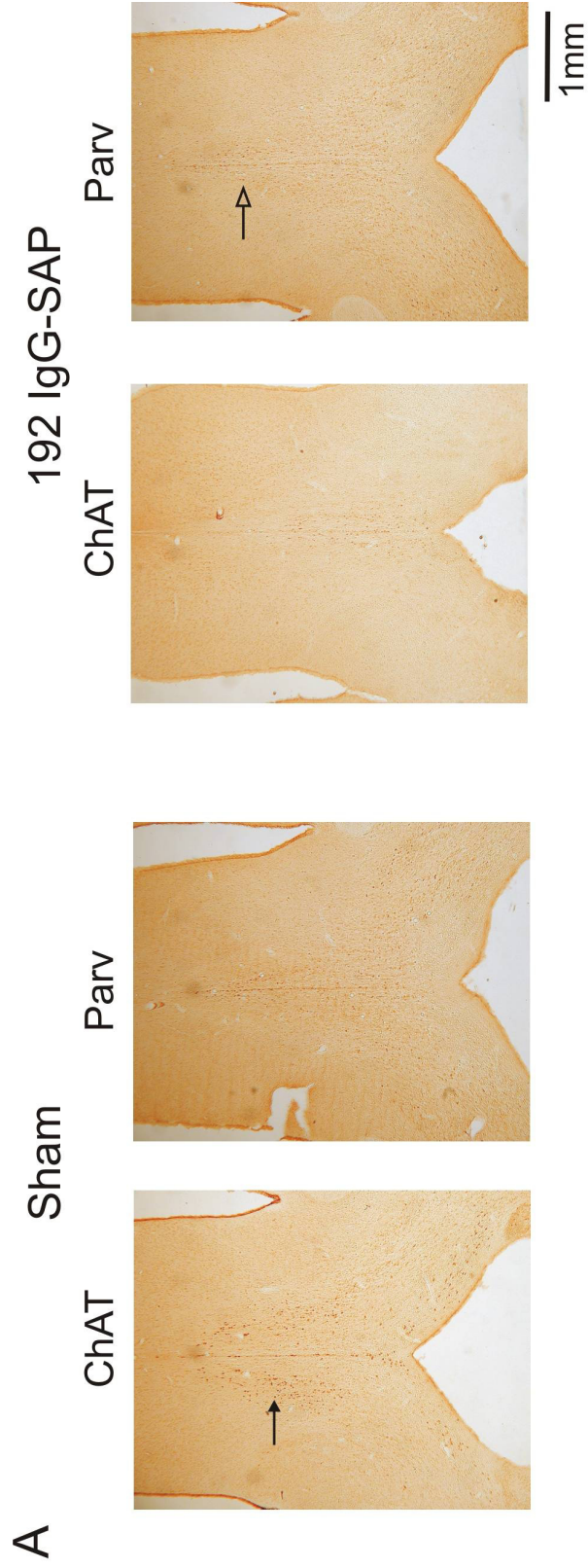


Fig. 3.5 Photomicrographs of representative coronal sections of the medial septum (MS) and the hippocampus in a sham-lesion and a 192 IgG-saporin (192 IgG-SAP) lesion rat. (A) Choline acetyltransferase (ChAT)- and parvalbumin (Parv) immunohistochemistry were performed on MS sections. (B) Hippocampal sections were stained for acetylcholinesterase (AChE). Note that there is a reduction of ChAT-immunopositive cholinergic neurons in the MS and a depletion of hippocampal AChE, as shown by a lighter stain, in the 192 IgG-SAP lesion rat. Parv-immunopositive GABAergic neurons in the MS were not affected. Solid and open arrows point to a ChAT- and Parv-immunopositive cell respectively.



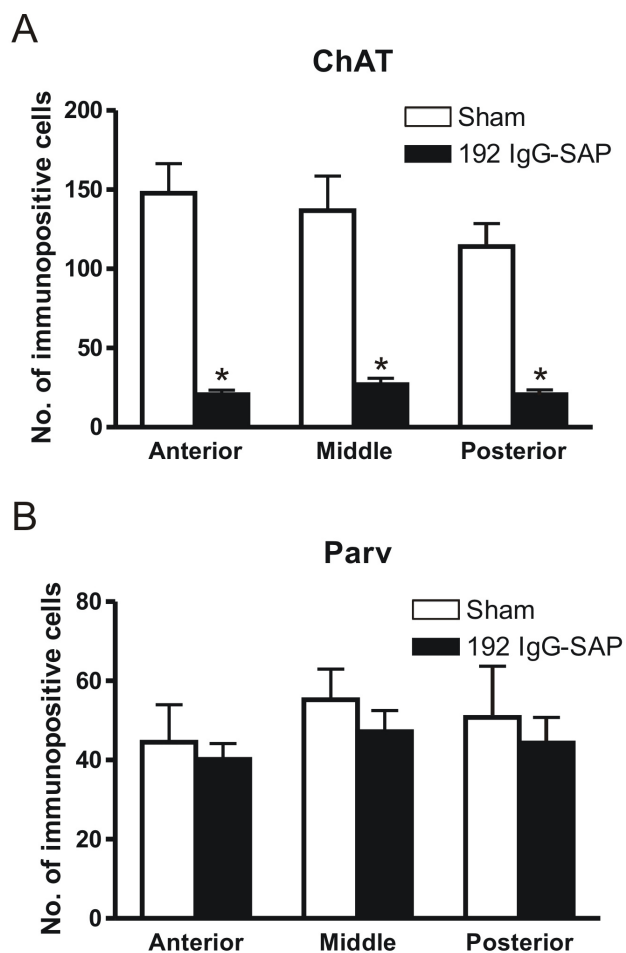


Fig. 3.6 Counts of choline acetyltransferase (ChAT)- and parvalbumin (Parv)-immunopositive cells from coronal sections of the medial septum (MS) of 192 IgG-saporin (192 IgG-SAP) lesion rats ($n = 6$) and sham-lesion rats ($n = 4$). (A) A significant decrease in the number of ChAT-immunopositive cholinergic neurons in 192 IgG-SAP as compared to sham lesion rats was observed in MS sections at three different anterior-posterior levels. (B) The number of Parv-immunopositive GABAergic neurons was not significantly different between sham and 192 IgG-SAP lesion rats. Values are expressed as mean \pm SEM. * $P < 0.01$: difference between 192 IgG-SAP lesion and sham-lesion rats at a particular level, using Newman-Keuls test after a significant two-way ANOVA.

enhanced for the entire 180 min post-tetanus, as demonstrated by Newman-Keuls post-hoc tests after a significant interaction effect ($F_{(9,27)} = 4.36$, $P < 0.002$) without a significant main effect ($F_{(1,3)} = 8.14$, $P = 0.065$; repeated measures block two-way ANOVA).

In contrast, distinct from sham-lesion rats, LTP induced during SPIN was not significantly different from that during IMM in 192 IgG-SAP lesion rats (Fig. 3.4B, D). At the stratum oriens electrode, repeated measures block two-way ANOVA did not show any significant main ($F_{(1,5)} = 4.13$, $P = 0.10$) or interaction ($F_{(9,45)} = 0.74$, $P = 0.67$) effect in 192 IgG-SAP lesion rats. Likewise, at the stratum radiatum electrode, there was no significant main ($F_{(1,5)} = 0.35$, $P = 0.58$) or interaction ($F_{(9,45)} = 0.41$, $P = 0.92$) effect in 192 IgG-SAP lesion rats.

When compared to control sham-lesion rats ($n = 4$), a decrease in the number of ChAT-immunopositive cells in the MS was found in 192 IgG-SAP lesion rats ($n = 6$; Fig. 3.5A, 3.6A). Two-way (group x section location) ANOVA showed a significant reduction in the number of ChAT-immunopositive neurons in 192 IgG-SAP lesion rats, as compared to sham-lesion rats ($F_{(1,2)} = 154.64$, $P < 0.0001$; Fig. 3.6A). Newman-Keuls post-hoc test displayed a significant decrease in the number of ChAT-immunopositive cells in 192 IgG-SAP lesion as compared to sham-lesion rats in all three frontal levels ($P < 0.01$, respectively). By contrast, the number of Parv-immunopositive cells in 192 IgG-SAP lesion rats was not different from that in sham-lesion rats, as confirmed by a two-way ANOVA ($F_{(1,2)} = 1.06$, $P = 0.31$; Fig. 3.5A, 3.6B). Moreover, there was a marked loss of AChE staining in the hippocampus in 192 IgG-SAP lesion rats, as compared with sham-lesion rats (Fig. 3.5B).

3.4 Discussion

This present study provides original results that vestibular stimulation by passive whole-body rotation enhanced hippocampal basal-dendritic LTP in freely behaving rats. LTP was facilitated when tetanus was delivered during rotation as compared to during awake-immobility. Systemic muscarinic cholinergic blockade by atropine sulfate or selective cholinotoxic (192 IgG-saporin) lesion of the MS abolished the enhancement of LTP. Therefore, LTP enhancement is mediated by activation of septohippocampal cholinergic neurons during rotation.

3.4.1 Vestibular stimulation enhances LTP

Basal dendritic LTP was enhanced when the tetanus was delivered during walking as compared to during awake-immobility (Leung et al., 2003). This is consistent with my results in which facilitation of LTP was observed when the rat was tetanized during whole-body passive rotation compared to during awake-immobility. A recent study showed that bilateral ablation of the vestibular apparatus had no effect on hippocampal LTP in behaving rats (Zheng et al., 2010). However, the latter study did not investigate LTP induced during different behaviors such as walking and rotation. To the best of my knowledge, there have been no studies demonstrating that vestibular stimulation can enhance hippocampal LTP in behaving rats.

Previous studies suggested that vestibular and other sensory information are transmitted to and processed in the hippocampus to facilitate spatial navigation (Berthoz,

1996; Etienne and Jeffery, 2004; Tsanov and Manahan-Vaughan, 2008). Vestibular inputs are necessary for path integration (O'Keefe and Nadel, 1978; Mittelstaedt and Mittelstaedt, 1980; McNaughton et al., 1996; McNaughton et al., 2006). Passive rotation has been shown to modulate the activity of place cells (Knierim et al., 1995; Wiener et al., 1995) while bilateral vestibular inactivation or damage abolished location-specific firing of place cells (Stackman et al., 2002; Russell et al., 2003). I suggest here that vestibular stimulation enhanced hippocampal LTP, which may be necessary for the formation of place fields (Muller et al., 1996; Dragoi et al., 2003; Isaac et al., 2009). Degradation of hippocampal place fields during walking by muscarinic blockade (Brazhnik et al., 2003) suggests that acetylcholine in the hippocampus is involved in place field formation, perhaps by enhancing LTP.

Besides depolarization by blocking potassium conductances (Krnjevic, 1993; Madison et al., 1987) and disinhibition by suppressing GABA release (Krnjevic et al., 1988), acetylcholine in the hippocampus may potentiate basal-dendritic LTP by facilitating NMDA receptors and their signaling pathways (Markram and Segal, 1992; Marino et al., 1998). LTP in hippocampal CA1 is sensitive to NMDA receptor antagonists including open-channel blocker MK-801 (Abraham and Mason, 1988; Leung and Shen, 1999). Moreover, NMDA receptor antagonists, including MK-801, dose-dependently impaired air righting, a set of complex movements requiring an intact vestibular labyrinth (Wayner et al., 2000).

I showed that LTP was larger when induced in the presence of a rotation-induced hippocampal theta rhythm than when induced during immobility when theta was absent. A theta rhythm was observed during passive rotation (Tai et al., 2011) and walking while

large irregular activity was observed during immobility (Vanderwolf, 1975; Leung, 1998). Walking (Dudar et al., 1979) and caloric vestibular stimulation (Horii et al., 1994; Horii et al., 1995) were shown to increase acetylcholine level in the hippocampus, and a high acetylcholine level was associated with the presence of a theta rhythm (Zhang et al., 2010; Keita et al., 2000; Vanderwolf, 1975; Leung, 1998; Leung and Vanderwolf, 1980). I showed here that muscarinic cholinergic activation during a rotation-induced theta rhythm is required for the enhancement of LTP. GABAergic and glutamatergic neurons in the MS may participate in generating a theta rhythm (Brazhnik and Fox, 1999; Alreja et al., 2000; Yoder and Pang, 2005; Huh et al., 2010), but the participation of these non-cholinergic inputs in hippocampal LTP during rotation and walking has not been shown.

3.4.2 Septohippocampal cholinergic modulation of LTP

Several *in vitro* studies have demonstrated a cholinergic enhancement of hippocampal LTP using cholinergic agonists or AChE inhibitors (Blitzer et al., 1990; Shimoshige et al., 1997; Hirotsu et al., 1989). In anesthetized rats, hippocampal LTP facilitated by tetanic stimulation of the MS was blocked by systemic administration of muscarinic cholinergic antagonists (Ovsepian et al., 2004). The duration of LTP in the dentate gyrus was prolonged after treatment with AChE inhibitors in aged behaving rats (Barnes et al., 2000). An AChE inhibitor physostigmine also facilitated basal dendritic LTP in CA1 of behaving rats during awake-immobility (Doralp and Leung, 2008).

I demonstrated that atropine sulfate and selective lesion of septohippocampal cholinergic neurons blocked the enhancement of LTP induced during rotation. Septal infusion of cholinotoxin 192 IgG-saporin effectively eliminated ~80% of cholinergic

ChAT-immunopositive cells, without affecting GABAergic Parv-immunopositive cells. Since the MS is the main source of acetylcholine for the hippocampus (Mesulam et al., 1983a; Mesulam et al., 1983b; Bagnoli et al., 1981), blockade of cholinergic influence on hippocampal physiology, in this case LTP, is expected to decrease drastically. The present results are consistent with previous studies in finding that pretreatment with muscarinic receptor antagonist scopolamine or specific M1 receptor antagonist pirenzepine or with septal 192-IgG-saporin lesion abolished the facilitation of LTP by walking as compared to immobility (Leung et al., 2003; Doralp and Leung, 2008). These results led us to propose that vestibular stimulation activates septohippocampal cholinergic neurons that release acetylcholine in the hippocampus, modulating hippocampal synaptic transmission and plasticity.

3.4.3 Conclusion

This present study provides original results that vestibular stimulation by passive whole-body rotation activates a septohippocampal cholinergic input, leading to enhancement of basal dendritic LTP in hippocampal CA1 of behaving rats. Activation of the vestibular system is a good model to investigate cholinergic modulation of LTP in behaving rats. Besides participating in formation of spatial memory (Hasselmo, 2006; Givens and Olton, 1995; Roland et al., 2008), septohippocampal cholinergic neurons may also be important for sensorimotor processing in which activation of the vestibular system provides a sensory signal to assist in motor planning (Bland and Oddie, 2001). A number of studies have demonstrated that vestibular stimulation can improve cognition in humans (reviewed in (Smith et al., 2010a; Smith et al., 2010b; Utz et al., 2010). Given

that synaptic plasticity is altered in patients with Alzheimer's disease (Gong and Lippa, 2010) and degeneration of basal forebrain cholinergic neurons is a pathological hallmark of this disease (Bartus et al., 1982; Francis et al., 1999; Wu et al., 2005; Wenk, 2006), vestibular stimulation may provide a novel treatment to improve hippocampal-dependent cognitive deficits in affected patients.

3.5 References

- Abraham WC, Mason SE (1988) Effects of the NMDA receptor/channel antagonists CPP and MK801 on hippocampal field potentials and long-term potentiation in anesthetized rats. *Brain Res* 462:40-46.
- Abraham WC, Williams JM (2003) Properties and mechanisms of LTP maintenance. *Neuroscientist* 9:463-474.
- Alreja M, Wu M, Liu W, Atkins JB, Leranath C, Shanabrough M (2000) Muscarinic tone sustains impulse flow in the septohippocampal GABA but not cholinergic pathway: implications for learning and memory. *J Neurosci* 20:8103-8110.
- Auerbach JM, Segal M (1996) Muscarinic receptors mediating depression and long-term potentiation in rat hippocampus. *J Physiol* 492 (Pt 2):479-493.
- Bagnoli P, Beaudet A, Stella M, Cuenod M (1981) Selective retrograde labeling of cholinergic neurons with [³H]choline. *J Neurosci* 1:691-695.
- Barnes CA, Rao G, Houston FP (2000) LTP induction threshold change in old rats at the perforant path--granule cell synapse. *Neurobiol Aging* 21:613-620.
- Bartus RT, Dean RL 3rd, Beer B, Lippa AS (1982) The cholinergic hypothesis of geriatric memory dysfunction. *Science* 217:408-414.
- Baxter MG, Bucci DJ, Gorman LK, Wiley RG, Gallagher M (1995) Selective immunotoxic lesions of basal forebrain cholinergic cells: effects on learning and memory in rats *Behav Neurosci* 109:714-722.
- Berger-Sweeney J, Heckers S, Mesulam MM, Wiley RG, Lappi DA, Sharma M (1994) Differential effects on spatial navigation of immunotoxin-induced cholinergic lesions of the medial septal area and nucleus basalis magnocellularis *J Neurosci* 14:4507-4519.
- Berthoz A (1996) How does the cerebral cortex process and utilize vestibular signals? In: *Disorders of the vestibular system*, (Baloh R, Halmagyi G eds), pp 113-125. Oxford: Oxford University Press.
- Bland BH, Oddie SD (2001) Theta band oscillation and synchrony in the hippocampal formation and associated structures: the case for its role in sensorimotor integration. *Behav Brain Res* 127:119-136.
- Bliss TV, Gardner-Medwin AR (1973) Long-lasting potentiation of synaptic transmission in the dentate area of the unanaesthetized rabbit following stimulation of the perforant path. *J Physiol* 232:357-374.

- Bliss TV, Lomo T (1973) Long-lasting potentiation of synaptic transmission in the dentate area of the anaesthetized rabbit following stimulation of the perforant path. *J Physiol* 232:331-356.
- Blitzer RD, Gil O, Landau EM (1990) Cholinergic stimulation enhances long-term potentiation in the CA1 region of rat hippocampus. *Neurosci Lett* 119:207-210.
- Brazhnik ES, Fox SE (1999) Action potentials and relations to the theta rhythm of medial septal neurons in vivo. *Exp Brain Res* 127:244-258.
- Brazhnik ES, Muller RU, Fox SE (2003) Muscarinic blockade slows and degrades the location-specific firing of hippocampal pyramidal cells *J Neurosci* 23:611-621.
- Chang Q, Gold PE (2004) Impaired and spared cholinergic functions in the hippocampus after lesions of the medial septum/vertical limb of the diagonal band with 192 IgG-saporin. *Hippocampus* 14:170-179.
- Doralp S, Leung LS (2008) Cholinergic modulation of hippocampal CA1 basal-dendritic long-term potentiation. *Neurobiol Learn Mem* 90:382-388.
- Dragoi G, Harris KD, Buzsaki G (2003) Place representation within hippocampal networks is modified by long-term potentiation. *Neuron* 39:843-853.
- Dudar JD, Whishaw IQ, Szerb JC (1979) Release of acetylcholine from the hippocampus of freely moving rats during sensory stimulation and running. *Neuropharmacology* 18:673-678.
- Etienne AS, Jeffery KJ (2004) Path integration in mammals. *Hippocampus* 14:180-192.
- Francis PT, Palmer AM, Snape M, Wilcock GK (1999) The cholinergic hypothesis of Alzheimer's disease: a review of progress. *J Neurol Neurosurg Psychiatry* 66:137-147.
- Givens B, Olton DS (1995) Bidirectional modulation of scopolamine-induced working memory impairments by muscarinic activation of the medial septal area. *Neurobiol Learn Mem* 63:269-276.
- Givens BS, Olton DS (1990) Cholinergic and GABAergic modulation of medial septal area: effect on working memory. *Behav Neurosci* 104:849-855.
- Gong Y, Lippa CF (2010) Review: disruption of the postsynaptic density in Alzheimer's disease and other neurodegenerative dementias. *Am J Alzheimers Dis Other Demen* 25:547-555.

- Hasselmo ME (2006) The role of acetylcholine in learning and memory. *Curr Opin Neurobiol* 16:710-715.
- Hirotsu I, Hori N, Katsuda N, Ishihara T (1989) Effect of anticholinergic drug on long-term potentiation in rat hippocampal slices. *Brain Res* 482:194-197.
- Horii A, Takeda N, Mochizuki T, Okakura-Mochizuki K, Yamamoto Y, Yamatodani A (1994) Effects of vestibular stimulation on acetylcholine release from rat hippocampus: an in vivo microdialysis study. *J Neurophysiol* 72:605-611.
- Horii A, Takeda N, Mochizuki T, Okakura-Mochizuki K, Yamamoto Y, Yamatodani A, Kubo T (1995) Vestibular modulation of the septo-hippocampal cholinergic system of rats. *Acta Otolaryngol Suppl* 520 Pt 2:395-398.
- Huh CY, Goutagny R, Williams S (2010) Glutamatergic neurons of the mouse medial septum and diagonal band of Broca synaptically drive hippocampal pyramidal cells: relevance for hippocampal theta rhythm. *J Neurosci* 30:15951-15961.
- Isaac JT, Buchanan KA, Muller RU, Mellor JR (2009) Hippocampal place cell firing patterns can induce long-term synaptic plasticity in vitro. *J Neurosci* 29:6840-6850.
- Jerusalinsky D, Kornisiuk E, Izquierdo I (1997) Cholinergic neurotransmission and synaptic plasticity concerning memory processing. *Neurochem Res* 22:507-515.
- Keita MS, Frankel-Kohn L, Bertrand N, Lecanu L, Monmaur P (2000) Acetylcholine release in the hippocampus of the urethane anaesthetised rat positively correlates with both peak theta frequency and relative power in the theta band. *Brain Res* 887:323-334.
- Kesner RP (1988) Reevaluation of the contribution of the basal forebrain cholinergic system to memory. *Neurobiol Aging* 9:609-616.
- Knierim JJ, Kudrimoti HS, McNaughton BL (1995) Place cells, head direction cells, and the learning of landmark stability. *J Neurosci* 15:1648-1659.
- Koelle GB, Friedenwald JS (1949) A histochemical method for localizing cholinesterase activity. *Proc Soc Exp Biol* 70:617-622.
- Krnjevic K (1993) Central cholinergic mechanisms and function. *Prog Brain Res* 98:285-292.
- Krnjevic K, Ropert N, Casullo J (1988) Septohippocampal disinhibition. *Brain Res* 438:182-192.
- Leung LS (1998) Generation of theta and gamma rhythms in the hippocampus. *Neurosci Biobehav Rev* 22:275-290.

- Leung LS, Peloquin P (2010) Cholinergic modulation differs between basal and apical dendritic excitation of hippocampal CA1 pyramidal cells. *Cereb Cortex* 20:1865-1877.
- Leung LS, Shen B (1999) N-methyl-D-aspartate receptor antagonists are less effective in blocking long-term potentiation at apical than basal dendrites in hippocampal CA1 of awake rats. *Hippocampus* 9:617-630.
- Leung LS, Shen B (1995) Long-term potentiation at the apical and basal dendritic synapses of CA1 after local stimulation in behaving rats. *J Neurophysiol* 73:1938-1946.
- Leung LS, Shen B (1993) Long-term potentiation in hippocampal CA1: effects of afterdischarges, NMDA antagonists, and anticonvulsants. *Exp Neurol* 119:205-214.
- Leung LS, Shen B, Rajakumar N, Ma J (2003) Cholinergic activity enhances hippocampal long-term potentiation in CA1 during walking in rats. *J Neurosci* 23:9297-9304.
- Leung LS, Vanderwolf CH (1980) Behavior-dependent evoked potentials in the hippocampal CA1 region of the rat. II. Effect of eserine, atropine, ether and pentobarbital. *Brain Res* 198:119-133.
- Luo T, Leung LS (2010) Endogenous histamine facilitates long-term potentiation in the hippocampus during walking. *J Neurosci* 30:7845-7852.
- Ma J, Shen B, Rajakumar N, Leung LS (2004) The medial septum mediates impairment of prepulse inhibition of acoustic startle induced by a hippocampal seizure or phencyclidine. *Behav Brain Res* 155:153-166.
- Madison DV, Lancaster B, Nicoll RA (1987) Voltage clamp analysis of cholinergic action in the hippocampus. *J Neurosci* 7:733-741.
- Marino MJ, Rouse ST, Levey AI, Potter LT, Conn PJ (1998) Activation of the genetically defined m1 muscarinic receptor potentiates N-methyl-D-aspartate (NMDA) receptor currents in hippocampal pyramidal cells. *Proc Natl Acad Sci U S A* 95:11465-11470.
- Markram H, Segal M (1992) The inositol 1,4,5-trisphosphate pathway mediates cholinergic potentiation of rat hippocampal neuronal responses to NMDA. *J Physiol* 447:513-533.
- Martin SJ, Grimwood PD, Morris RG (2000) Synaptic plasticity and memory: an evaluation of the hypothesis. *Annu Rev Neurosci* 23:649-711.

- McMahan RW, Sobel TJ, Baxter MG (1997) Selective immunolesions of hippocampal cholinergic input fail to impair spatial working memory *Hippocampus* 7:130-136.
- McNaughton BL, Barnes CA, Gerrard JL, Gothard K, Jung MW, Knierim JJ, Kudrimoti H, Qin Y, Skaggs WE, Suster M, Weaver KL (1996) Deciphering the hippocampal polyglot: the hippocampus as a path integration system. *J Exp Biol* 199:173-185.
- McNaughton BL, Battaglia FP, Jensen O, Moser EI, Moser MB (2006) Path integration and the neural basis of the 'cognitive map'. *Nat Rev Neurosci* 7:663-678.
- Mesulam MM, Mufson EJ, Levey AI, Wainer BH (1983a) Cholinergic innervation of cortex by the basal forebrain: cytochemistry and cortical connections of the septal area, diagonal band nuclei, nucleus basalis (substantia innominata), and hypothalamus in the rhesus monkey *J Comp Neurol* 214:170-197.
- Mesulam MM, Mufson EJ, Wainer BH, Levey AI (1983b) Central cholinergic pathways in the rat: an overview based on an alternative nomenclature (Ch1-Ch6). *Neuroscience* 10:1185-1201.
- Mittelstaedt ML, Mittelstaedt H (1980) Homing by path integration in a mammal. *Naturewissenschaften* 67:556-567.
- Muller RU, Stead M, Pach J (1996) The hippocampus as a cognitive graph. *J Gen Physiol* 107:663-694.
- Neves G, Cooke SF, Bliss TV (2008) Synaptic plasticity, memory and the hippocampus: a neural network approach to causality. *Nat Rev Neurosci* 9:65-75.
- O'Keefe J, Nadel L (1978) *The hippocampus as a cognitive map*. pp 570. Oxford: Clarendon Press.
- Ovsepian SV, Anwyl R, Rowan MJ (2004) Endogenous acetylcholine lowers the threshold for long-term potentiation induction in the CA1 area through muscarinic receptor activation: in vivo study. *Eur J Neurosci* 20:1267-1275.
- Paxinos G, Watson C (1997) *The rat brain in stereotaxic coordinates*. San Diego: Academic Press.
- Roland JJ, Mark K, Vetreno RP, Savage LM (2008) Increasing hippocampal acetylcholine levels enhance behavioral performance in an animal model of diencephalic amnesia. *Brain Res* 1234:116-127.
- Russell NA, Horii A, Smith PF, Darlington CL, Bilkey DK (2003) Long-term effects of permanent vestibular lesions on hippocampal spatial firing. *J Neurosci* 23:6490-6498.

- Sarter M, Hasselmo ME, Bruno JP, Givens B (2005) Unraveling the attentional functions of cortical cholinergic inputs: interactions between signal-driven and cognitive modulation of signal detection. *Brain Res Brain Res Rev* 48:98-111.
- Shen J, Barnes CA, Wenk GL, McNaughton BL (1996) Differential effects of selective immunotoxic lesions of medial septal cholinergic cells on spatial working and reference memory. *Behav Neurosci* 110:1181-1186.
- Shimoshige Y, Maeda T, Kaneko S, Akaike A, Satoh M (1997) Involvement of M2 receptor in an enhancement of long-term potentiation by carbachol in Schaffer collateral-CA1 synapses of hippocampal slices. *Neurosci Res* 27:175-180.
- Shin J (2010) Passive rotation-induced theta rhythm and orientation homeostasis response. *Synapse* 64:409-415.
- Shin J, Kim D, Bianchi R, Wong RK, Shin HS (2005) Genetic dissection of theta rhythm heterogeneity in mice. *Proc Natl Acad Sci U S A* 102:18165-18170.
- Smith PF, Darlington CL, Zheng Y (2010a) Move it or lose it--is stimulation of the vestibular system necessary for normal spatial memory? *Hippocampus* 20:36-43.
- Smith PF, Geddes LH, Baek JH, Darlington CL, Zheng Y (2010b) Modulation of memory by vestibular lesions and galvanic vestibular stimulation. *Front Neurol* 1:141.
- Stackman RW, Clark AS, Taube JS (2002) Hippocampal spatial representations require vestibular input. *Hippocampus* 12:291-303.
- Tai SK, Ma J, Ossenkopp KP, Leung LS (2011) Activation of immobility-related hippocampal theta by cholinergic septohippocampal neurons during vestibular stimulation. *Hippocampus* doi: 10.1002/hipo.20955.
- Tsanov M, Manahan-Vaughan D (2008) Synaptic plasticity from visual cortex to hippocampus: systems integration in spatial information processing. *Neuroscientist* 14:584-597.
- Utz KS, Dimova V, Oppenlander K, Kerkhoff G (2010) Electrified minds: transcranial direct current stimulation (tDCS) and galvanic vestibular stimulation (GVS) as methods of non-invasive brain stimulation in neuropsychology--a review of current data and future implications. *Neuropsychologia* 48:2789-2810.
- Vanderwolf CH (1975) Neocortical and hippocampal activation relation to behavior: effects of atropine, eserine, phenothiazines, and amphetamine. *J Comp Physiol Psychol* 88:300-323.

- Walsh TJ, Herzog CD, Gandhi C, Stackman RW, Wiley RG (1996) Injection of IgG 192-saporin into the medial septum produces cholinergic hypofunction and dose-dependent working memory deficits. *Brain Res* 726:69-79.
- Wayner MJ, Tracy HA, Armstrong DL, Phelix CF (2000) Air righting: role of the NMDA receptor channel and hippocampal LTP. *Physiol Behav* 69:505-510.
- Wenk GL (2006) Neuropathologic changes in Alzheimer's disease: potential targets for treatment. *J Clin Psychiatry* 67 Suppl 3:3-7; quiz 23.
- Wiener SI, Korshunov VA, Garcia R, Berthoz A (1995) Inertial, substratal and landmark cue control of hippocampal CA1 place cell activity. *Eur J Neurosci* 7:2206-2219.
- Wiley RG, Oeltmann TN, Lappi DA (1991) Immunolesioning: selective destruction of neurons using immunotoxin to rat NGF receptor. *Brain Res* 562:149-153.
- Wu CK, Thal L, Pizzo D, Hansen L, Masliah E, Geula C (2005) Apoptotic signals within the basal forebrain cholinergic neurons in Alzheimer's disease. *Exp Neurol* 195:484-496.
- Yoder RM, Pang KC (2005) Involvement of GABAergic and cholinergic medial septal neurons in hippocampal theta rhythm. *Hippocampus* 15:381-392.
- Zhang H, Lin SC, Nicolelis MA (2010) Spatiotemporal coupling between hippocampal acetylcholine release and theta oscillations in vivo. *J Neurosci* 30:13431-13440.
- Zheng Y, Mason-Parker SE, Logan B, Darlington CL, Smith PF, Abraham WC (2010) Hippocampal synaptic transmission and LTP in vivo are intact following bilateral vestibular deafferentation in the rat. *Hippocampus* 20:461-468.

Chapter 4

Activation of Septohippocampal GABAergic Neurons Facilitates Population Spike and Modulates Single Unit Activities in the Dentate Gyrus

4.1 Introduction

As a result of the pathological loss of cholinergic neurons in the basal forebrain observed in patients with Alzheimer's disease, much attention has been focused on the cholinergic neurons in the medial septum (MS) which are the primary source of acetylcholine (Mesulam et al., 1983; Nyakas et al., 1987) for the hippocampus, a structure important in memory function (Givens and Olton, 1990; Chang and Gold, 2004). However, other neurons in the MS such as the septohippocampal GABAergic cells which are known to selectively innervate hippocampal GABAergic interneurons (Freund and Antal, 1988) may also play a role. Several selective immunotoxin lesion studies indicated that the integrity of septal GABAergic neurons, but not septal cholinergic neurons, is essential for spatial performance in rats. For instance, depletion of cholinergic neurons by intraseptal injection of the immunotoxin 192 immunoglobulin G-saporin (192 IgG-saporin) produced no or mild effects in spatial memory tasks (Berger-Sweeney et al., 1994; Baxter et al., 1995; Dornan et al., 1997; McMahan et al., 1997; Pang and Nocera, 1999), but some impairments were reported in other studies (Walsh et al., 1996; Chang and Gold, 2004). Recently, lesion of septal GABAergic neurons with orexin-saporin

impaired spatial memory in the Morris water maze (Smith and Pang, 2005; LeCourtier et al., 2010).

Hippocampal theta rhythm, an EEG wave implicated in sensorimotor integration, learning and memory, has a frequency that ranges from 3 to 6 Hz in anesthetized rats and from 4 to 10 Hz in behaving animals (Bland, 1986; Leung, 1998; Buzsaki, 2002). Previous studies, primarily using muscarinic receptor antagonist atropine, suggested that spontaneous theta in urethane-anesthetized rats (Stumpf, 1965; Kramis et al., 1975; Monmaur et al., 1993) and immobility-related theta in behaving rats (Monmaur and Breton, 1991) depend on septal cholinergic input. However, several studies have shown otherwise. For example, lesion of cholinergic cells by intracerebroventricular injection of 192 IgG-saporin failed to abolish spontaneous hippocampal theta in anesthetized rats (Apartis et al., 1998) or immobility-related theta in freely moving (Bassant et al., 1995) and unanesthetized restrained rats (Apartis et al., 1998). In addition, GABAergic septal cells displayed tight phase coupling (i.e. firing preferentially at theta peak or trough) with hippocampal theta (Borhegyi et al., 2004; Varga et al., 2008). Meanwhile, cholinergic septal cells did not show theta-related burst or tonic activity (Simon et al., 2006), suggesting that GABAergic septal cells play a key role in theta generation.

Septal pulse stimulation prior to perforant path pulse stimulation facilitated the dentate population spike (Fantie and Goddard, 1982; Bilkey and Goddard, 1985). This facilitation was eliminated by hippocampal administration of the GABA_A receptor antagonist picrotoxin (Bilkey and Goddard, 1985), but was unaffected by systemic injections of muscarinic and nicotinic cholinergic antagonists (Fantie and Goddard, 1982), implying that septal facilitation is GABA-mediated. However, it is unclear if

GABAergic neurons in the MS or the hippocampus are involved. In the present study, selective lesion of septal GABAergic neurons was carried out by intraseptal infusion of orexin-saporin as outlined previously (Berchtold et al., 2002; Smith and Pang, 2005; LeCourtier et al., 2010). EEGs and evoked field potentials were recorded in the DG of urethane-anesthetized and behaving rats, following paired-pulse stimulation of the medial perforant path (MPP). Unit activities were also recorded in anesthetized rats. I hypothesize that the loss of septal GABAergic cells reduces the disinhibition of granule cells by enhancing hippocampal GABAergic inhibition. Preliminary results of this report were presented in an abstract (Tai and Leung, 2009).

4.2 Material and methods

4.2.1 Lesion, sham and control rats

Experiments were conducted on 62 adult male Long Evans hooded rats (250-420 g; Charles River Canada, St. Constant, Quebec, Canada). All animals were given food and water ad libitum and housed in pairs in Plexiglas cages under climate-controlled conditions on a 12 h light/dark cycle (lights on at 7:00 A.M.). Three groups of rats were used: (i) rats with septal GABAergic neurons lesioned with orexin-saporin, (ii) rats with saline infused into the MS (Sham) and (iii) control rats consisting of intact rats with no lesions. All experimental procedures were approved by the local Animal Use Committee and conducted according to the guidelines of Canadian Council for Animal Care. All efforts were taken to minimize pain and suffering of animals.

4.2.2 Lesion of GABAergic cells in the medial septum

GABAergic neurons in the MS were lesioned using orexin-saporin (Advanced Targeting Systems, San Diego, CA) under sodium pentobarbital (60 mg/kg i.p.) anesthesia. Orexin-saporin is a neurotoxin created by conjugating the orexin-2 receptor-binding ligand orexin to a ribosome-inactivating toxin saporin. Although orexin-2 receptor is highly expressed in both GABAergic and cholinergic neurons in the MS, a dose of 100 ng/ μ l was shown to preferentially eliminate GABAergic cells while leaving most cholinergic cells intact (Smith and Pang, 2005). Orexin-saporin was diluted with sterile saline to 100 ng/ μ l. Two 30-gauge needles, each attached to a Hamilton syringe, were inserted bilaterally into the MS (A +0.5, L \pm 0.5; units in mm) using the atlas of Paxinos and Watson (1997). The needles were first lowered to 5.7 mm ventral to the skull surface (V) where 0.3 μ l of orexin-saporin was injected, and then to V 7.8 where 0.4 μ l was injected. Sham rats were infused with sterile saline in the same manner. All infusions were performed at a constant rate of 0.5 μ l/10 minutes via an infusion pump (Harvard Apparatus, South Natick, MA). The needles remained in place for 10 minutes after each infusion. Hippocampal EEGs, evoked potentials and single unit activities were recorded 2-4 weeks following lesion.

4.2.3 Electrophysiological procedure in anesthetized rats

Under urethane anesthesia (1.2–1.5 g/kg i.p.), the rat was placed in a stereotaxic frame and maintained at a body temperature of 37°C. The recording electrode (16-channel silicon probe or tungsten microelectrode) was positioned in the dentate gyrus

(DG; P 3.8-4.2, L 2.4-3). Stimulating electrodes (125 μm Teflon-insulated wires except at the cut tip) were placed in the PNO (P 7.5, L 1, V 7-8) and medial perforant path (MPP; P 8, L 4-4.5, V 3.3-3.6). A jeweller's screw in the skull plate over the frontal cortex served as the anode, while another screw over the cerebellum served as a recording ground. Cathodal stimulus currents were delivered (with pulse duration of 0.2 ms) through a photo-isolated stimulus isolation unit (PSIU6, Astro-Med/Grass Instruments, West Warwick, RI). Stimulation repetition rate was at 0.1 Hz. At the end of the experiments, lesion was made by passing a DC current of 0.3 mA for 0.5 s through the stimulating electrodes.

In a urethane-anesthetized rat, hippocampal theta rhythm occurs spontaneously or more reliably induced by tail pinching or electrical stimulation of the brainstem such as the PNO (Vertes, 1981; Bland et al., 1994; Heynen and Bilkey, 1994; Jiang and Khanna, 2004). Signals triggering theta arise from the PNO ascend to the MS before reaching the hippocampus (Bland, 1986; Vertes and Kocsis, 1997; Takano and Hanada, 2009). As a result, electrical stimulation of PNO induces a hippocampal theta in anesthetized rats (Barrenechea et al., 1995; Kirk et al., 1996; Teruel-Marti et al., 2008; Leung and Peloquin, 2010). In my experiments, a 100-Hz train stimulation of 1 s duration was applied to PNO (pulses of 150 μA and 0.2 ms duration) to elicit a hippocampal theta rhythm (Leung and Peloquin, 2010), with thresholds 60 - 75 μA . PNO-induced theta had amplitude and phase profiles that resembled the physiological theta (Heynen and Bilkey, 1994). Direct stimulation of the MS was not used in this study because it would directly activate all septal neurons simultaneously without reliably inducing a hippocampal theta

rhythm (Kramis et al., 1980); in addition, backfiring of hippocamptoseptal afferents is possible.

4.2.4 Recordings from the 16-channel probe in anesthetized rats

Silicon recording probes (NeuroNexus Technologies, Ann Arbor, MI) had 16 recording sites spaced 50 μm apart on a vertical shank. The signals were amplified 200–1000x by preamplifier and amplifier, passed through a high-pass filter with 0.08 Hz corner frequency, and acquired by custom made software using a Tucker Davis Technologies (Alachua, FL) real-time processor system RA-16 (Townsend et al., 2002; Leung and Peloquin, 2010). Single and averaged ($n = 4$) sweeps were stored and one-dimensional current source density (CSD) as a function of depth z and time t was calculated by a second-order differencing formula (Freeman and Nicholson, 1975; Leung, 2010):

$$\text{CSD}(z, t) = \sigma [2\Phi(z, t) - \Phi(z + \Delta z, t) - \Phi(z - \Delta z, t)] / (\Delta z)^2$$

where $\Phi(z, t)$ is the potential at depth z and time t , Δz is the spacing (50 μm) between adjacent electrodes on the 16-channel probe. Since simultaneously acquired signals were sufficiently noise free, no spatial smoothing of the CSDs was necessary. The conductivity σ was assumed to be constant and the CSDs were reported in units of V/mm^2 .

Field potentials recorded from the probe were subjected to CSD analysis. The excitatory current sink (E1) was measured by its maximal slope during the falling phase at the depth of the sink maximum (i.e., the middle third of the molecular layer). The population spike amplitude (P1) was measured from the CSD trace at the granule cell

layer by dropping a vertical line from the negative sink to the tangent between the two positive peaks. A paired-pulse stimulation protocol consisted of two pulses of equal stimulus intensity delivered to MPP at various interpulse intervals (30, 50, 80, 100, 150, 200 and 400 ms). The stimulus intensity of these pulses (P1) was set at 50-70% of the maximal population spike amplitude. The magnitude of the inhibitory effect of hippocampal GABAergic interneurons on the activity of granule cells was reflected by the P2/P1 (or E2/E1) ratio which was calculated by dividing the amplitude (or slope) of the second or test pulse P2 (or E2) by that of the first or conditioning pulse P1 (or E1). The larger the ratio, the smaller is the effect of inhibition.

After 1 s of PNO activation, 1.67 s of EEG was analyzed by Fast Fourier Transform and shown as autopower spectra with 0.75 Hz resolution (Leung, 1985). Only the electrode of the silicon probe (4-6th electrode, in the molecular layer) showing the largest theta power was used for analyzing theta power. Theta peak frequency and power were measured at the peak of the power spectra.

4.2.5 Recordings from the tungsten microelectrode in anesthetized rats

Single unit activity and evoked field potentials in the granule cell layer were recorded using an epoxyite-insulated tungsten microelectrode (9-12 M Ω impedance at 1 kHz; FHC Inc., ME) lowered using an Inchworm piezoelectric micromanipulator (Exfo Burleigh Products Group, Victor, NY). Localization was assessed by the characteristic waveforms elicited by MPP stimulation and by the increase in unit activity upon entering CA1 and dentate cell layer. The signal was amplified (100x for field potentials, 5000x for unit activity) and filtered (band-pass 1-10 kHz for field potentials, 500-5 kHz for unit

activity). The signal was digitized at 100 kHz using SciWorks 7 program (DataWave Technologies, Berthoud, CO). Units that crossed a set detection threshold were recorded and analyzed off-line. Interneurons and granule cells were distinguished on the basis of their waveform parameters (e.g. spike width and valley amplitude) such that they form separate dense patches of points (clusters). To improve clustering, principal component analysis (PCA) was used. It maps the data from a high-dimensional space to a space with lower (fewer) dimensional in a way that variance of the data is maximized. Therefore, the first principal component (PC1) represents the direction with the largest variation.

Spontaneous units ($n = 37$) prior to MPP stimulation but immediately following PNO stimulation were analyzed. In the paired-pulse stimulation experiment, unit recordings were made with 20 and 25 ms IPIs. Since 20 ms IPI resulted in greater paired pulse depression than 25 ms IPI, only units evoked by the test pulse with 20 ms IPI ($n = 24$) were presented in this study. Histograms showing temporal relations of unit occurrences to itself (autocorrelogram) and to the occurrence of units in the other identified cluster (cross-correlogram) were plotted. In addition, peristimulus time histograms showing the timing of unit firings upon the onset of the conditioning MMP pulse was plotted. The firing frequency of a cell at each bin was divided by the total firing frequency of each cell following each pulse of MPP stimulation. Bin size for all histograms was set at 1 ms. Probability of activation of each cluster was calculated from unit activities of at least 25 paired-pulse responses at five different stimulus intensities (below EPSP threshold, EPSP threshold, above EPSP threshold, population spike threshold, above population spike threshold).

4.2.6 Electrophysiological procedure and recordings in behaving rats

Under sodium pentobarbital (60 mg/kg i.p.) anesthesia, bipolar electrodes were placed bilaterally in the DG (P 3.8, L 2.5). Recording electrodes were implanted such that the deep and surface electrodes were located in the polymorphic (hilus) and the molecular layers respectively. The dorsal-ventral depth was optimized by monitoring field potentials while stimulating the ipsilateral MPP (P 7.5, L 4.4, V 3.3-3.6). Each electrode comprised of a 125- μ m stainless steel wire insulated with Teflon, except at the cut end. A jeweler's screw, placed over the occipital bone plate, served as recording reference. Additional screws were inserted to anchor the implant to the skull. All electrodes and screws were fixed on the skull with dental cement.

After allowing at least 7 days to recover from the last surgery, hippocampal EEG and field potentials was recorded during awake immobility and walking. During awake immobility (Imm), the rat stood motionless in an alert state with eyes opened and head held above ground. Walking behavior (Walk) consisted of horizontal walking and rearing. EEG recorded from the surface electrode was sampled at 200 Hz after averaging 5 consecutive samples digitized at 1 KHz, which contributed 3 dB and 10 dB attenuation points at 84 Hz and 180 Hz, respectively. Artifact-free segments of the EEG were manually selected, with each segment consisting of 1024 points or 5.12 s duration. A power spectrum was constructed from at least 6 segments, and after smoothing and averaging, spectral estimates had 0.195 Hz resolution, 2.15 Hz bandwidth (interval of smoothing) and >60 degrees of freedom (Leung, 1985).

Field potentials from the deep electrodes were recorded, following paired-pulse stimulation of the ipsilateral MPP at various interpulse intervals (20, 30, 50, 80, 100, 150

and 200 ms). In each rat, an average evoked potential (average of 8 sweeps) was recorded following stimulation at two times the population spike threshold (25-120 μ A, 0.2 ms pulse duration, repeated at 0.1 Hz). The population spike amplitudes (P1 and P2) were measured by dropping a vertical line from the trough to the tangent between the two positive peaks. Walking-to-immobility ratio was calculated by dividing the population spike amplitude during walking by that during immobility. P2/P1 ratio was calculated in the same manner as in anesthetized rats.

4.2.7 Histology

Rats were deeply anesthetized with 30% urethane and perfused through the heart with 400 ml of cold saline followed by 500 ml of cold 4% paraformaldehyde solution in 0.1 M phosphate buffer (PB; pH 7.4). The brain was removed and post-fixed overnight in the latter solution at 4°C. Later, the brain was immersed in 18% sucrose in phosphate-buffered saline for at least 72 hrs at 4°C. Choline acetyltransferase (ChAT) and parvalbumin (Parv) immunohistochemistry were carried out on MS sections. Using a freezing microtome, the MS was sectioned at 40 μ m and they were first incubated in 1% sodium borohydride in 0.1 M PB for 15 minutes and subsequently rinsed in PB. They were incubated in 10% normal goat serum (Sigma, St. Louis, MO) in 0.1 M PB containing 0.1% Triton X-100 (Sigma) for 1 hr at room temperature to block non-specific labeling. The sections were rinsed briefly in PB and incubated at 4°C for 48 hrs in primary antibody solution containing mouse monoclonal ChAT (1:200; Cedarlane, Burlington, Ontario, Canada) or Parv (1:100; Sigma-Aldrich, St. Louis, MO) in 1% normal goat serum. Sections were rinsed in three changes of PB and followed by

incubation in biotin-conjugated goat anti-mouse secondary antiserum (1:200; Jackson ImmunoResearch, West Grove, PA) for 1 hr in room temperature. The sections were then rinsed several times in PB. ABC complex solution (Vector Laboratories, Burlington, Ontario, Canada) was prepared 20 minutes before use by adding equal volumes of solutions A and B in PB (1:1:100). The sections were incubated in the ABC complex solution for 1 hr at room temperature. Following three washes in PB, the sections were developed in a solution containing 0.05% diaminobenzidine tetrahydrochloride (DAB, Sigma) and 0.03% hydrogen peroxide in PB at room temperature in a fume hood until they reached the desired color intensity (1-3 min). The sections were then rinsed several times in PB, mounted on glass slides. Finally, they were dehydrated in a series of 70%, 95% and 100% ethyl alcohol, cleared in xylene (5 minutes x 2) and cover-slipped with DePex (BDH, VWR International Mississauga, Ontario, Canada) mounting medium.

The number of ChAT- and Parv-positive cells was quantified in three representative coronal sections (40 μm) at anterior ($\sim\text{A } 0.7$), middle ($\sim\text{A } 0.4$) and posterior ($\sim\text{A } 0.2$) levels of the medial septum-diagonal band of Broca region. Images of selected sections were captured with a digital camera using x100 magnification in a microscope, and cells were counted from the digital images by a person who was unaware of the treatment history. Electrode placements were histologically verified in 40 μm thionin-stained brain sections (DG: Fig. 4.1A, MPP: Fig. 4.1B, PNO: Fig. 4.1C).

4.2.8 Statistical analysis

Student's *t*-tests (paired and unpaired) were performed. In addition, one- or two-way ANOVAs (randomized and repeated) were carried out, followed by post-hoc

Bonferroni or Fisher's Least Significant Difference tests if the main or interaction effect was statistically significant ($P < 0.05$). Fisher's exact test was used on frequency occurrence data. All statistical analyses were performed using Prism 4.0 (GraphPad Software Inc., La Jolla, CA) and GB Stat (Dynamic Microsystems Inc., Silver Spring, MD).

4.3 Results

4.3.1 Effect of orexin-saporin lesion on theta rhythm and population spike in anesthetized rats

In both control and lesion rats, high-frequency stimulation of the PNO for 1 s activated a hippocampal theta rhythm during and after stimulation (Fig. 4.1D, E). The EEG at the DG molecular layer immediately after PNO stimulation was analyzed by power spectra. The peak theta frequency was not significantly different (unpaired t-test, $P = 0.36$) between control (2.90 ± 0.08 Hz, $n = 9$) and lesion rats (2.65 ± 0.25 Hz, $n = 9$). However, peak theta power was lower in lesion rats (0.06 ± 0.23 log units) as compared to control rats (0.78 ± 0.08 log units; $P < 0.01$, unpaired t-test; Fig. 4.1E).

Stimulation of MPP evoked a negative field potential (-100 μm depth in Fig. 4.2A1, B1) corresponding to an excitatory synaptic sink (E1 in Fig. 4.2A2, B2) in the middle molecular layer. This synaptic current flowed into the middle dendrites (sink) and out of the distal dendrites and the soma (source: -250 to -150 μm and 0 to 50 μm depth in Fig. 4.2A2, B2). Meanwhile, a population spike appeared as a sink (P1 in Fig. 4.2A2, B2)

Fig. 4.1 Electrode placements and hippocampal theta rhythm following electrical stimulation of pontis nucleus oralis (PNO). (A-C) Representative coronal sections stained with thionin showing the locations of the 16-channel silicon recording probe (arrow) in the dentate gyrus (DG, in A) and the stimulating electrodes in the medial perforant path (MPP, in B) and PNO (C). (D) Electroencephalogram (EEG) was recorded in the DG of control rats during baseline without (upper trace) or with high frequency 1-s stimulation of PNO (lower trace). (E) Power spectra were constructed from the last 1.67 s of artifact-free EEG shown in D, and the average power spectra for different conditions were plotted. Although PNO stimulation induced a hippocampal theta rhythm (θ) in control ($n = 9$) and lesion rats ($n = 9$), a reduction in theta peak power was observed in orexin-lesion rats.

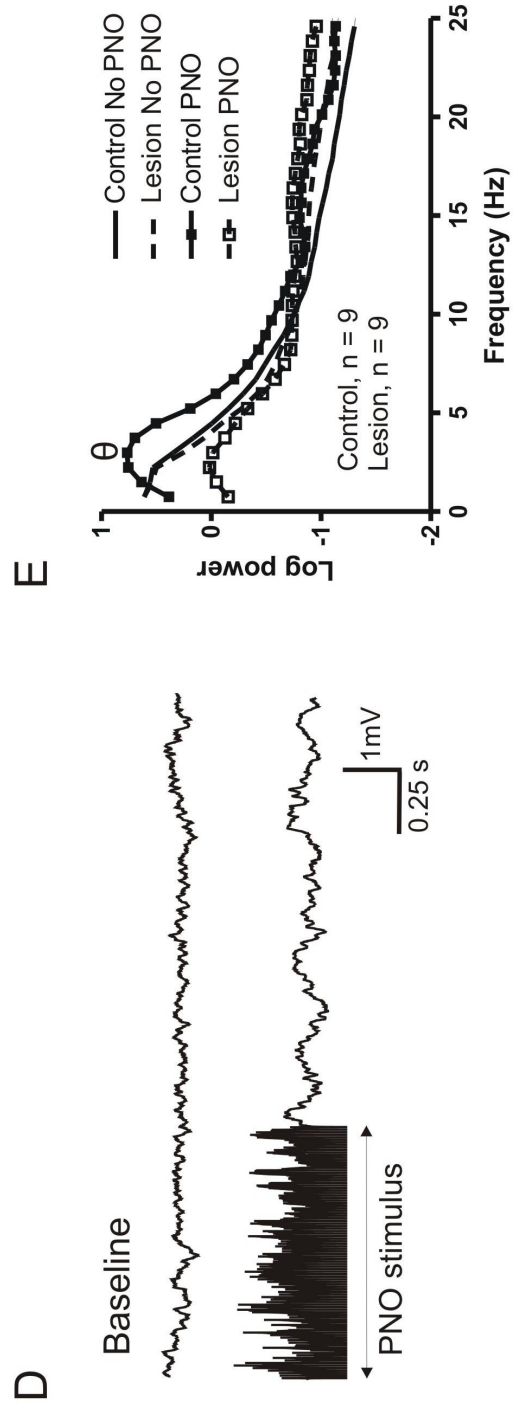
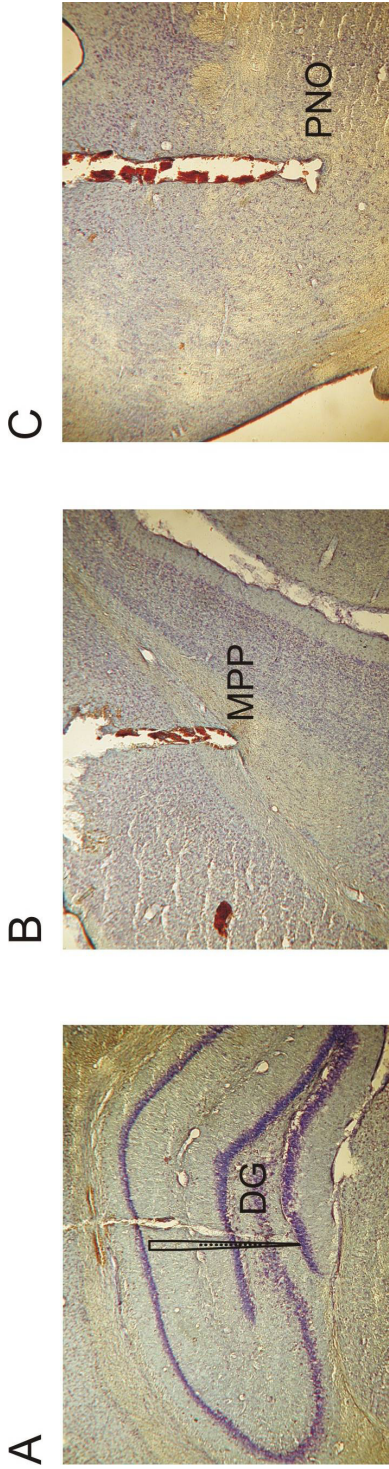
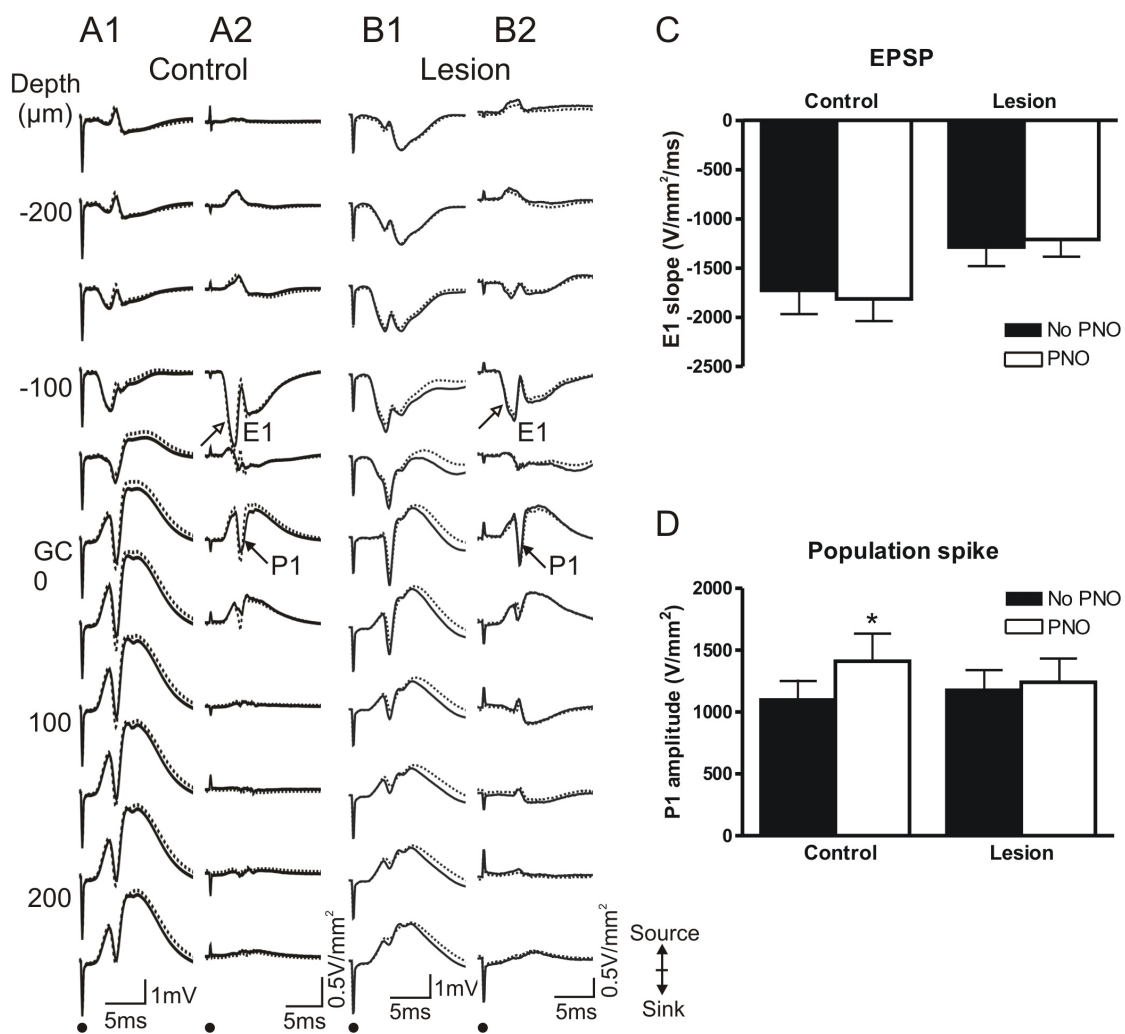


Fig. 4.2 (A-B) Depth profiles of averaged evoked potentials (A1, B1) and its corresponding current source densities on the right (A2, B2) following PNO stimulation (dotted traces) in control and lesion rats. Baseline conditions (No PNO) are displayed as solid traces. Stimulation of the medial perforant path at an intensity 50-70 % of the maximal population spike amplitude resulted in a dendritic excitatory sink (E1, empty arrow) at depth -100 μm , accompanied by a population spike (P1, filled arrow) in the granule cell layer (GC) at depth 0 μm . (C) E1 slopes during baseline or following PNO stimulation was not significantly different between control ($n = 9$) and lesion ($n = 9$) rats. (D) P1 amplitude following PNO stimulation as compared to baseline was larger in control rats ($n = 9$), but not in lesion rats ($n = 9$). Values are expressed as mean + SEM. * $P < 0.01$: difference between baseline (No PNO) and PNO stimulation, using paired t-test.



superimposed on the rising phase of the synaptic current source at the granule cell layer, reflecting the synchronous firing of granule cells.

At a stimulus intensity that evoked 50-70 % of the maximal population spike amplitude, the slopes of fEPSP (empty arrow in Fig. 4.2A2) were not affected in control rats with (dotted traces; -1813 ± 225 V/mm²/ms) and without PNO stimulation (solid traces; -1727 ± 241 V/mm²/ms) in control rats ($P = 0.25$, paired t-test; $n = 9$; Fig. 4.2C). Similar results were also found in lesion rats (Fig. 4.2B2). A paired t-test reported no significant difference between baseline (no PNO: -1287 ± 192 V/mm²/ms) and PNO stimulation (-1210 ± 174 V/mm²/ms) in lesion rats ($P = 0.10$, $n = 9$; Fig. 4.2C).

When compared to baseline (no PNO stimulation), a larger MPP-evoked population spike (filled arrow; P1) was observed following PNO stimulation in control rats (Fig. 4.2A2), but not in lesion rats (Fig. 4.2B2). In control rats, paired t-tests showed a significant increase in P1 amplitude of 26.4 ± 8.8 % following PNO stimulation as compared to baseline (baseline: 1097 ± 155 V/mm² vs PNO: 1411 ± 223 V/mm²; $P < 0.01$). In lesion rats, no significant difference in P1 amplitudes was observed between baseline (1176 ± 164 V/mm²) and PNO stimulation (1241 ± 192 V/mm²; $P = 0.45$; Fig. 4.2D).

4.3.2 Effect of orexin-saporin lesion on paired-pulse responses in anesthetized rats

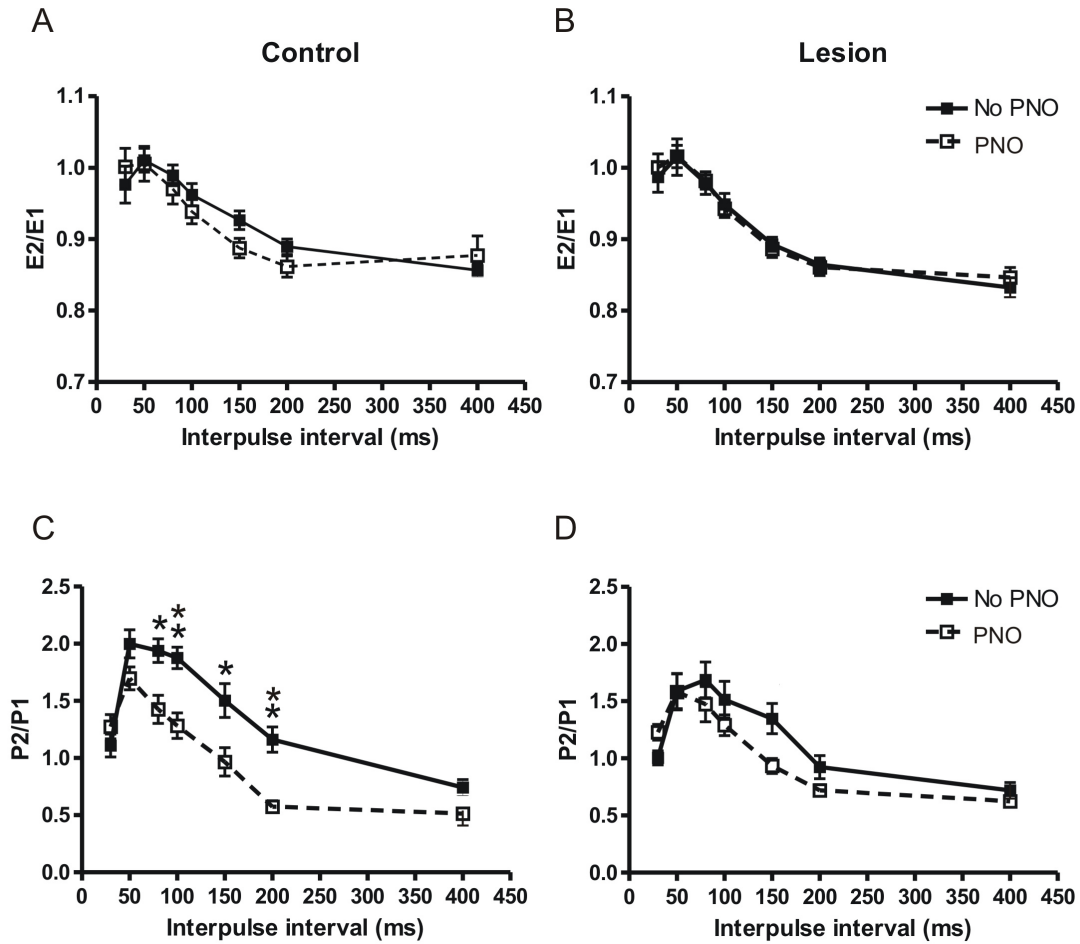
To study the strength of inhibition exerted by hippocampal GABAergic interneurons on granule cells, paired pulses were delivered to MPP at various interpulse intervals at an intensity that evoked 50-70% of the maximal population spike amplitude.

In control and lesion rats, paired-pulse excitatory sink responses at the dendrites of granule cells (E2/E1 ratio) were largely depressed at >50 ms IPI. E2/E1 ratios were not significantly different between baseline and PNO stimulation in control (Fig. 4.3A) or lesion rats (Fig. 4.3B), as shown by a repeated measures two-way ANOVA (control: $F_{(1,16)} = 0.23$, $P = 0.64$; lesion: $F_{(1,16)} = 0.02$, $P = 0.90$).

In control rats, paired-pulse population spike responses recorded at the granule cell layer (P2/P1 ratio) during baseline condition were facilitated at IPI 50-200 ms, and depressed at 400 ms (Fig. 4.3C). Following PNO stimulation as compared to baseline, a decrease in P2/P1 ratio was observed and paired-pulse depression occurred at 150-400 ms IPI. Repeated measures two-way ANOVA revealed a significant decrease in P2/P1 ratio following PNO stimulation as compared to baseline ($F_{(1,16)} = 15.71$, $P < 0.002$). Bonferroni posthoc tests showed a difference in P2/P1 ratio between baseline and PNO stimulation at all IPIs except at 30, 50 and 400 ms. In contrast, no significant change in P2/P1 ratio were observed in lesion rats between PNO stimulation and baseline conditions (Fig. 4.3D), as confirmed with a repeated measures 2-way ANOVA ($F_{(1,16)} = 1.53$, $P = 0.23$).

In addition, P2/P1 ratios during baseline condition were significantly larger in control rats (Fig. 4.3C) as compared to lesion rats (Fig. 4.3D). In control rats, paired-pulse facilitation peaked at 50 ms IPI with $P2/P1 \approx 2$, while in lesion rats, paired-pulse facilitation peaked at 80 ms IPI with $P2/P1 \approx 1.7$. Two-way ANOVA showed that P2/P1 ratio was lower in lesion rats as compared to control rats ($F_{(1,112)} = 12.32$, $P < 0.0007$). On the contrary, there was no significant difference in P2/P1 ratios following PNO

Fig. 4.3 Paired-pulse responses as a function of interpulse interval (IPI). Paired pulses were delivered to MPP at various IPIs (30 - 400 ms) at an intensity that evoked 50-70% of the maximal population spike amplitude. Paired-pulse responses are expressed as a ratio of the excitatory current sink evoked by the 2nd pulse (E2) to that evoked by the 1st pulse (E1) recorded at the middle molecular layer, or a ratio of the population spike sink evoked by the 2nd pulse (P2) to that evoked by the 1st pulse (P1) recorded at the granule cell layer. No significant difference in E2/E1 ratios was found between baseline (No PNO) and PNO stimulation in control (n = 9; A) and lesion rats (n = 9; B). Paired-pulse population spike responses (P2/P1) decreased following PNO stimulation in control rats (C), but not in lesion rats (D). Values are expressed as mean \pm SEM. * $P < 0.01$, ** $P < 0.001$: difference between baseline (No PNO) and PNO stimulation, using Bonferroni test after a significant repeated two-way ANOVA.



stimulation between control and lesion rats, as shown by a two-way ANOVA ($F_{(1,112)} = 0.09, P = 0.76$).

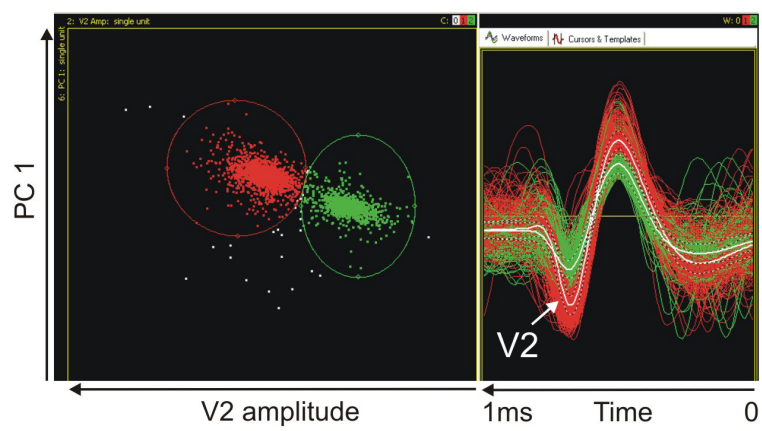
4.3.3 Effect of orexin-saporin lesion on single units in anesthetized rats

Interneurons and granule cells were distinguished on the basis of their waveform parameters and firing patterns. They appeared as separate clusters after spike sorting (Fig. 4.4A). When compared with granule cells (green), interneurons (red) had a narrower spike width and deeper valley due to a fast afterhyperpolarization, largely caused by voltage-gated Kv3 channels (Du et al., 1996; Martina et al., 1998; Rudy and McBain, 2001; Fig. 4.4A). Autocorrelation function showed an interneuron that fired rhythmically at a frequency of ~ 4 Hz, while no obvious rhythmicity was observed in the granule cell (Fig. 4.4B). Since most principal cells innervate adjacent interneurons via axon collaterals, interneurons were shown to fire shortly after principal cells (Csicsvari et al., 1998). This is demonstrated in a cross-correlogram that showed an interneuron firing with a peak latency of 2 ms following a granule cell (Fig. 4.4C).

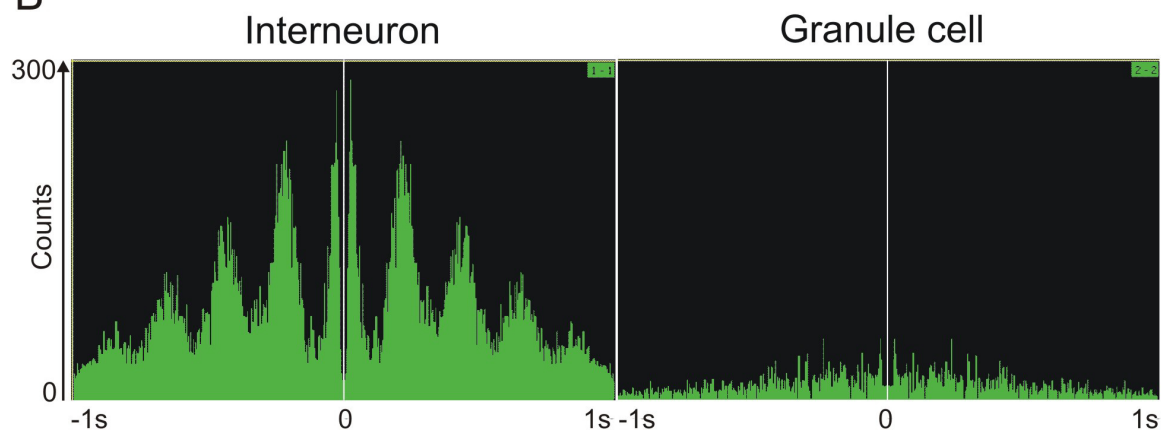
Analysis of spontaneous unit activity in the time window (40 ms) immediately after PNO stimulation but before the MPP stimulus pulse showed that the probability of granule cell activation was significantly higher following PNO stimulation than during baseline condition in sham rats ($n = 18$; Fig. 4.5A), as confirmed by repeated measures two-way ANOVA ($F_{(1,136)} = 15.09, P < 0.0003$). In contrast, in lesion rats ($n = 19$), there was no significant difference between granule cell activities observed following PNO stimulation as compared to baseline (repeated measures two-way ANOVA; $F_{(1,144)} = 2.93, P = 0.09$). In addition, the probability of granule cell activation was significantly

Fig. 4.4 Identification of interneurons and granule cells. (A) Spike sorting was carried out to distinguish interneurons (red) and granule cells (green) from each other such that clusters were formed in x-y plot (left). The x-axis represents the amplitude of the valley (V2) following the positive component and the y-axis represents the first principal component (PC1) which corresponds to the direction with the largest variation after principal component analysis (PCA). PCA transforms the data to a space with fewer dimensions while maximizing variance. Individual traces were superimposed and the average waveform of each cell type is displayed in white (right). Interneurons had a narrower spike width and deeper valley (V2) as compared to granule cells. (B) Autocorrelograms of an interneuron and a granule cell; the vertical axis represents the number of times the cell fired in each time bin before and after each spike. The interneuron displayed a rhythmic firing pattern at a frequency of 4 Hz (left), but not the granule cell (right). (C) Cross-correlogram of interneuronal firing with respect to firing of a granule cell at time zero on the horizontal axis. The vertical axis represents the number of times the interneuron fired at a time ± 0.5 ms after the granule cell. The interneuron fired at a peak latency of 2 ms after a granule cell. Bin size of all histograms is 1 ms.

A



B



C

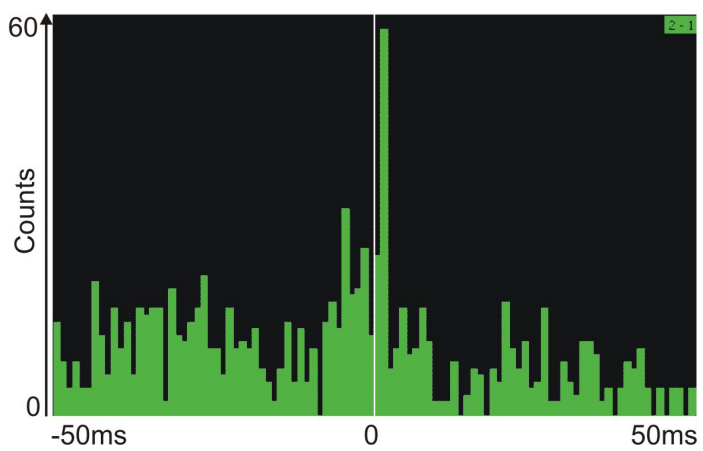
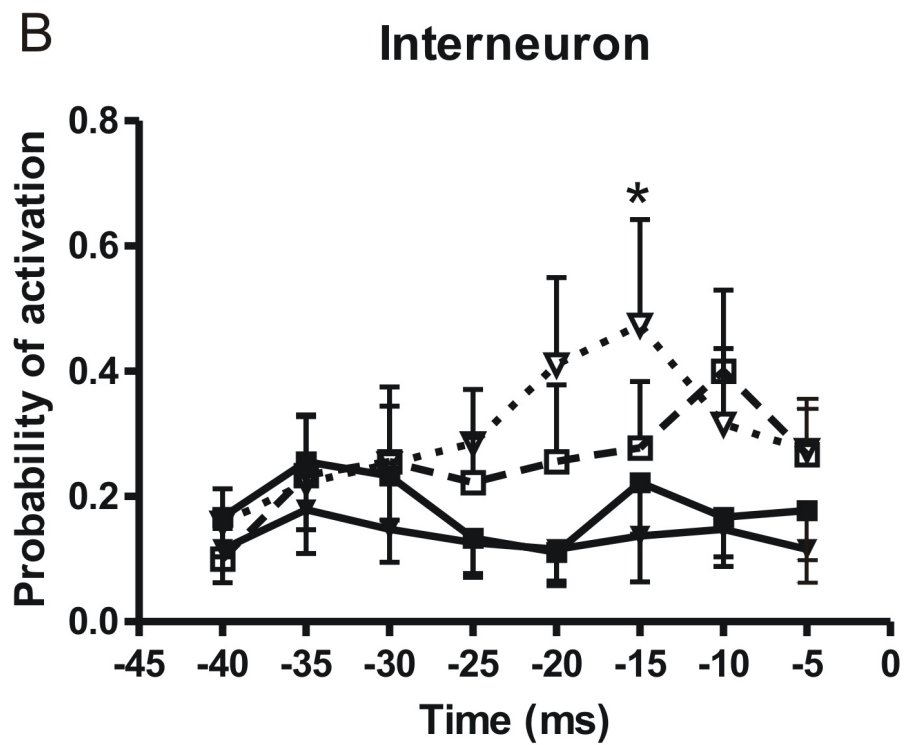
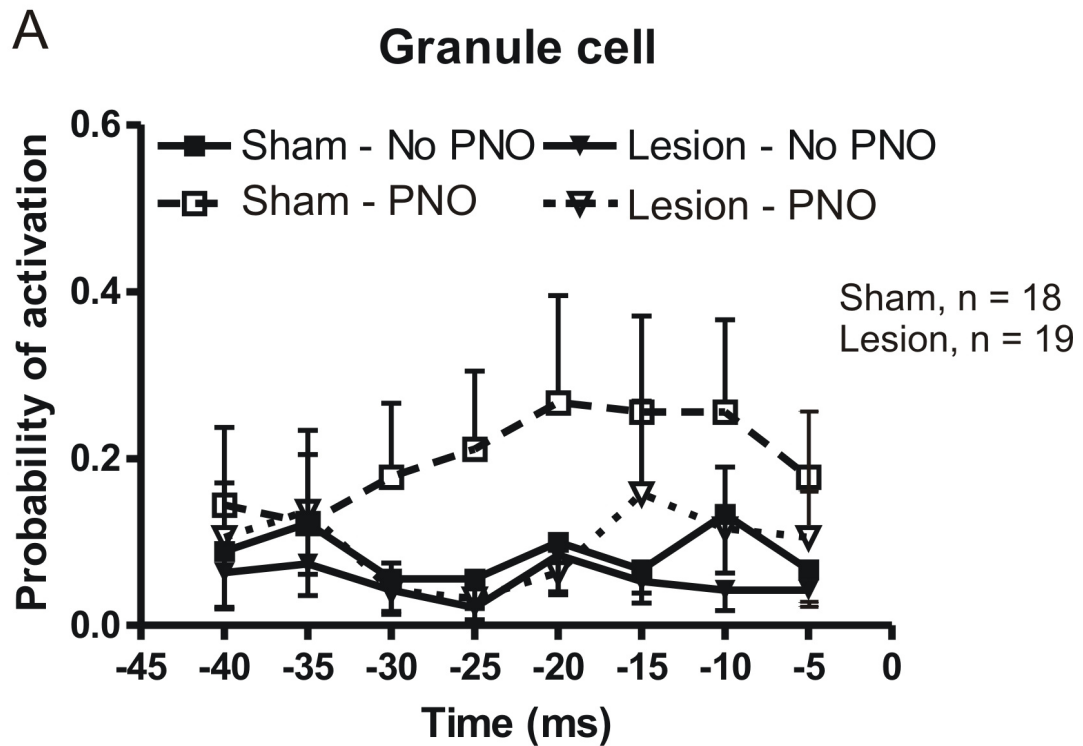


Fig. 4.5 Probability of unit activation (mean and SEM in one direction) in the 40-ms time window immediately following PNO stimulation and before MPP stimulation. For each unit, firing in each 5-ms bin was evaluated in at least 25 sweeps of PNO stimulation or baseline. Following PNO stimulation, (A) granule cells were more active in sham (n = 19 cells) than lesion rats (n = 18 cells), whereas (B) interneurons were more active in lesion than sham rats. * $P < 0.05$: difference between baseline (No PNO) and PNO stimulation, using Bonferroni test after a significant repeated two-way ANOVA.



higher in sham rats than in lesion rats following PNO stimulation (two-way ANOVA; $F_{(1,280)} = 6.29$, $P < 0.02$). However, there was no significant difference between sham and lesion rats during baseline condition as confirmed by a two-way ANOVA ($F_{(1,280)} = 2.43$, $P = 0.12$).

The probability of spontaneous interneuron activity was significantly higher following PNO stimulation than during baseline condition in lesion rats ($n = 19$; Fig. 4.5B), as confirmed by repeated two-way ANOVA ($F_{(1,144)} = 17.29$, $P < 0.0001$). Bonferroni posthoc tests showed a difference at 15 ms prior to MPP pulse stimulation ($P < 0.05$). In sham rats ($n = 18$), interneuron activity showed a trend of increase following PNO stimulation as compared to baseline (repeated two-way ANOVA; $F_{(1,136)} = 3.51$, $P = 0.06$). The probability of interneuron activation was not significantly different between sham and lesion rats during baseline condition (two-way ANOVA; $F_{(1,280)} = 2.06$, $P = 0.15$) or following PNO stimulation ($F_{(1,280)} = 0.79$, $P = 0.37$).

To evaluate the activity of DG cells following paired-pulse stimulation of MPP (IPI = 20 ms) at a stimulus intensity above population spike threshold, peristimulus time histograms were plotted such that the firing frequency of a cell at each bin (1 ms) was normalized with respect to the total firing frequency of each cell following a pulse of MPP stimulation. In sham ($n = 9$ cells) and lesion rats ($n = 15$ cells), units began firing 1-2 ms after each pulse. Granule cell and interneuron activity was maximal at 3 ms after the conditioning pulse. Interneuron activity peaked 3 ms after the test pulse, whereas granule cell activity peaked later (7-9 ms) after the test pulse. PNO stimulation did not significantly alter the firing frequency of granule cells (Fig. 4.6A, B) and interneurons (Fig. 4.6C, D) in sham and lesion rats following each pulse (at least $P > 0.3$, repeated

measures two-way ANOVA). Additionally, granule cell and interneuron firing frequency between sham (Fig. 4.6A, C) and lesion rats (Fig. 4.6B, D) following each pulse remain unchanged with ($P > 0.6$) and without PNO stimulation ($P > 0.7$, two-way ANOVA).

Granule cells (Fig. 4.7A) and interneurons (Fig. 4.7B) exhibited a high probability of activation by the conditioning pulse when MPP stimulus intensity was at (level 4) or above the population spike threshold (level 5). As stimulus intensity increases, the probability of granule cell activation was significantly lower in lesion rats ($n = 19$) than in sham rats ($n = 18$). Two-way ANOVA revealed that granule cells were less active in lesion rats, compared to sham rats ($F_{(1,175)} = 16.28$, $P < 0.0001$; Fig. 4.7A). However, no significant difference in the probability of interneuron activation as a function of stimulus intensity between sham and lesion rats, as demonstrated by a two-way ANOVA ($F_{(1,175)} = 0.27$, $P = 0.61$; Fig. 4.7B).

At stimulus intensity above population spike threshold, the probability of granule cell activation by the conditioning pulse was lower in lesion rats ($n = 19$) than in sham rats ($n = 18$) with ($P < 0.05$) or without PNO stimulation ($P < 0.04$, unpaired t-tests; Fig. 4.7C). However, no significant difference was observed between baseline condition and PNO stimulation in sham ($P = 0.62$) and lesion rats ($P = 0.83$, paired t-tests). In addition, the probability of granule cell activation by the test pulse was not significantly different between sham ($n = 9$) and lesion ($n = 15$) rats regardless of PNO stimulation (at least $P > 0.4$, unpaired t-tests; Fig. 4.7E). Moreover, there was no significant difference in the activity evoked by the test pulse between baseline condition and PNO stimulation, in either sham or lesion rats (at least $P > 0.5$, paired t-tests). Furthermore, no significant difference in interneuron activity evoked by the conditioning pulse was observed between

Fig. 4.6 Normalized peristimulus time histograms (PETHs) of granule cells and interneurons in sham and lesion rats. Granule cells (A, B) and interneurons (C, D) following paired-pulse stimulation of MPP (IPI = 20 ms) at a stimulus intensity above population spike threshold were recorded and plotted as PETHs (bin size = 1 ms) such that the firing frequency of a cell at each bin was normalized with respect to the total firing frequency of each cell following a pulse of MPP stimulation. PNO stimulation did not alter the firing frequency of granule cells and interneurons in sham (n = 9 cells) and lesion rats (n = 15 cells).

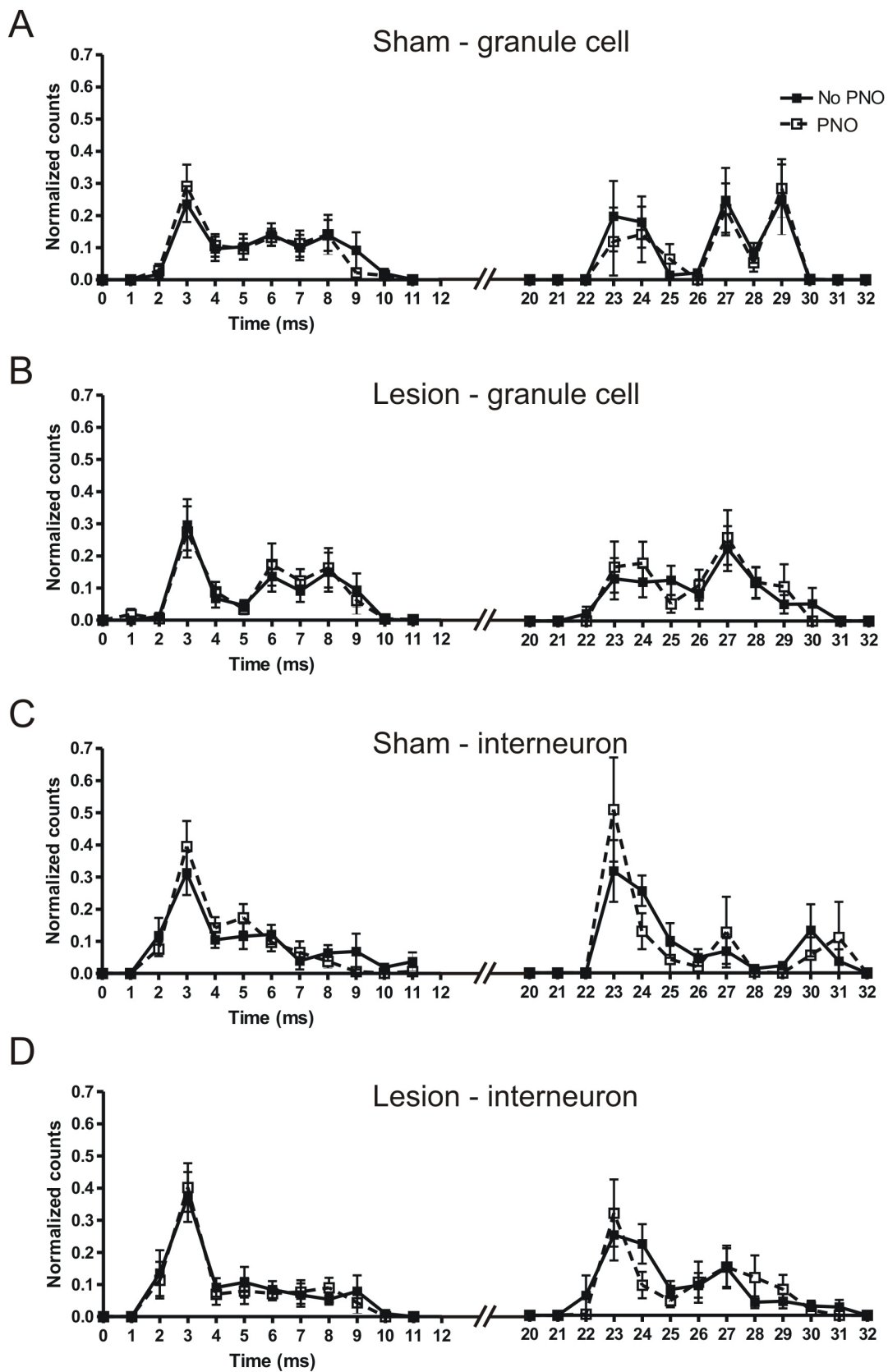
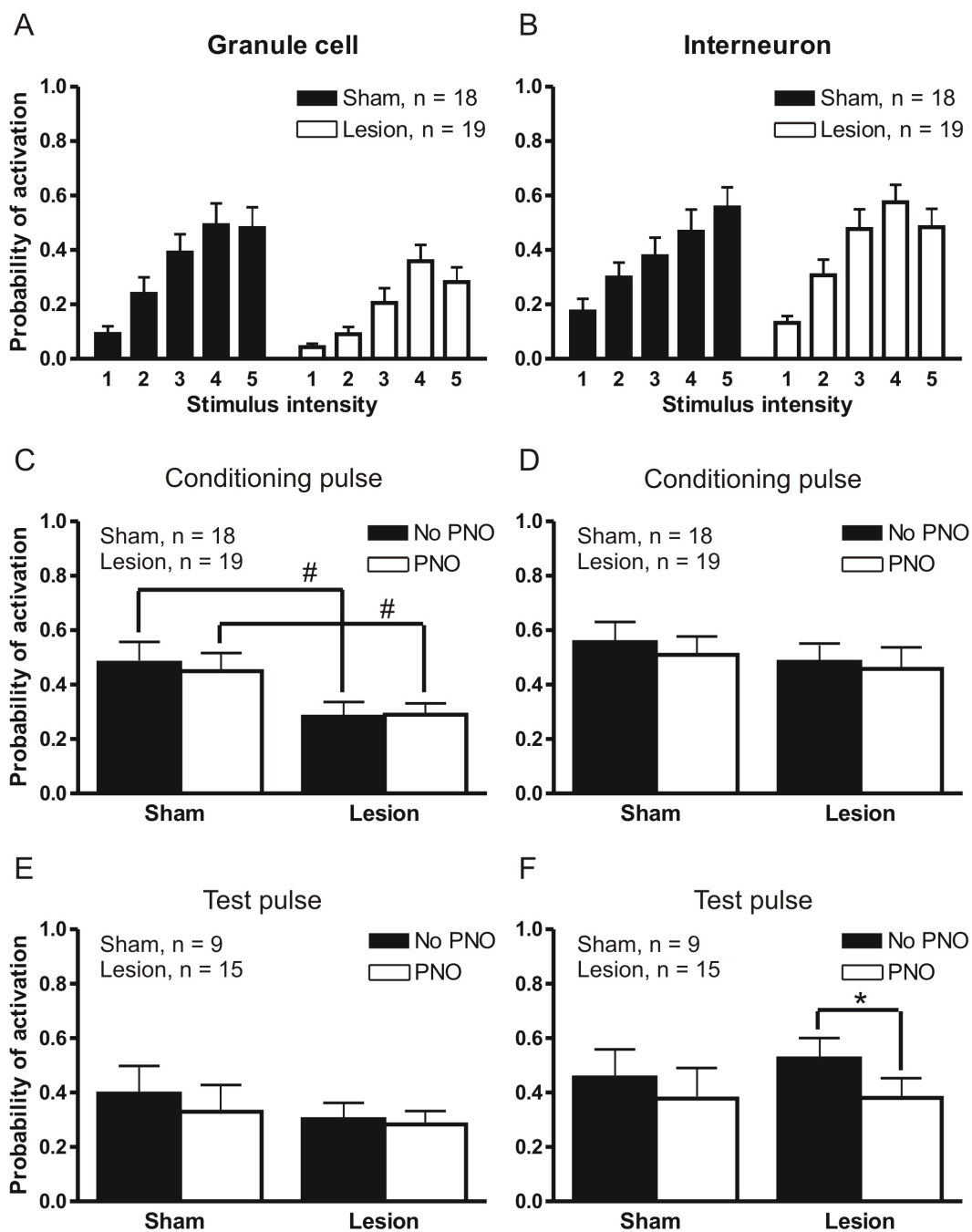


Fig. 4.7 Probability of activation of units by conditioning (1st) and test (2nd) stimulus pulses delivered to the medial perforant path (MPP) in sham and lesion rats. The probability of granule cell (A) and interneuron (B) activation was calculated from unit activities of at least 25 paired-pulse sweeps for each of five different stimulus intensities (1: below EPSP threshold, 2: EPSP threshold, 3: above EPSP threshold, 4: population spike threshold, 5: above population spike threshold). As stimulus intensity increases, firing probability of granule cells was lower in lesion rats (n = 19 cells) as compared to sham rats (n = 18 cells; two-way ANOVA, $P < 0.0001$). (C-F) At stimulus intensity 5 (above population spike threshold), the probability of granule cell (C, E) and interneuron (D, F) activation by the conditioning and test pulses were analyzed. Evoked activity among granule cells following conditioning pulse was lower in lesion rats (n = 19 cells) than in sham rats (n = 18 cells), with or without PNO stimulation (C). Evoked activity in interneurons by the test pulse (F) was reduced following PNO stimulation as compared to baseline in lesion rats (n = 15 cells). Values are expressed as mean + SEM. # $P < 0.05$: difference between sham and lesion rats, using unpaired t-tests. * $P < 0.05$: difference between baseline condition (No PNO) and PNO stimulation in lesion rats, using paired t-test.



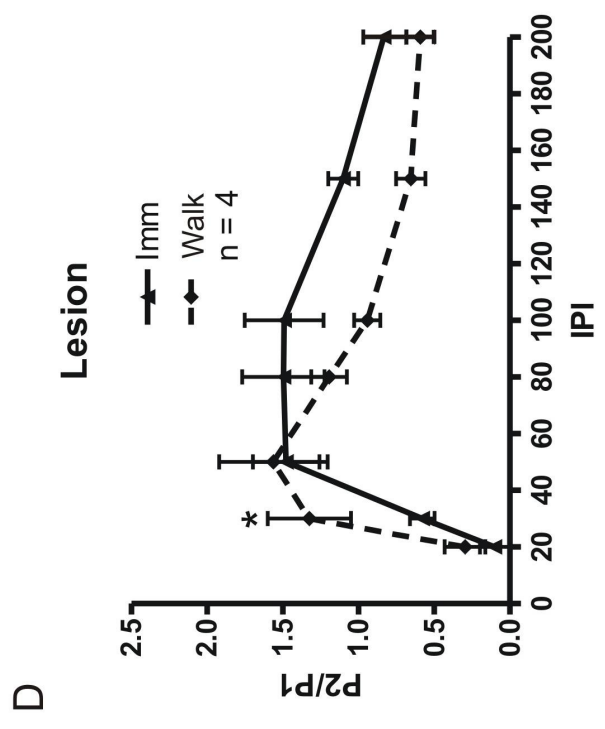
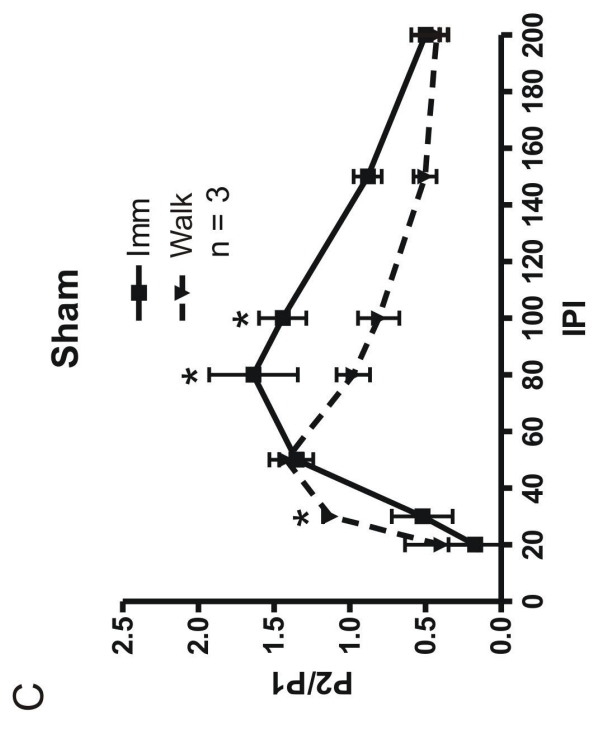
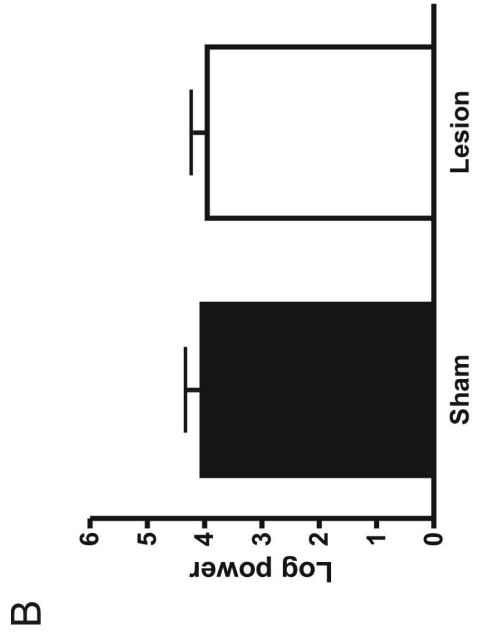
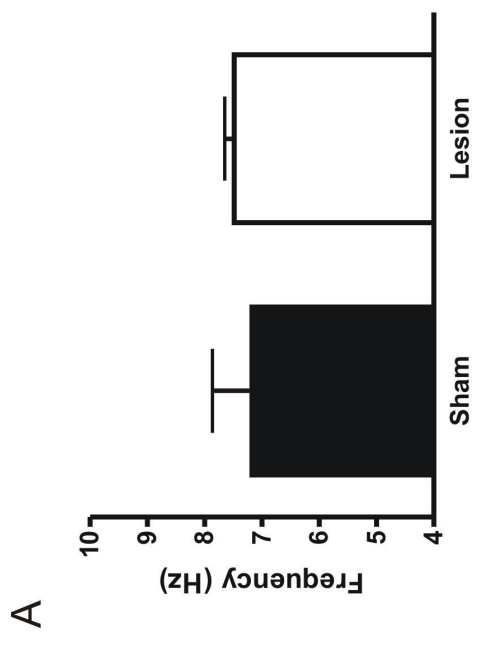
sham ($n = 18$) and lesion ($n = 19$) rats (at least $P > 0.4$, unpaired t-tests), with or without PNO stimulation (at least $P > 0.1$, paired t-tests; Fig. 4.7D). The probability of interneuron activation evoked by the test pulse following PNO stimulation, as compared to baseline, was lower in lesion rats ($n = 15$; $P < 0.05$), but not significantly different in sham rats ($n = 9$; $P = 0.50$, paired t-tests; Fig. 4.7F). However, no significant difference in interneuron activity evoked by the test pulse was observed between sham and lesion rats, for a given condition (baseline or PNO stimulation) (at least $P > 0.5$, unpaired t-tests).

4.3.4 Effect of orexin-saporin lesion in behaving rats

To investigate hippocampal function without the influence of anesthesia, EEG at the molecular layer and field potentials at the hilus were recorded via the surface and deep electrodes respectively during walking (Walk) and awake immobility (Imm). In sham and lesion rats, a theta rhythm was observed during walking, but not during awake immobility. Theta peak frequency was not significantly different between sham (7.18 ± 0.69 Hz, $n = 3$) and lesion rats (7.49 ± 0.17 Hz, $n = 4$; $P = 0.64$, unpaired t-test; Fig. 4.8A). Similarly, no significant difference in theta peak power was found between sham (4.05 ± 0.29 log units) and lesion rats (3.96 ± 0.28 log units; $P = 0.83$, unpaired t-test; Fig. 4.8B).

Stimulation of MPP (25-120 μ A) evoked a population spike at the hilus. At a stimulus intensity which was two times the population spike threshold, the amplitudes of population spike (an average of eight sweeps) were measured and expressed as a ratio of the amplitude evoked during walking to that evoked during immobility. Walking-to-

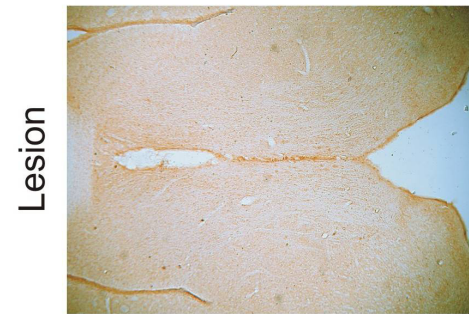
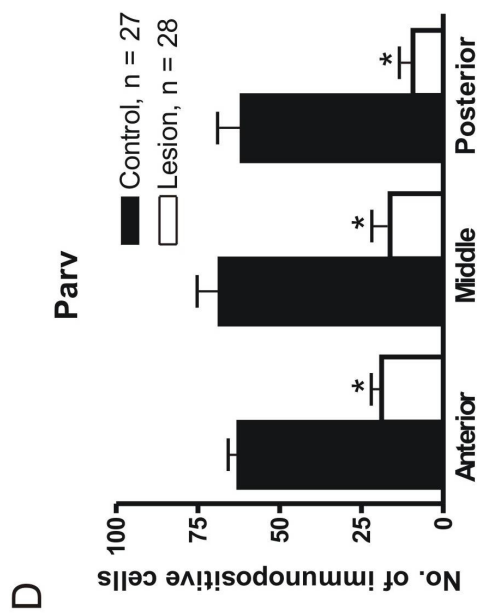
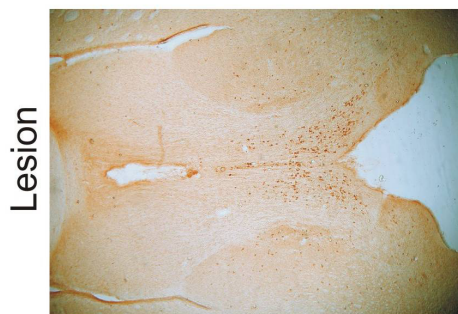
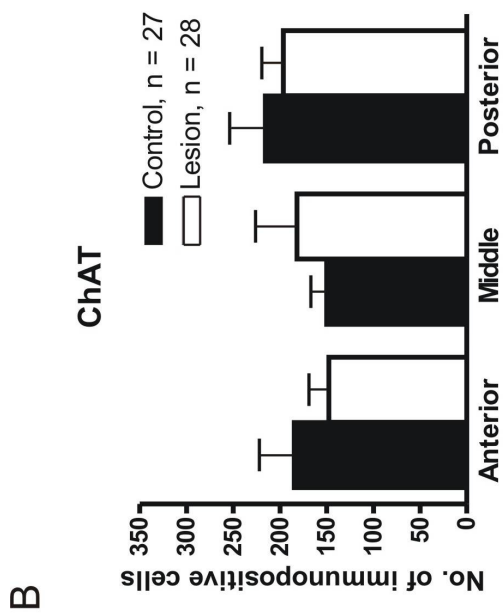
Fig. 4.8 Effect of orexin-saporin on theta rhythm and paired-pulse responses in behaving rats. In sham ($n = 3$) and lesion rats ($n = 4$), EEG at the molecular layer (A, B) and field potentials at the hilus (C, D) were recorded during walking and awake immobility. Power (arbitrary logarithmic units) and frequency (Hz) at theta peak were obtained from power spectra following fast Fourier Transform (FFT) of artifact-free EEG segments recorded during walking. Theta peak frequency (A) and power (B) were not significantly different between sham and lesion rats. In each rat, an average evoked potential (average of 8 sweeps) was recorded following paired-pulse stimulation of the ipsilateral MPP at various interpulse intervals (20, 30, 50, 80, 100, 150 and 200 ms). Stimulus intensity was fixed at two times the population spike threshold. Population spike amplitudes (P1 and P2) were measured and expressed as P2/P1 ratio. When compared to immobility (Imm), paired-pulse population spike responses (P2/P1) increased at 30 ms and decreased at 80-100 ms during walking (Walk) in sham rats (C), whereas paired pulse facilitation occurred at 30 ms in lesion rats (D). Values are expressed as mean \pm SEM. * $P < 0.01$: difference between baseline (No PNO) and PNO stimulation, using Fisher's Least Significant Difference test after a significant repeated two-way ANOVA.



immobility population spike ratio was not significantly different between sham (1.02 ± 0.03 , $n = 3$) and lesion rats (0.96 ± 0.02 , $n = 4$; $P = 0.16$, unpaired t-test). Furthermore, the frequency occurrence of walking-induced change in population spike amplitude was not significantly different in sham ($n = 3$) and lesion rats ($n = 4$), as shown by Fisher's exact test ($P = 0.49$).

In sham rats, paired-pulse population spike responses (P2/P1 ratio) recorded during immobility were depressed except at 50-100 ms IPI (Fig. 4.8C). During walking, an increase in P2/P1 ratios was observed at 30 ms IPI and paired-pulse depression occurred at >80 ms IPI. Although repeated two-way ANOVA did not show a significant main effect between immobility and walking ($F_{(1,4)} = 1.47$, $P = 0.29$), a significant interaction effect was observed ($F_{(6,24)} = 5.15$, $P < 0.002$). Fisher's Least Significant Difference (LSD) posthoc tests showed a difference in P2/P1 ratio at 30, 80 and 100 ms IPI. In lesion rats, paired-pulse facilitation was observed at 50-150 ms IPI during immobility (Fig. 4.8D). During walking, P2/P1 ratio increased at 30 ms IPI and paired-pulse depression occurred at >100 ms IPI. Repeated two-way ANOVA did not reveal a significant main effect between immobility and walking ($F_{(1,6)} = 0.22$, $P = 0.66$), but a significant interaction effect was observed ($F_{(6,36)} = 3.76$, $P < 0.006$). However, Fisher's LSD posthoc tests showed a difference in P2/P1 ratio at 30 ms IPI. P2/P1 ratios between sham (Fig. 4.8C) and lesion (Fig. 4.8D) during immobility or walking were not significantly different, as confirmed by a two-way ANOVA (immobility: $F_{(1,35)} = 0.68$, $P = 0.41$; walking: $F_{(1,35)} = 1.86$, $P = 0.18$).

Fig. 4.9 Counts of choline acetyltransferase (ChAT)- and parvalbumin (Parv)-immunopositive cells in coronal MS sections of sham and lesion rats. ChAT-immunopositive cholinergic cells were located mostly lateral to the midline (A) while Parv-immunopositive GABAergic neurons were observed along the midline (C). A significant decrease in the number of Parv-immunopositive GABAergic neurons was observed in all three coronal MS sections (D) following bilateral injections of orexin-aporin in the MS as compared to sham. However, ChAT-immunopositive cholinergic cells were unaffected (B). * $P < 0.003$: difference between lesion and sham rats at a particular anterior-posterior level, using paired t-tests.



A

C

4.3.5 Effect of orexin-saporin lesion on cells in the MS

In lesion rats, numerous ChAT-immunopositive cholinergic cells were seen (Fig. 4.9A), mostly lateral to the midline while a decrease in Parv-immunopositive GABAergic neurons in the MS were observed, normally found along the midline (Fig. 4.9C). When compared to sham rats, Parv-immunopositive cells numbers were significantly reduced at all three coronal levels (anterior: 63 ± 3 vs 19 ± 3 ; middle: 68 ± 7 vs 16 ± 6 ; posterior: 62 ± 8 vs 9 ± 2 ; at least $P < 0.003$, paired t-tests; Fig. 4.9D), while the number of ChAT-immunopositive cells remained about the same (at least $P > 0.3$, paired t-tests; Fig. 4.9B).

4.4 Discussion

The present study showed that orexin-saporin lesion of septal GABAergic neurons decreased various PNO-modulated but not the baseline (no PNO stimulation) neural activities in the DG. In anesthetized control rats, PNO stimulation as compared to baseline induced a hippocampal theta rhythm, increased single-pulse population spike amplitude (P1), spontaneous granule cell activity and paired-pulse depression of population spikes at 80-200 ms IPI. Orexin-saporin lesion rats as compared to control rats showed a decrease in PNO-induced theta peak power and paired-pulse depression of population spikes, and an abolition of PNO-induced enhancement of P1. Moreover, PNO-induced spontaneous granule cell activity decreased while PNO-induced spontaneous interneuronal activity increased in lesion rats. This is the first report investigating the role of septal GABAergic neurons on hippocampal unit activity *in vivo*.

4.4.1 Orexin-saporin lesion attenuates PNO-induced theta

In this study, intraseptal infusion of orexin-saporin led to a marked decrease in Parv-immunopositive GABAergic neurons but not ChAT-immunopositive cholinergic neurons, as first reported by Smith and Pang (2005). I found that the hippocampal theta induced by PNO stimulation under urethane anesthesia was lower in peak power but similar in peak frequency in lesion as compared to control rats. The latter result is also consistent with previous differential lesion of GABAergic septal neurons by excitotoxin kainic acid (Malthe-Sorensen et al., 1980; Pang et al., 2001; Yoder and Pang, 2005), which resulted in a theta rhythm of lower peak amplitude but similar peak frequency as control rats under urethane anesthesia (Yoder and Pang, 2005). These results demonstrate that septal GABAergic neurons participate in hippocampal theta generation under urethane anesthesia.

In behaving rats, I showed no difference in peak power and frequency of the theta rhythm during walking between orexin-saporin lesion and control rats. This contrasts with a reduction of the theta peak amplitude during walking after lesion of septal GABAergic neurons with kainic acid (Yoder and Pang, 2005). Potential damage of septal glutamatergic neurons by kainic acid was not examined (Yoder and Pang, 2005) and may contribute to lower theta power during walking.

In the present study, walking-induced theta survived orexin-saporin treatment (100 ng/ μ l) which preferentially destroys GABAergic cells. Theta was abolished only when both GABAergic and cholinergic neurons were destroyed, for example when a higher concentration (200 ng/ μ l) of orexin-saporin was administered (Gerashchenko et

al., 2001) or following electrolytic lesion of the medial septum (Green and Arduini, 1954; Winson, 1978; Leung, 1987). It is likely that both septal GABAergic and cholinergic inputs to the hippocampus are important for theta generation, supported by recent studies demonstrating that pacing of theta is mediated by GABAergic neurons (Borhegyi et al., 2004; Varga et al., 2008; Hangya et al., 2009) while putative cholinergic neurons increases theta power (Zhang et al., 2011).

4.4.2 Orexin-saporin lesion blocks PNO-induced population spike facilitation

The present study demonstrated that PNO stimulation facilitated the DG population spike evoked by a MPP pulse, and that this facilitation required septal GABAergic neurons. Although previous studies showed that population spike facilitation is not mediated by muscarinic receptors (Fantie and Goddard, 1982), the participation of other septal neurons has not been shown. A GABA-mediated effect was suggested when hippocampal infusion of GABA_A receptor antagonist picrotoxin eliminated facilitation (Bilkey and Goddard, 1985), but GABAergic contribution from the MS or within the hippocampus was not addressed. I showed that orexin-saporin lesion of septal GABAergic neurons blocked the PNO-induced population spike facilitation in the DG. Population spike facilitation in the DG of control rats is likely a result of disinhibition of granule cells due to inhibition of interneurons by septal GABAergic neurons following PNO stimulation.

In this study, no behavior-mediated changes in population spike amplitude between walking and immobility were observed which is consistent with previous studies

(Green et al., 1993; Hargreaves et al., 1990). However, population spike amplitude was smaller during walking as compared to during drinking or grooming (Buzsaki et al., 1981). In addition, transient increases in population spike amplitude can occur following novelty-related changes such as transitions between environments (Sharp et al., 1989; Green et al., 1990). Therefore, mechanisms other than septal GABAergic disinhibition are likely involved.

4.4.3 Orexin-saporin lesion blocks changes in paired-pulse population spike response

The present study demonstrated a significant decrease in paired-pulse population spike ratio (P2/P1) following PNO stimulation as compared to baseline in control rats at 80-200 ms IPI, but not in orexin-saporin lesion rats. Similarly, in behaving sham rats, a suppression of paired-pulse facilitation (PPF) during walking as compared to immobility was observed at 80-100 ms IPI, but not in orexin-saporin lesion rats. My results correspond to a study in anesthetized mice whereby septal activation by MS pulse stimulation reduced PPF at 60-80 ms IPI (Sanchez-Alavez et al., 2002), suggesting a decrease in P2 amplitude due to a stronger interneuronal activation following septal stimulation. I further suggest that septal stimulation may involve septohippocampal GABAergic neurons acting possibly on GABAergic interneuronal circuits in the DG.

Paired-pulse stimulation in the DG results in a typical triphasic depression/facilitation/depression response curve (Lomo, 1971; Racine and Milgram, 1983; Robinson and Racine, 1986). The early depression, lasting for about 30 ms, results from GABA_A mediated recurrent inhibition (Adamec et al., 1981; Tuff et al., 1993). This

is followed by a facilitation phase that has been suggested to be mediated by NMDA-receptors on granule cells (Joy and Albertson, 1993). The mechanism underlying the late depression phase is yet to be fully elucidated. Total blockade of GABA_B receptors by local injection of GABA_B antagonist CGP35348 abolished paired-pulse depression at 200-1000 ms and reduced PPF at 50-70 ms (Canning and Leung, 2000), and increased paired-pulse depression at 50-400 ms in rats with early-life seizures (Tsai et al., 2008). The reduction of PPF at <100 ms is likely mediated by GABAergic neuronal circuits acting on GABA_A receptors, and these GABAergic neurons are more active after GABA_B receptor blockade or following PNO/septal stimulation of septohippocampal GABAergic neurons. The suppression of PPF at 80–200 ms following PNO stimulation or during walking may be mediated by the same GABAergic neuronal network in the DG, with the long-latency paired-pulse depression mediated by GABA_B receptors on granule cells.

The firing of DG neurons initiated by a conditioning pulse is expected to excite an extensive network of heterogeneous interneurons (reviewed in Freund and Buzsaki, 1996), which include cells (e.g., basket cells, axo-axonic cells) that project to the cell bodies or axon initial segments of granule cells (Scharfman et al., 1990) and interneuron (e.g., molecular layer perforant path-associated cells) whose axons terminate on the granule cells dendrites (Leranth et al., 1990; Halasy and Somogyi, 1993). The former attenuates population spike amplitude evoked by the test-pulse (P2), while the latter inhibits fEPSP slope (E2) of the test pulse (Moser, 1996). Since the present study reported that P2/P1 decreased but no E2/E1 change occurred following PNO stimulation in control rats, PNO stimulation is suggested to affect hippocampal interneurons that synapse on the cell bodies instead of the dendrites of granule cells.

4.4.4 Orexin-saporin lesion results in changes in single unit activity

The lack of PNO-induced increase in granule cell activity in orexin-saporin lesion rats compared to control rats suggest that one function of septal GABAergic cells in normal rats is to enhance granule cell activity, perhaps by inhibition of hippocampal interneurons (Freund and Antal, 1988). The same septohippocampal GABAergic neuron-mediated disinhibition of granule cells also accounts for P1 facilitation following PNO stimulation in control rats but not in lesion rats. At first glance, my evoked unit data does not seem to support this because no difference in granule cell activity during conditioning pulse was found in sham rats between baseline (no PNO) and PNO stimulation. However, granule cell activity during the conditioning pulse was significantly attenuated with or without PNO stimulation in orexin-saporin lesion rats as compared to sham rats. In addition, in the absence of PNO stimulation, the probability of granule cell activation with respect to stimulus intensity in orexin-saporin lesion rats was significantly lower than that in sham rats. Furthermore, when spontaneous unit activities were analyzed in the time window (40 ms) between the end of PNO stimulation and the conditioning pulse, granule cells in sham rats were more active following PNO stimulation than during baseline, but no change was observed in orexin-saporin lesion rats. It is possible that due to the lack of disinhibition from septal GABAergic cells in orexin-saporin lesion rats, granule cells are less likely to be activated. Therefore, my results suggest the loss of septal GABAergic neurons leads to a reduction in granule cell activity. Disinhibition of hippocampal pyramidal cells (Toth et al., 1997) has been shown, but I am not aware of reports of disinhibition of granule cells in the literature.

Previous studies demonstrated an increase in spontaneous activity of hippocampal interneurons during theta activity (Ranck, 1973; O'Keefe, 1976; Buzsaki and Eidelberg, 1983). This is consistent with a trend of increased spontaneous interneuronal activity following PNO stimulation in sham rats. In addition, there was a significant increase spontaneous interneuronal activity following PNO stimulation in orexin-saporin lesion rats, as compared to baseline, suggesting that the loss of septal GABAergic inhibition of interneurons increases interneuronal inhibitory tone. Although a decrease in P2/P1 ratio generally indicates greater inhibition from interneurons which leads to attenuation of test spike, interneuronal activity evoked by the test pulse decreased in orexin-saporin lesion rats following PNO stimulation, as compared to baseline. It is likely that interneurons that target interneurons (Acsady et al., 1996) are recruited later during theta, thereby lowering interneuronal activity.

4.4.5 Conclusion

Septal GABAergic neurons participate in theta generation under urethane anesthesia and are responsible for DG population spike facilitation following septal activation. Septal GABAergic disinhibition increased interneuronal inhibition as demonstrated by the suppression of paired-pulse facilitation in control rats, as compared to orexin-saporin lesion rats. With the loss of disinhibition from septal GABAergic cells in orexin-saporin lesion rats, tonic interneuronal inhibition is increased and granule cells are less likely to be activated. This is the first report investigating the role of septal GABAergic neurons on dentate unit activity in which septal GABAergic disinhibition of granule cells was demonstrated. I provide results suggesting that septal GABAergic

neurons can help regulate granule cell excitability by reducing inhibitory tone of the interneurons. In animals, orexin-saporin lesion of septal GABAergic neurons has been shown to impair hippocampal-dependent spatial reference memory in the Morris water maze (Smith and Pang, 2005; LeCourtier et al., 2010). In humans, the decrease in cortical GABAergic tone, which is suppressed by GABAergic neurons through the basal forebrain corticopetal system, is correlated with the severity of depression, a symptom of Alzheimer's disease (Garcia-Alloza et al., 2006). In addition, synthesis of beta-amyloid precursor protein which forms characteristic plaques in Alzheimer's disease is triggered by an increased septal GABAergic tone and a benzodiazepine receptor antagonist was found to be neuroprotective (Marczynski et al., 1995). It is likely that a certain level of septal GABAergic inhibition is required for normal brain function. Development of procedures targeting septal GABAergic function may offer a new way to approach this neurodegenerative disease.

4.5 References

- Acsady L, Gorcs TJ, Freund TF (1996) Different populations of vasoactive intestinal polypeptide-immunoreactive interneurons are specialized to control pyramidal cells or interneurons in the hippocampus. *Neuroscience* 73:317-334.
- Adamec RE, McNaughton B, Racine R, Livingston KE (1981) Effects of diazepam on hippocampal excitability in the rat: action in the dentate area. *Epilepsia* 22:205-215.
- Apartis E, Poindessous-Jazat FR, Lamour YA, Bassant MH (1998) Loss of rhythmically bursting neurons in rat medial septum following selective lesion of septohippocampal cholinergic system. *J Neurophysiol* 79:1633-1642.
- Barrenechea C, Pedemonte M, Nunez A, Garcia-Austt E (1995) In vivo intracellular recordings of medial septal and diagonal band of Broca neurons: relationships with theta rhythm. *Exp Brain Res* 103:31-40.
- Bassant MH, Apartis E, Jazat-Poindessous FR, Wiley RG, Lamour YA (1995) Selective immunolesion of the basal forebrain cholinergic neurons: effects on hippocampal activity during sleep and wakefulness in the rat. *Neurodegeneration* 4:61-70.
- Baxter MG, Bucci DJ, Gorman LK, Wiley RG, Gallagher M (1995) Selective immunotoxic lesions of basal forebrain cholinergic cells: effects on learning and memory in rats *Behav Neurosci* 109:714-722.
- Berchtold NC, Kesslak JP, Cotman CW (2002) Hippocampal brain-derived neurotrophic factor gene regulation by exercise and the medial septum. *J Neurosci Res* 68:511-521.
- Berger-Sweeney J, Heckers S, Mesulam MM, Wiley RG, Lappi DA, Sharma M (1994) Differential effects on spatial navigation of immunotoxin-induced cholinergic lesions of the medial septal area and nucleus basalis magnocellularis *J Neurosci* 14:4507-4519.
- Bilkey DK, Goddard GV (1985) Medial septal facilitation of hippocampal granule cell activity is mediated by inhibition of inhibitory interneurons. *Brain Res* 361:99-106.
- Bland BH (1986) The physiology and pharmacology of hippocampal formation theta rhythms. *Prog Neurobiol* 26:1-54.
- Bland BH, Oddie SD, Colom LV, Vertes RP (1994) Extrinsic modulation of medial septal cell discharges by the ascending brainstem hippocampal synchronizing pathway. *Hippocampus* 4:649-660.

- Borhegyi Z, Varga V, Szilagyi N, Fabo D, Freund TF (2004) Phase segregation of medial septal GABAergic neurons during hippocampal theta activity. *J Neurosci* 24:8470-8479.
- Buzsaki G (2002) Theta oscillations in the hippocampus. *Neuron* 33:325-340.
- Buzsaki G, Eidelberg E (1983) Phase relations of hippocampal projection cells and interneurons to theta activity in the anesthetized rat. *Brain Res* 266:334-339.
- Buzsaki G, Grastyan E, Czopf J, Kellenyi L, Prohaska O (1981) Changes in neuronal transmission in the rat hippocampus during behavior. *Brain Res* 225:235-247.
- Canning KJ, Leung LS (2000) Excitability of rat dentate gyrus granule cells in vivo is controlled by tonic and evoked GABA(B) receptor-mediated inhibition. *Brain Res* 863:271-275.
- Chang Q, Gold PE (2004) Impaired and spared cholinergic functions in the hippocampus after lesions of the medial septum/vertical limb of the diagonal band with 192 IgG-saporin. *Hippocampus* 14:170-179.
- Csicsvari J, Hirase H, Czurko A, Buzsaki G (1998) Reliability and state dependence of pyramidal cell-interneuron synapses in the hippocampus: an ensemble approach in the behaving rat. *Neuron* 21:179-189.
- Dornan WA, McCampbell AR, Tinkler GP, Hickman LJ, Bannon AW, Decker MW, Gunther KL (1997) Comparison of site specific injections into the basal forebrain on water maze and radial arm maze performance in the male rat after immunolesioning with 192 IgG saporin. *Behav Brain Res* 86:181-189.
- Du J, Zhang L, Weiser M, Rudy B, McBain CJ (1996) Developmental expression and functional characterization of the potassium-channel subunit Kv3.1b in parvalbumin-containing interneurons of the rat hippocampus. *J Neurosci* 16:506-518.
- Fantie BD, Goddard GV (1982) Septal modulation of the population spike in the fascia dentata produced by perforant path stimulation in the rat *Brain Res* 252:227-237.
- Freeman JA, Nicholson C (1975) Experimental optimization of current source-density technique for anuran cerebellum. *J Neurophysiol* 38:369-382.
- Freund TF, Antal M (1988) GABA-containing neurons in the septum control inhibitory interneurons in the hippocampus. *Nature* 336:170-173.
- Freund TF, Buzsaki G (1996) Interneurons of the hippocampus. *Hippocampus* 6:347-470.

- Garcia-Alloza M, Tsang SW, Gil-Bea FJ, Francis PT, Lai MK, Marcos B, Chen CP, Ramirez MJ (2006) Involvement of the GABAergic system in depressive symptoms of Alzheimer's disease. *Neurobiol Aging* 27:1110-1117.
- Gerashchenko D, Salin-Pascual R, Shiromani PJ (2001) Effects of hypocretin-saporin injections into the medial septum on sleep and hippocampal theta. *Brain Res* 913:106-115.
- Givens BS, Olton DS (1990) Cholinergic and GABAergic modulation of medial septal area: effect on working memory. *Behav Neurosci* 104:849-855.
- Green EJ, Barnes CA, McNaughton BL (1993) Behavioral state dependence of homo- and hetero-synaptic modulation of dentate gyrus excitability. *Exp Brain Res* 93:55-65.
- Green EJ, McNaughton BL, Barnes CA (1990) Exploration-dependent modulation of evoked responses in fascia dentata: dissociation of motor, EEG, and sensory factors and evidence for a synaptic efficacy change. *J Neurosci* 10:1455-1471.
- Green JD, Arduini AA (1954) Hippocampal electrical activity in arousal. *J Neurophysiol* 17:533-557.
- Halasy K, Somogyi P (1993) Distribution of GABAergic synapses and their targets in the dentate gyrus of rat: a quantitative immunoelectron microscopic analysis. *J Hirnforsch* 34:299-308.
- Hangya B, Borhegyi Z, Szilagyi N, Freund TF, Varga V (2009) GABAergic neurons of the medial septum lead the hippocampal network during theta activity. *J Neurosci* 29:8094-8102.
- Hargreaves EL, Cain DP, Vanderwolf CH (1990) Learning and behavioral-long-term potentiation: importance of controlling for motor activity. *J Neurosci* 10:1472-1478.
- Heynen AJ, Bilkey DK (1994) Effects of perforant path procaine on hippocampal type 2 rhythmical slow-wave activity (theta) in the urethane-anesthetized rat. *Hippocampus* 4:683-695.
- Jiang F, Khanna S (2004) Reticular stimulation evokes suppression of CA1 synaptic responses and generation of theta through separate mechanisms. *Eur J Neurosci* 19:295-308.
- Joy RM, Albertson TE (1993) NMDA receptors have a dominant role in population spike-paired pulse facilitation in the dentate gyrus of urethane-anesthetized rats. *Brain Res* 604:273-282.

- Kirk IJ, Oddie SD, Konopacki J, Bland BH (1996) Evidence for differential control of posterior hypothalamic, supramammillary, and medial mammillary theta-related cellular discharge by ascending and descending pathways. *J Neurosci* 16:5547-5554.
- Kramis R, Vanderwolf CH (1980) Frequency-specific RSA-like hippocampal patterns elicited by septal, hypothalamic, and brain stem electrical stimulation. *Brain Res* 192:383-398.
- Kramis R, Vanderwolf CH, Bland BH (1975) Two types of hippocampal rhythmical slow activity in both the rabbit and the rat: relations to behavior and effects of atropine, diethyl ether, urethane, and pentobarbital. *Exp Neurol* 49:58-85.
- Lecourtier L, de Vasconcelos AP, Leroux E, Cosquer B, Geiger K, Lithfous S, Cassel JC (2010) Septohippocampal pathways contribute to system consolidation of a spatial memory: Sequential implication of gabaergic and cholinergic neurons. *Hippocampus*
- Leranth C, Malcolm AJ, Frotscher M (1990) Afferent and efferent synaptic connections of somatostatin-immunoreactive neurons in the rat fascia dentata. *J Comp Neurol* 295:111-122.
- Leung LS (2010) Field potential and current source density analysis. In: *Electrophysiological Recording Techniques*, Vol. 54 (Vertes RP, Stackman J, Robert W. eds), Totowa, NJ: Springer Science+Business Media, LLC.
- Leung LS (1998) Generation of theta and gamma rhythms in the hippocampus. *Neurosci Biobehav Rev* 22:275-290.
- Leung LS, Peloquin P (2010) Cholinergic modulation differs between basal and apical dendritic excitation of hippocampal CA1 pyramidal cells. *Cereb Cortex* 20:1865-1877.
- Leung LW (1987) Hippocampal electrical activity following local tetanization. I. Afterdischarges. *Brain Res* 419:173-187.
- Leung LW (1985) Spectral analysis of hippocampal EEG in the freely moving rat: effects of centrally active drugs and relations to evoked potentials. *Electroencephalogr Clin Neurophysiol* 60:65-77.
- Lomo T (1971) Potentiation of monosynaptic EPSPs in the perforant path-dentate granule cell synapse. *Exp Brain Res* 12:46-63.
- Malthe-Sorensen D, Odden E, Walaas I (1980) Selective destruction by kainic acid of neurons innervated by putative glutamergic afferents in septum and nucleus of the diagonal band. *Brain Res* 182:461-465.

- Marczynski TJ (1995) GABAergic deafferentation hypothesis of brain aging and Alzheimer's disease; pharmacologic profile of the benzodiazepine antagonist, flumazenil. *Rev Neurosci* 6:221-258.
- Martina M, Schultz JH, Ehmke H, Monyer H, Jonas P (1998) Functional and molecular differences between voltage-gated K⁺ channels of fast-spiking interneurons and pyramidal neurons of rat hippocampus. *J Neurosci* 18:8111-8125.
- McMahan RW, Sobel TJ, Baxter MG (1997) Selective immunolesions of hippocampal cholinergic input fail to impair spatial working memory. *Hippocampus* 7:130-136.
- Mesulam MM, Mufson EJ, Wainer BH, Levey AI (1983) Central cholinergic pathways in the rat: an overview based on an alternative nomenclature (Ch1-Ch6). *Neuroscience* 10:1185-1201.
- Monmaur P, Ayadi K, Breton P (1993) Hippocampal EEG responses induced by carbachol and atropine infusions into the septum and the hippocampus in the urethane-anaesthetized rat. *Brain Res* 631:317-324.
- Monmaur P, Breton P (1991) Elicitation of hippocampal theta by intraseptal carbachol injection in freely moving rats. *Brain Res* 544:150-155.
- Moser EI (1996) Altered inhibition of dentate granule cells during spatial learning in an exploration task. *J Neurosci* 16:1247-1259.
- Nyakas C, Luiten PG, Spencer DG, Traber J (1987) Detailed projection patterns of septal and diagonal band efferents to the hippocampus in the rat with emphasis on innervation of CA1 and dentate gyrus. *Brain Res Bull* 18:533-545.
- O'Keefe J (1976) Place units in the hippocampus of the freely moving rat. *Exp Neurol* 51:78-109.
- Pang KC, Nocera R (1999) Interactions between 192-IgG saporin and intraseptal cholinergic and GABAergic drugs: role of cholinergic medial septal neurons in spatial working memory. *Behav Neurosci* 113:265-275.
- Pang KC, Nocera R, Secor AJ, Yoder RM (2001) GABAergic septohippocampal neurons are not necessary for spatial memory. *Hippocampus* 11:814-827.
- Paxinos G, Watson C (1997) *The rat brain in stereotaxic coordinates*. San Diego: Academic Press.
- Racine RJ, Milgram NW (1983) Short-term potentiation phenomena in the rat limbic forebrain. *Brain Res* 260:201-216.

- Ranck JB Jr (1973) Studies on single neurons in dorsal hippocampal formation and septum in unrestrained rats. I. Behavioral correlates and firing repertoires. *Exp Neurol* 41:461-531.
- Robinson GB, Racine RJ (1986) Interactions between septal and entorhinal inputs to the rat dentate gyrus: facilitation effects. *Brain Res* 379:63-67.
- Rudy B, McBain CJ (2001) Kv3 channels: voltage-gated K⁺ channels designed for high-frequency repetitive firing. *Trends Neurosci* 24:517-526.
- Sanchez-Alavez M, Gallegos RA, Kalafut MA, Games D, Henriksen SJ, Criado JR (2002) Loss of medial septal modulation of dentate gyrus physiology in young mice overexpressing human beta-amyloid precursor protein. *Neurosci Lett* 330:45-48.
- Scharfman HE, Kunkel DD, Schwartzkroin PA (1990) Synaptic connections of dentate granule cells and hilar neurons: results of paired intracellular recordings and intracellular horseradish peroxidase injections. *Neuroscience* 37:693-707.
- Sharp PE, McNaughton BL, Barnes CA (1989) Exploration dependent modulation of evoked responses in fascia dentata. Fundamental observations and time course. *Psychobiology* 17:257-269.
- Simon AP, Poindessous-Jazat F, Dutar P, Epelbaum J, Bassant MH (2006) Firing properties of anatomically identified neurons in the medial septum of anesthetized and unanesthetized restrained rats. *J Neurosci* 26:9038-9046.
- Smith HR, Pang KC (2005) Orexin-saporin lesions of the medial septum impair spatial memory. *Neuroscience* 132:261-271.
- Stumpf C (1965) Drug action on the electrical activity of the hippocampus. *Int Rev Neurobiol* 8:77-138.
- Tai SK, Leung LS (2009) Facilitation of dentate gyrus population spike may involve septohippocampal GABAergic input. *Society for Neuroscience Abstract* 566.18/EE33:
- Takano Y, Hanada Y (2009) The driving system for hippocampal theta in the brainstem: an examination by single neuron recording in urethane-anesthetized rats. *Neurosci Lett* 455:65-69.
- Teruel-Marti V, Cervera-Ferri A, Nunez A, Valverde-Navarro AA, Olucha-Bordonau FE, Ruiz-Torner A (2008) Anatomical evidence for a ponto-septal pathway via the nucleus incertus in the rat. *Brain Res* 1218:87-96.
- Toth K, Freund TF, Miles R (1997) Disinhibition of rat hippocampal pyramidal cells by GABAergic afferents from the septum. *J Physiol* 500 (Pt 2):463-474.

- Townsend G, Peloquin P, Kloosterman F, Hetke JF, Leung LS (2002) Recording and marking with silicon multichannel electrodes. *Brain Res Brain Res Protoc* 9:122-129.
- Tsai ML, Shen B, Leung LS (2008) Seizures induced by GABAB-receptor blockade in early-life induced long-term GABA(B) receptor hypofunction and kindling facilitation. *Epilepsy Res* 79:187-200.
- Tuff LP, Racine RJ, Adamec R (1983) The effects of kindling on GABA-mediated inhibition in the dentate gyrus of the rat. I. Paired-pulse depression. *Brain Res* 277:79-90.
- Varga V, Hangya B, Kranitz K, Ludanyi A, Zemankovics R, Katona I, Shigemoto R, Freund TF, Borhegyi Z (2008) The presence of pacemaker HCN channels identifies theta rhythmic GABAergic neurons in the medial septum. *J Physiol* 586:3893-3915.
- Vertes RP (1981) An analysis of ascending brain stem systems involved in hippocampal synchronization and desynchronization. *J Neurophysiol* 46:1140-1159.
- Vertes RP, Kocsis B (1997) Brainstem-diencephalo-septohippocampal systems controlling the theta rhythm of the hippocampus. *Neuroscience* 81:893-926.
- Walsh TJ, Herzog CD, Gandhi C, Stackman RW, Wiley RG (1996) Injection of IgG 192-saporin into the medial septum produces cholinergic hypofunction and dose-dependent working memory deficits. *Brain Res* 726:69-79.
- Winson J (1978) Loss of hippocampal theta rhythm results in spatial memory deficit in the rat. *Science* 201:160-163.
- Yoder RM, Pang KC (2005) Involvement of GABAergic and cholinergic medial septal neurons in hippocampal theta rhythm. *Hippocampus* 15:381-392.
- Zhang H, Lin SC, Nicolelis MA (2011) A distinctive subpopulation of medial septal slow-firing neurons promote hippocampal activation and theta oscillations. *J Neurophysiol* (in press).

Chapter 5

General Discussion

5.1 Introduction

In this thesis, I investigated the effects of selective lesion of septohippocampal cholinergic and GABAergic neurons on theta rhythm, synaptic plasticity, population and unit activity in the hippocampus of urethane-anesthetized and freely behaving rats. Lesion of cholinergic and GABAergic neurons were carried out by intraseptal infusion of 192 IgG-saporin and orexin-saporin respectively.

In Chapters 2 and 3, I focused on the role of cholinergic septohippocampal cells in theta rhythm and synaptic plasticity in hippocampal CA1 during vestibular stimulation of behaving rats. Specifically, in Chapter 2, I showed that vestibular stimulation by passive whole body rotation induced an atropine-sensitive theta rhythm in the hippocampus. The rotation-induced theta was attenuated after systemic cholinergic blockade with atropine sulfate, septal 192 IgG-saporin lesion or bilateral vestibular lesion with sodium arsenite. Modulation of field excitatory postsynaptic potentials (fEPSPs), observed during rotation as compared to during immobility, was sensitive to muscarinic cholinergic blockade and septal 192 IgG-saporin lesion. In Chapter 3, I provided original results that rotation enhanced hippocampal basal-dendritic LTP. LTP was facilitated when tetanus was delivered during rotation as compared to during immobility. Systemic muscarinic cholinergic blockade by atropine sulfate or septal 192 IgG-saporin lesion abolished the enhancement of LTP.

In Chapter 4, I investigated the effects of septal orexin-saporin lesion on population and unit activity in the hippocampal DG of anesthetized and behaving rats. I showed that septal orexin-saporin lesioned GABAergic neurons, attenuated pontis nucleus oralis (PNO)-induced theta and blocked PNO-induced population spike facilitation. Orexin-saporin lesion also blocked paired-pulse depression of population spikes observed in anesthetized rats following PNO stimulation and in behaving rats during walking. Moreover, PNO-induced spontaneous granule cell activity decreased while PNO-induced spontaneous interneuronal activity increased in orexin-saporin lesion rats.

As specific results were discussed earlier (Chapter 2-4), only the general associations of the results will be discussed in this chapter.

5.2 Advantages and limitations of immunotoxin lesions

Immunolesioning is a powerful technique used in the study of nervous system function, brain-related diseases and disorders. As opposed to non-specific electrolytic lesion and surgical transection of fibers, immunotoxins can selectively destroy a target neuronal population as long as it expresses a specific cell surface marker. An immunotoxin is made by conjugating an antibody or protein that binds to a cell surface molecule with a ribosome-inactivating toxin saporin. Once injected, the immunotoxin attaches to its target receptor and is internalized. The bond between saporin and the targeting agent is broken intracellularly. Saporin inactivates the ribosome, inhibiting protein synthesis which results in cell death. Cells which do not express the target receptor will be spared. Pilot experiments are necessary to determine the optimal dose,

injection site and volume of injection to achieve the desired lesion. Although loss of neuronal function may be observed 2-7 days after injection, a delay of up to 2 weeks is required for complete dissolution of the targeted population (Wiley, 2001).

5.2.1 192 IgG-saporin lesion of septal cholinergic neurons

In my studies (Chapters 2 and 3), 192 IgG-saporin, a conjugate of the monoclonal p75 receptor antibody 192 IgG and saporin, was infused into the MS. Since cholinergic neurons are the only cells in the MS that express p75 receptor, 192 IgG-saporin destroys cholinergic neurons without affecting non-cholinergic cells (Wiley et al., 1991; Wrenn and Wiley, 1998). Septal 192 IgG-saporin lesion effectively eliminated 80-83 % of cholinergic ChAT-immunopositive cells, sparing GABAergic Parv-immunopositive cells.

Septal 192 IgG-saporin lesion attenuated rotation-induced theta (Chapter 2) which is consistent with previous studies (Lee et al., 1994; Bassant et al., 1995; Gerashchenko et al., 2001). Others have reported no or mild deficits in learning and memory following 192 IgG-saporin lesion, despite a marked loss of ChAT-immunopositive neurons and significant reduction in other markers of cholinergic function (i.e. AChE) in the hippocampus (Berger-Sweeney et al., 1994; Baxter et al., 1995; Pang and Nocera, 1999). Since it is possible that incomplete lesions can occur, some researchers suggest that a threshold level of damage ($\geq 75\%$) must be achieved before impairments become apparent (Leanza et al., 1995; Wrenn and Wiley, 1998). In addition, compensatory mechanisms which include sprouting of the remaining acetylcholine terminals, up-regulation of synthesis and storage of acetylcholine may also account for the lack of effect (Lapchak et al., 1991; Chang and Gold, 2004). These mechanisms may be

responsible for the residual acetylcholine release in the hippocampus that is estimated to remain at 30-40% of control levels (Dornan et al., 1996; McMahan et al., 1997; Chang and Gold, 2004).

5.2.2 Orexin-saporin lesion of septal GABAergic neurons

Orexin-saporin is a conjugate of orexin-2 receptor binding ligand and saporin. Although orexin-2 receptors are expressed on most septal cells (Berchtold et al., 2002; Wu et al., 2002), intraseptal infusion of orexin-saporin lesion (100 ng/ μ l) successfully eradicated ~77% of GABAergic Parv-immunopositive cells without damaging cholinergic ChAT-immunopositive cells (Chapter 4). Walking-induced theta remained unchanged whereas PNO-induced theta was attenuated following septal orexin-saporin lesion. Theta is abolished (Gerashchenko et al., 2001) and spatial memory in the Morris water maze is impaired (Smith and Pang, 2005) when both septal GABAergic and cholinergic neurons are destroyed by a higher concentration (200 ng/ μ l) of orexin-saporin. However, no studies have been conducted to evaluate the relative distribution of orexin-2 receptors, which may help explain the differential susceptibility between GABAergic and cholinergic neurons.

5.2.3 Septal glutamatergic neurons

Before the discovery of septohippocampal glutamatergic neurons (Manns et al., 2003; Sotty et al, 2003; Colom et al., 2005), cholinergic cells represented roughly two thirds (~65%) of the total septohippocampal projecting neurons while GABAergic cells

made up the remaining one third (Kohler et al., 1984; Amaral and Kurz, 1985; Freund and Antal, 1988; Kiss et al., 1990). At present, septal glutamatergic neurons are estimated to form ~23% of the septohippocampal projection (Colom et al., 2005), but the relative percentages of the remaining two cell types remain to be established. Septal glutamatergic neurons have been shown to burst in relation to hippocampal theta (Huh et al., 2010), however, the question of whether glutamatergic septal neurons are damaged by 192 IgG-saporin or orexin-saporin lesions has not been addressed in literature.

5.3 Significance of studies

Alzheimer's disease (AD) is an irreversible and progressive neurodegenerative disease that slowly destroys memory and thinking skills, and eventually the ability to carry out the simplest tasks. In 2010, half a million Canadians had AD or a related dementia and it cost Canadians \$15 billion a year. Approximately 1 in 11 Canadians over the age of 65 has AD or a related dementia (Alzheimer Society of Canada, 2010). AD is the leading form of dementia. Hence, there is a great need to develop ways to delay its onset, retard its progress, and prevent and treat the disease.

In this thesis, I provided original results that vestibular stimulation by rotation activates a cholinergic input from the medial septum to the hippocampus, mediating synaptic modulation, an atropine-sensitive theta rhythm and enhancement of LTP in hippocampal CA1 of behaving rats. Therefore, activation of the vestibular system is a good model to investigate septohippocampal cholinergic activation in behaving rats. Septohippocampal cholinergic input may participate in sensorimotor processing whereby activation of the vestibular system may serve as a sensory signal to assist in motor

planning (Bland and Oddie, 2001). In addition, atropine-sensitive theta induced during vestibular stimulation may represent the cholinergic activation that is necessary for formation of spatial memory (Givens and Olton, 1995; Hasselmo, 2006; Roland et al., 2008). Previous studies have demonstrated that vestibular stimulation by caloric and galvanic vestibular stimulation can improve cognition (reviewed in Smith et al., 2010a, 2010b; Utz et al., 2010). Hippocampal-dependent cognitive abilities are greatly compromised in patients suffering from AD, and degeneration of cholinergic neurons in the basal forebrain is a pathological hallmark of this disease (Bartus et al., 1982; Francis et al., 1999; Wenk, 2006). Therefore, vestibular stimulation provides a physiological method to activate septohippocampal cholinergic neurons which may ameliorate some of the hippocampal-dependent cognitive deficits due to cholinergic dysfunction in AD.

In addition, I presented evidence showing that septal GABAergic neurons participate in theta generation and are responsible for the population spike facilitation in the DG following septal activation under urethane anesthesia. Septal GABAergic disinhibition increased interneuronal inhibition as demonstrated by the suppression of paired-pulse facilitation in anesthetized and behaving rats. This is the first report investigating the role of septal GABAergic neurons on dentate unit activity in which septal GABAergic disinhibition of granule cells was demonstrated. Following PNO stimulation, an increase in spontaneous granule cell activity was observed in sham-lesion rats, but not in orexin-saporin lesion rats. My results suggest that septal GABAergic neurons regulate granule cell excitability by reducing inhibitory tone of the interneurons. In animals, orexin-saporin lesion of septal GABAergic neurons has been shown to impair hippocampal-dependent spatial reference memory in the Morris water maze (Smith and

Pang, 2005; LeCourtier et al., 2010). In humans, the decrease in cortical GABAergic tone, which is suppressed by GABAergic neurons through the basal forebrain corticopetal system, is correlated with the severity of depression, a symptom of Alzheimer's disease (Garcia-Alloza et al., 2006). In addition, synthesis of beta-amyloid precursor protein which forms characteristic plaques in AD is triggered by an increased septal GABAergic tone and a GABA_A receptor antagonist was found to be neuroprotective (Marczynski et al., 1995). Development of procedures targeting septal GABAergic function may offer a new way to approach this neurodegenerative disease.

5.4 Further studies

While this thesis has advanced the understanding of the septal cholinergic and GABAergic neurons in hippocampal function, several experiments may further extend my findings are reported below.

1. The role of septal GABAergic neurons in the activation of vestibular system is currently unknown. My studies (Chapters 2 and 3) demonstrated that rotation activates a septal cholinergic input to the hippocampus. Whether septal GABAergic neurons are also involved will require further investigation.
2. The role of septal cholinergic neurons on hippocampal single unit activity has yet to be explored. Although muscarinic antagonists blocked PNO-induced modulation of excitatory sink and population spike in hippocampal CA1 of anesthetized rats (Leung and Peloquin, 2010), no studies relating to single unit

activity were carried out. It will be interesting to study the effects of 192 IgG-saporin lesion on hippocampal single unit activity.

3. At present, there are no studies looking at the damage of glutamatergic neurons following intraseptal infusion of immunotoxins. Immunostaining for a vesicular transporter of glutamate VGLUT2 shall be performed to evaluate possible damage of glutamatergic neurons following septal immunotoxin lesion of cholinergic or GABAergic neurons.

5.5 References

- Alzheimer Society of Canada (2010) Rising tide: the impact of dementia on Canadian society. 1-65.
- Amaral DG, Kurz J (1985) An analysis of the origins of the cholinergic and noncholinergic septal projections to the hippocampal formation of the rat. *J Comp Neurol* 240:37-59.
- Bartus RT, Dean RL 3rd, Beer B, Lippa AS (1982) The cholinergic hypothesis of geriatric memory dysfunction. *Science* 217:408-414.
- Bassant MH, Apartis E, Jazat-Poindessous FR, Wiley RG, Lamour YA (1995) Selective immunolesion of the basal forebrain cholinergic neurons: effects on hippocampal activity during sleep and wakefulness in the rat. *Neurodegeneration* 4:61-70.
- Baxter MG, Bucci DJ, Gorman LK, Wiley RG, Gallagher M (1995) Selective immunotoxic lesions of basal forebrain cholinergic cells: effects on learning and memory in rats *Behav Neurosci* 109:714-722.
- Berchtold NC, Kesslak JP, Cotman CW (2002) Hippocampal brain-derived neurotrophic factor gene regulation by exercise and the medial septum. *J Neurosci Res* 68:511-521.
- Berger-Sweeney J, Heckers S, Mesulam MM, Wiley RG, Lappi DA, Sharma M (1994) Differential effects on spatial navigation of immunotoxin-induced cholinergic lesions of the medial septal area and nucleus basalis magnocellularis *J Neurosci* 14:4507-4519.
- Bland BH, Oddie SD (2001) Theta band oscillation and synchrony in the hippocampal formation and associated structures: the case for its role in sensorimotor integration. *Behav Brain Res* 127:119-136.
- Chang Q, Gold PE (2004) Impaired and spared cholinergic functions in the hippocampus after lesions of the medial septum/vertical limb of the diagonal band with 192 IgG-saporin. *Hippocampus* 14:170-179.
- Colom LV, Castaneda MT, Reyna T, Hernandez S, Garrido-Sanabria E (2005) Characterization of medial septal glutamatergic neurons and their projection to the hippocampus. *Synapse* 58:151-164.
- Dornan WA, McCampbell AR, Tinkler GP, Hickman LJ, Bannon AW, Decker MW, Gunther KL (1996) Comparison of site-specific injections into the basal forebrain on

- water maze and radial arm maze performance in the male rat after immunolesioning with 192 IgG saporin. *Behav Brain Res* 82:93-101.
- Francis PT, Palmer AM, Snape M, Wilcock GK (1999) The cholinergic hypothesis of Alzheimer's disease: a review of progress. *J Neurol Neurosurg Psychiatry* 66:137-147.
- Freund TF, Antal M (1988) GABA-containing neurons in the septum control inhibitory interneurons in the hippocampus. *Nature* 336:170-173.
- Garcia-Alloza M, Tsang SW, Gil-Bea FJ, Francis PT, Lai MK, Marcos B, Chen CP, Ramirez MJ (2006) Involvement of the GABAergic system in depressive symptoms of Alzheimer's disease. *Neurobiol Aging* 27:1110-1117.
- Gerashchenko D, Salin-Pascual R, Shiromani PJ (2001) Effects of hypocretin-saporin injections into the medial septum on sleep and hippocampal theta. *Brain Res* 913:106-115.
- Givens BS, Olton DS (1990) Cholinergic and GABAergic modulation of medial septal area: effect on working memory. *Behav Neurosci* 104:849-855.
- Hasselmo ME (2006) The role of acetylcholine in learning and memory. *Curr Opin Neurobiol* 16:710-715.
- Huh CY, Goutagny R, Williams S (2010) Glutamatergic neurons of the mouse medial septum and diagonal band of Broca synaptically drive hippocampal pyramidal cells: relevance for hippocampal theta rhythm. *J Neurosci* 30:15951-15961.
- Kiss J, Patel AJ, Freund TF (1990) Distribution of septohippocampal neurons containing parvalbumin or choline acetyltransferase in the rat brain. *J Comp Neurol* 298:362-372.
- Kohler C, Chan-Palay V, Wu JY (1984) Septal neurons containing glutamic acid decarboxylase immunoreactivity project to the hippocampal region in the rat brain. *Anat Embryol (Berl)* 169:41-44.
- Lapchak PA, Jenden DJ, Hefti F (1991) Compensatory elevation of acetylcholine synthesis in vivo by cholinergic neurons surviving partial lesions of the septohippocampal pathway. *J Neurosci* 11:2821-2828.
- Leanza G, Nilsson OG, Wiley RG, Bjorklund A (1995) Selective lesioning of the basal forebrain cholinergic system by intraventricular 192 IgG-saporin: behavioural, biochemical and stereological studies in the rat. *Eur J Neurosci* 7:329-343.

- Lecourtier L, de Vasconcelos AP, Leroux E, Cosquer B, Geiger K, Lithfous S, Cassel JC (2010) Septohippocampal pathways contribute to system consolidation of a spatial memory: Sequential implication of gabaergic and cholinergic neurons. *Hippocampus*
- Lee MG, Chrobak JJ, Sik A, Wiley RG, Buzsaki G (1994) Hippocampal theta activity following selective lesion of the septal cholinergic system. *Neuroscience* 62:1033-1047.
- Leung LS, Peloquin P (2010) Cholinergic modulation differs between basal and apical dendritic excitation of hippocampal CA1 pyramidal cells. *Cereb Cortex* 20:1865-1877.
- Manns ID, Alonso A, Jones BE (2003) Rhythmically discharging basal forebrain units comprise cholinergic, GABAergic, and putative glutamatergic cells. *J Neurophysiol* 89:1057-1066.
- Marczynski TJ (1995) GABAergic deafferentation hypothesis of brain aging and Alzheimer's disease; pharmacologic profile of the benzodiazepine antagonist, flumazenil. *Rev Neurosci* 6:221-258.
- McMahan RW, Sobel TJ, Baxter MG (1997) Selective immunolesions of hippocampal cholinergic input fail to impair spatial working memory. *Hippocampus* 7:130-136.
- Pang KC, Nocera R (1999) Interactions between 192-IgG saporin and intraseptal cholinergic and GABAergic drugs: role of cholinergic medial septal neurons in spatial working memory. *Behav Neurosci* 113:265-275.
- Roland JJ, Mark K, Vetreno RP, Savage LM (2008) Increasing hippocampal acetylcholine levels enhance behavioral performance in an animal model of diencephalic amnesia. *Brain Res* 1234:116-127.
- Rorsman I, Magnusson M, Johansson BB (1999) Reduction of visuo-spatial neglect with vestibular galvanic stimulation. *Scand J Rehabil Med* 31:117-124.
- Smith HR, Pang KC (2005) Orexin-saporin lesions of the medial septum impair spatial memory. *Neuroscience* 132:261-271.
- Smith PF, Darlington CL, Zheng Y (2010a) Move it or lose it--is stimulation of the vestibular system necessary for normal spatial memory? *Hippocampus* 20:36-43.
- Smith PF, Geddes LH, Baek JH, Darlington CL, Zheng Y (2010b) Modulation of memory by vestibular lesions and galvanic vestibular stimulation. *Front Neurol* 1:141.
- Sotty F, Danik M, Manseau F, Laplante F, Quirion R, Williams S (2003) Distinct electrophysiological properties of glutamatergic, cholinergic and GABAergic rat

- septohippocampal neurons: novel implications for hippocampal rhythmicity. *J Physiol* 551:927-943.
- Utz KS, Dimova V, Oppenlander K, Kerkhoff G (2010) Electrified minds: transcranial direct current stimulation (tDCS) and galvanic vestibular stimulation (GVS) as methods of non-invasive brain stimulation in neuropsychology--a review of current data and future implications. *Neuropsychologia* 48:2789-2810.
- Wenk GL (2006) Neuropathologic changes in Alzheimer's disease: potential targets for treatment. *J Clin Psychiatry* 67 Suppl 3:3-7; quiz 23.
- Wiley RG (2001) Targeting toxins to neural antigens and receptors. *Methods Mol Biol* 166:267-276.
- Wiley RG, Oeltmann TN, Lappi DA (1991) Immunolesioning: selective destruction of neurons using immunotoxin to rat NGF receptor. *Brain Res* 562:149-153.
- Wrenn CC, Wiley RG (1998) The behavioral functions of the cholinergic basal forebrain: lessons from 192 IgG-saporin. *Int J Dev Neurosci* 16:595-602.
- Wu M, Zhang Z, Leranth C, Xu C, van den Pol AN, Alreja M (2002) Hypocretin increases impulse flow in the septohippocampal GABAergic pathway: implications for arousal via a mechanism of hippocampal disinhibition. *J Neurosci* 22:7754-7765.

Copyright Transfer Agreement

JOHN WILEY AND SONS LICENSE

TERMS AND CONDITIONS

Jun 17, 2011

This is a License Agreement between Siew Kian Tai ("You") and John Wiley and Sons ("John Wiley and Sons") provided by Copyright Clearance Center ("CCC"). The license consists of your order details, the terms and conditions provided by John Wiley and Sons, and the payment terms and conditions.

All payments must be made in full to CCC. For payment instructions, please see information listed at the bottom of this form.

License Number: 2691180667072

License date: Jun 17, 2011

Licensed content publisher: John Wiley and Sons

Licensed content publication: Hippocampus

Licensed content title: Activation of immobility - related hippocampal theta by cholinergic septohippocampal neurons during vestibular stimulation

Licensed content author: Siew Kian Tai, Jingyi Ma, Klaus - Peter Ossenkopp, L. Stan Leung

Licensed content date: Jan 1, 2011

Start page: n/a

End page: n/a

Type of use: Dissertation/Thesis

Requestor type: Author of this Wiley article

Format: Print and electronic

Portion: Full article

Will you be translating?: No

Order reference number

Total: 0.00 USD

Terms and Conditions

TERMS AND CONDITIONS

This copyrighted material is owned by or exclusively licensed to John Wiley & Sons, Inc. or one of its group companies (each a "Wiley Company") or a society for whom a Wiley Company has exclusive publishing rights in relation to a particular journal (collectively "WILEY"). By clicking "accept" in connection with completing this licensing

transaction, you agree that the following terms and conditions apply to this transaction (along with the billing and payment terms and conditions established by the Copyright Clearance Center Inc., ("CCC's Billing and Payment terms and conditions"), at the time that you opened your Rightslink account (these are available at any time at <http://myaccount.copyright.com>)

Terms and Conditions

1. The materials you have requested permission to reproduce (the "Materials") are protected by copyright.
2. You are hereby granted a personal, non-exclusive, non-sublicensable, non-transferable, worldwide, limited license to reproduce the Materials for the purpose specified in the licensing process. This license is for a one-time use only with a maximum distribution equal to the number that you identified in the licensing process. Any form of republication granted by this licence must be completed within two years of the date of the grant of this licence (although copies prepared before may be distributed thereafter). The Materials shall not be used in any other manner or for any other purpose. Permission is granted subject to an appropriate acknowledgement given to the author, title of the material/book/journal and the publisher and on the understanding that nowhere in the text is a previously published source acknowledged for all or part of this Material. Any third party material is expressly excluded from this permission.
3. With respect to the Materials, all rights are reserved. Except as expressly granted by the terms of the license, no part of the Materials may be copied, modified, adapted (except for minor reformatting required by the new Publication), translated, reproduced, transferred or distributed, in any form or by any means, and no derivative works may be made based on the Materials without the prior permission of the respective copyright owner. You may not alter, remove or suppress in any manner any copyright, trademark or other notices displayed by the Materials. You may not license, rent, sell, loan, lease, pledge, offer as security, transfer or assign the Materials, or any of the rights granted to you hereunder to any other person.
4. The Materials and all of the intellectual property rights therein shall at all times remain the exclusive property of John Wiley & Sons Inc or one of its related companies (WILEY) or their respective licensors, and your interest therein is only that of having possession of and the right to reproduce the Materials pursuant to Section 2 herein during the continuance of this Agreement. You agree that you own no right, title or interest in or to the Materials or any of the intellectual property rights therein. You shall have no rights hereunder other than the license as provided for above in Section 2. No right, license or interest to any trademark, trade name, service mark or other branding ("Marks") of WILEY or its licensors is granted hereunder, and you agree that you shall not assert any such right, license or interest with respect thereto.
5. NEITHER WILEY NOR ITS LICENSORS MAKES ANY WARRANTY OR REPRESENTATION OF ANY KIND TO YOU OR ANY THIRD PARTY, EXPRESS,

IMPLIED OR STATUTORY, WITH RESPECT TO THE MATERIALS OR THE ACCURACY OF ANY INFORMATION CONTAINED IN THE MATERIALS, INCLUDING, WITHOUT LIMITATION, ANY IMPLIED WARRANTY OF MERCHANTABILITY, ACCURACY, SATISFACTORY QUALITY, FITNESS FOR A PARTICULAR PURPOSE, USABILITY, INTEGRATION OR NON-INFRINGEMENT AND ALL SUCH WARRANTIES ARE HEREBY EXCLUDED BY WILEY AND ITS LICENSORS AND WAIVED BY YOU.

6. WILEY shall have the right to terminate this Agreement immediately upon breach of this Agreement by you.

7. You shall indemnify, defend and hold harmless WILEY, its Licensors and their respective directors, officers, agents and employees, from and against any actual or threatened claims, demands, causes of action or proceedings arising from any breach of this Agreement by you.

8. IN NO EVENT SHALL WILEY OR ITS LICENSORS BE LIABLE TO YOU OR ANY OTHER PARTY OR ANY OTHER PERSON OR ENTITY FOR ANY SPECIAL, CONSEQUENTIAL, INCIDENTAL, INDIRECT, EXEMPLARY OR PUNITIVE DAMAGES, HOWEVER CAUSED, ARISING OUT OF OR IN CONNECTION WITH THE DOWNLOADING, PROVISIONING, VIEWING OR USE OF THE MATERIALS REGARDLESS OF THE FORM OF ACTION, WHETHER FOR BREACH OF CONTRACT, BREACH OF WARRANTY, TORT, NEGLIGENCE, INFRINGEMENT OR OTHERWISE (INCLUDING, WITHOUT LIMITATION, DAMAGES BASED ON LOSS OF PROFITS, DATA, FILES, USE, BUSINESS OPPORTUNITY OR CLAIMS OF THIRD PARTIES), AND WHETHER OR NOT THE PARTY HAS BEEN ADVISED OF THE POSSIBILITY OF SUCH DAMAGES. THIS LIMITATION SHALL APPLY NOTWITHSTANDING ANY FAILURE OF ESSENTIAL PURPOSE OF ANY LIMITED REMEDY PROVIDED HEREIN.

9. Should any provision of this Agreement be held by a court of competent jurisdiction to be illegal, invalid, or unenforceable, that provision shall be deemed amended to achieve as nearly as possible the same economic effect as the original provision, and the legality, validity and enforceability of the remaining provisions of this Agreement shall not be affected or impaired thereby.

10. The failure of either party to enforce any term or condition of this Agreement shall not constitute a waiver of either party's right to enforce each and every term and condition of this Agreement. No breach under this agreement shall be deemed waived or excused by either party unless such waiver or consent is in writing signed by the party granting such waiver or consent. The waiver by or consent of a party to a breach of any provision of this Agreement shall not operate or be construed as a waiver of or consent to any other or subsequent breach by such other party.

11. This Agreement may not be assigned (including by operation of law or otherwise) by you without WILEY's prior written consent.

12. Any fee required for this permission shall be non-refundable after thirty (30) days from receipt.

13. These terms and conditions together with CCC's Billing and Payment terms and conditions (which are incorporated herein) form the entire agreement between you and WILEY concerning this licensing transaction and (in the absence of fraud) supersedes all prior agreements and representations of the parties, oral or written. This Agreement may not be amended except in writing signed by both parties. This Agreement shall be binding upon and inure to the benefit of the parties' successors, legal representatives, and authorized assigns.

14. In the event of any conflict between your obligations established by these terms and conditions and those established by CCC's Billing and Payment terms and conditions, these terms and conditions shall prevail.

15. WILEY expressly reserves all rights not specifically granted in the combination of (i) the license details provided by you and accepted in the course of this licensing transaction, (ii) these terms and conditions and (iii) CCC's Billing and Payment terms and conditions.

16. This Agreement will be void if the Type of Use, Format, Circulation, or Requestor Type was misrepresented during the licensing process.

17. This Agreement shall be governed by and construed in accordance with the laws of the State of New York, USA, without regards to such state's conflict of law rules. Any legal action, suit or proceeding arising out of or relating to these Terms and Conditions or the breach thereof shall be instituted in a court of competent jurisdiction in New York County in the State of New York in the United States of America and each party hereby consents and submits to the personal jurisdiction of such court, waives any objection to venue in such court and consents to service of process by registred or certified mail, return receipt requested, at the last known address of such party. . BY CLICKING ON THE "I ACCEPT" BUTTON, YOU ACKNOWLEDGE THAT YOU HAVE READ AND FULLY UNDERSTAND EACH OF THE SECTIONS OF AND PROVISIONS SET FORTH IN THIS AGREEMENT AND THAT YOU ARE IN AGREEMENT WITH AND ARE WILLING TO ACCEPT ALL OF YOUR OBLIGATIONS AS SET FORTH IN THIS AGREEMENT.

v1.4

Gratis licenses (referencing \$0 in the Total field) are free. Please retain this printable license for your reference. No payment is required.

If you would like to pay for this license now, please remit this license along with your payment made payable to "COPYRIGHT CLEARANCE CENTER" otherwise you will be invoiced within 48 hours of the license date. Payment should

be in the form of a check or money order referencing your account number and this invoice number RLNK11005755

Once you receive your invoice for this order, you may pay your invoice by credit card. Please follow instructions provided at that time.

Make Payment To:

**Copyright Clearance Center
Dept 001
P.O. Box 843006
Boston, MA 02284-3006**

For suggestions or comments regarding this order, contact Rightslink Customer Support: customercare@copyright.com or +1-877-622-5543 (toll free in the US) or +1-978-646-2777.

Curriculum Vitae

Name: Siew Kian Tai

Address: Medical Science Building, Rm 240
Department of Physiology and Pharmacology
University of Western Ontario
London, Ontario N6A5C1

Post-secondary Education and Degrees:

2006-Present PhD Candidate
Graduate Program in Neuroscience
School of Graduate and Postdoctoral Studies
University of Western Ontario, Canada

2002-2005 M.Sc.
Department of Physiology
National University of Singapore, Singapore

2001-2002 B.Sc. (Hons)
Department of Microbiology
National University of Singapore, Singapore

1998-2001 B.Sc. (Biomedical science)
National University of Singapore, Singapore

Honors and Awards:

2006-2010 Canadian Commonwealth Scholarship
Canadian Bureau for International Education
Foreign Affairs and International Trade Canada

2007-2010 Western Graduate Research Scholarship
University of Western Ontario

2002-2005 Graduate Research Scholarship
National University of Singapore

Related work experience:

2006-2011 Graduate Research Assistant
University of Western Ontario

Publications:

Tai S.K., Ma J., Ossenkopp K-P. and Leung L.S. (2011) Activation of immobility-related hippocampal theta by cholinergic septohippocampal neurons during vestibular stimulation. *Hippocampus* doi: 10.1002/hipo.20955.

Ma J., **Tai S.K.** and Leung L.S. (2009) Ketamine-induced deficit of auditory gating in the hippocampus of rats is alleviated by medial septal inactivation and antipsychotic drugs. *Psychopharmacology*. 206 (3):457-467.

Tai S.K., Huang F-D., Moochhala S. and Khanna S. (2006) Hippocampal theta functional state in relation to formalin nociception. *Pain*. 121 (1-2): 29-42.

Tai S.K., Tan O. J-K. , Chow V. T-K, Jin R., Jones J.L., Tan P-H., Jayasurya A. and Bay B-H. (2003) Differential Expression of Metallothionein 1 and 2 isoforms in breast cancer lines with different invasive potential: identification of a novel non-silent MT-1H mutant variant. *American Journal of Pathology*. 163 (5): 2009-2019.

Abstracts and presentations:

Tai S.K. and Leung L.S. (2009) Facilitation of dentate gyrus population spike may involve septohippocampal GABAergic input. *Soc Neurosci Abstr* 566.18/EE33 (Chicago, USA)

Tai S.K., Ma J. and Leung L.S. (2007) Vestibular activation stimulates cholinergic system in the hippocampus. *Soc Neurosci Abstr* 399.21/OO13 (San Diego, USA)

Ma J., **Tai S.K.**, Leung L.S. (2007) Ketamine-induced gating deficit of hippocampal auditory evoked potentials in rats is alleviated by medial septum inactivation and antipsychotic drugs. *Soc Neurosci Abstr* 498.12/GG19 (San Diego, USA)

Tai S.K., Ma J., Ossenkopp K-P. and Leung L.S. (2007) Vestibular activation stimulates cholinergic system in the hippocampus. *Margaret Moffat Graduate Research Day* (University of Western Ontario, Canada)

Tai S.K., Moochhala S. and Khanna S. (2004) Hippocampal nociceptive activation in behaving rat. *Singapore International Neuroscience Conference* 1524-P27 (Singapore)